ELEMENTA
Science of the Anthropocene

Gkatzelis, GI, et al. 2021. The global impacts of COVID-19 lockdowns on urban air pollution: A critical review and recommendations. *Elem Sci Anth*, 9: 1. DOI: https://doi.org/10.1525/elementa.2021.00176

REVIEW

The global impacts of COVID-19 lockdowns on urban air pollution: A critical review and recommendations

Georgios I. Gkatzelis[1], Jessica B. Gilman[2], Steven S. Brown[2], Henk Eskes[3], A. Rita Gomes[1], Anne C. Lange[1], Brian C. McDonald[2], Jeff Peischl[2,4], Andreas Petzold[1], Chelsea R. Thompson[2,4], and Astrid Kiendler-Scharr[1,*]

The coronavirus-19 (COVID-19) pandemic led to government interventions to limit the spread of the disease which are unprecedented in recent history; for example, stay at home orders led to sudden decreases in atmospheric emissions from the transportation sector. In this review article, the current understanding of the influence of emission reductions on atmospheric pollutant concentrations and air quality is summarized for nitrogen dioxide (NO_2), particulate matter ($PM_{2.5}$), ozone (O_3), ammonia, sulfur dioxide, black carbon, volatile organic compounds, and carbon monoxide (CO). In the first 7 months following the onset of the pandemic, more than 200 papers were accepted by peer-reviewed journals utilizing observations from ground-based and satellite instruments. Only about one-third of this literature incorporates a specific method for meteorological correction or normalization for comparing data from the lockdown period with prior reference observations despite the importance of doing so on the interpretation of results. We use the government stringency index (SI) as an indicator for the severity of lockdown measures and show how key air pollutants change as the SI increases. The observed decrease of NO_2 with increasing SI is in general agreement with emission inventories that account for the lockdown. Other compounds such as O_3, $PM_{2.5}$, and CO are also broadly covered. Due to the importance of atmospheric chemistry on O_3 and $PM_{2.5}$ concentrations, their responses may not be linear with respect to primary pollutants. At most sites, we found O_3 increased, whereas $PM_{2.5}$ decreased slightly, with increasing SI. Changes of other compounds are found to be understudied. We highlight future research needs for utilizing the emerging data sets as a preview of a future state of the atmosphere in a world with targeted permanent reductions of emissions. Finally, we emphasize the need to account for the effects of meteorology, emission trends, and atmospheric chemistry when determining the lockdown effects on pollutant concentrations.

Keywords: COVID-19 lockdown, Air quality, Urban pollution

1. Introduction

The global spread of severe acute respiratory syndrome coronavirus 2 (SARS-CoV-2) in early 2020 was an unprecedented, highly disruptive event. Lockdowns instituted to control the subsequent coronavirus disease 2019 (COVID-19) pandemic led to rapid, unforeseen decreases in economic and social activity and associated emissions of air pollutants and greenhouse gases worldwide. It has been suggested in a number of perspective articles and comments that this episode provides a unique scientific opportunity to detect, attribute, and understand the impacts of anthropogenic emissions on the Earth's atmosphere at all spatial scales, from regional to global (Forster et al., 2020; He et al., 2020; Kroll et al., 2020; Le Quéré et al., 2020; Liu et al., 2020d), and on the Earth System and climate generally (Diffenbaugh et al., 2020; Phillips et al., 2020; Raymond et al., 2020). Of particular interest have been shifts in regional air quality that have been documented by ground-level monitoring networks and spaceborne remote sensing instruments. Such changes, occurring to a varying extent on every continent except Antarctica, have been the subject of intense interest among the general public and within the scientific and regulatory communities charged with understanding the air quality impacts of anthropogenic emissions. These transient shifts within particular emissions sectors have the potential to test the efficacy of air pollution control strategies and may even provide a preview of the future state of the atmosphere in a world with more permanent reductions in emissions from certain sectors.

[1] IEK-8: Troposphere, Forschungszentrum Jülich GmbH, Jülich, Germany

[2] NOAA Chemical Sciences Laboratory, Boulder, CO, USA

[3] Royal Netherlands Meteorological Institute (KNMI), De Bilt, the Netherlands

[4] Cooperative Institute for Research in Environmental Sciences, University of Colorado Boulder, Boulder, CO, USA

* Corresponding author:
Email: a.kiendler-scharr@fz-juelich.de

Table 1. Overview of compounds of relevance for ambient air quality and the respective guideline values as stated in the 2005 global update of the World Health Organization (WHO) air quality guidelines. DOI: https://doi.org/10.1525/elementa.2021.00176.t1

Compound	WHO Guideline Value ($\mu g/m^3$) or Comment	Additional Definition ($\mu g/m^3$) or Comment
NO_2	$40^{/\text{annual mean}}$	$200^{/\text{1-h mean}}$
NMVOCs		Some NMVOCs considered for indoor air guidelines
SO_2	$20^{/\text{24-h mean}}$	$500^{/\text{10-min mean}}$
NH_3		Not defined
O_3	$100^{/\text{8-h mean}}$	No WHO guideline values for annual or 24-h mean exist
$PM_{2.5}$	$10^{/\text{annual mean}}$	$25^{/\text{24-h mean}}$
PM_{10}	$20^{/\text{annual mean}}$	$50^{/\text{24-h mean}}$
CO	Chinese guideline value	$4^{/\text{24-h mean}}$ mg m^{-3}, $10^{/\text{1-h mean}}$ mg m^{-3}
	European guideline value	$10^{/\text{24-h mean}}$ mg m^{-3}
	U.S. guideline value	$10^{/\text{8-h mean}}$ mg m^{-3}, $40^{/\text{1-h mean}}$ mg m^{-3}

NMVOC = nonmethane volatile organic compound; NO_2 = nitrogen dioxide; SO_2 = sulfur dioxide; NH_3 = ammonia; O_3 = ozone; PM = particulate matter; CO = carbon monoxide.

The concept of air quality acknowledges the health burden attributable to atmospheric pollutants (World Health Organization [WHO], 2019). The WHO assesses that air pollution is the number one environmental health risk globally, causing 7.1 million premature deaths per year, of which 4.2 million are attributable to outdoor air pollutants. The WHO defines guideline values for key air pollutants (see **Table 1**), yet national regulatory limit values vary widely and are often less stringent than the WHO guideline values. The air quality index (AQI) is a common term used by government agencies to define standards for the simultaneous presence of multiple pollutants. Individual pollutant concentrations are combined to derive the AQI and determine air quality levels. However, no agreed upon definition for AQI exists, with AQI determined in different ways for each country (Bishoi et al., 2009; Fareed et al., 2020).

In addition to emission and deposition processes, both sources and sinks of air quality relevant trace compounds are determined by atmospheric chemistry. Species that are emitted directly to the atmosphere are considered primary, whereas species formed through atmospheric chemical processes are referred to as secondary. The main species of concern for human health are particulate matter (PM) and tropospheric ozone (O_3; Gakidou et al., 2017). PM has both primary and secondary sources, while ozone is formed almost exclusively through atmospheric chemistry, that is, it is secondary in nature. Major pollutants that serve as precursors to O_3 and secondary PM include nitrogen oxides (NO_x = NO + nitrogen dioxide [NO_2]), volatile organic compounds (VOCs), sulfur dioxide (SO_2), carbon monoxide (CO), and ammonia (NH_3; see **Figure 1**).

Observational and laboratory approaches to understand relevant atmospheric chemical processes are complemented by modeling approaches to determine atmospheric composition on regional and global scales. Atmospheric chemical transport models (CTMs) account for (1) emissions from anthropogenic and natural sources, (2) atmospheric chemistry, and (3) transport, dilution, and deposition processes. The ability of CTMs to correctly simulate atmospheric composition is traditionally verified through comparisons of model and observational outputs. Extreme events, such as volcanic eruptions (Kristiansen et al., 2016; Wilkins et al., 2016; Beckett et al., 2020), wildfires (Liu et al., 2010), and heatwaves (Churkina et al., 2017; Zhao et al., 2019), play a particularly important role in this regard, as such events can expose model biases or missing processes.

The various national, statewide, and municipal lockdowns and implementations of social distancing for pandemic control of COVID-19 offer an "extreme" real-world experiment in which various anthropogenic sector-specific emissions of air pollutants have been suddenly and significantly reduced. This link of changes in human behavior and reduced anthropogenic emissions is expected (Beirle et al., 2003). In particular, during the pandemic, emissions from the transportation sector were reduced as a consequence of stay-at-home orders, as revealed by mobility data sets (Forster et al., 2020; Venter et al., 2020), for example. Early reports of observed decreases in NO_x and PM in various regions of the world are now complemented by data sets showing varied responses in the secondary pollutants O_3 and PM resulting from the nonlinear interactions involved in atmospheric chemistry (Seinfeld, 2006). The COVID-19 lockdowns, therefore, offer a unique opportunity to (1) verify emission inventories and (2) explore the sensitivity of secondary pollutants to emission changes. Several review articles have already been published as of the writing of this article. Shakil et al. (2020) used 23 publications through May 2020 to highlight the effects of lockdowns and environmental factors on air quality and recommended that future analyses include meteorological corrections. Srivastava et al. (2020) focused on the link between PM pollution and the

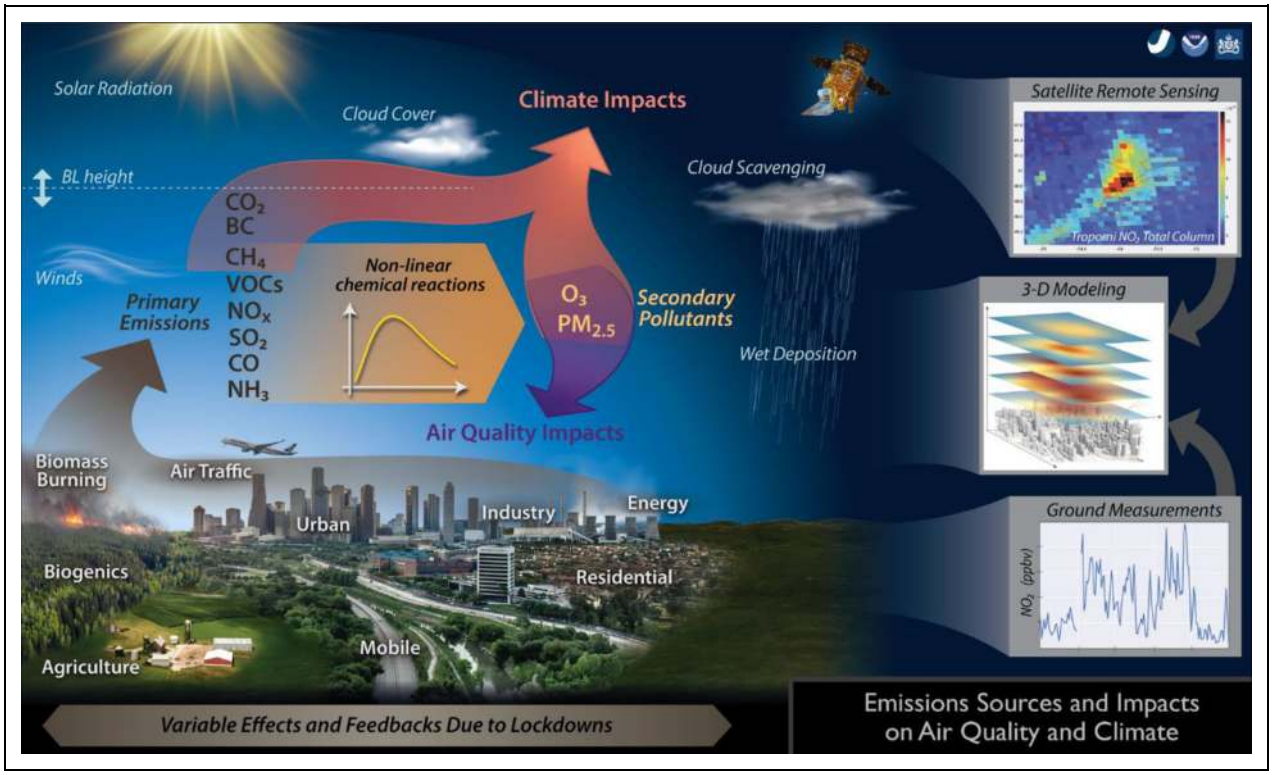

Figure 1. Schematic of major emission sectors and primary emissions, meteorological and chemical processes, impacts to air quality and climate, and measurement and analysis tools used to analyze the effects of emissions changes. DOI: https://doi.org/10.1525/elementa.2021.00176.f1

positive correlation to COVID-19 cases as well as the impact of weather on pollutant concentrations that affect morbidity and mortality. Kumar et al. (2020) highlighted the key findings of 28 publications on the effects of lockdowns on pollutant concentrations. Finally, Le et al. (2020b) discussed 16 publications related to PM concentration reductions during the pandemic.

In this review, we summarize the available literature through September 30, 2020, comprising more than 200 publications, and the approaches used to quantify changes in atmospheric pollutant levels. We focus on species that are of relevance as air pollutants and short-lived climate forcers, namely, NO_2, $PM_{2.5}$, O_3, NH_3, SO_2, black carbon (BC), VOCs, and CO. We further provide an outlook on the tools and analyses required to expand from individual case studies to a global framework of readily comparable results. To enhance the readability of the text, we present the references in tables, which allows for structured overviews of all references relevant to respective methods, regions, or compounds. With the pandemic, and hence lockdowns, ongoing as of this writing, this review intends to serve as a milestone in identifying and quantifying the overall impacts of emission reductions to air quality.

2. Methods

2.1. Literature review process

Analysis of ground- and satellite-based observations of pollutants has received intense scientific focus in 2020. During the 7 months following the onset of the pandemic (March–September 2020), more than 200 manuscripts were accepted for publication in peer-reviewed journals. There are undoubtedly many others that are in preparation and review at the time of this writing or that have been published after October 2020. Subsequent reviews will be required to fully assess the breadth of this literature. The goal of this review is to provide an initial synthesis of this rapidly developing literature, as well as to provide some critical assessment of the state of the initial literature that may be useful for authors of manuscripts that follow.

To generate the database of peer-reviewed scientific articles used in this study, we utilized Google Scholar (Google, 2020) and searched the websites of prominent publishers of environmental scientific journals to find as many relevant and newly accepted papers as possible. We used the following search terms to query subject matter content: "COVID* AND air AND pollution" or "COVID* AND air AND quality." The wildcard "*" accounted for common iterations such as "COVID-19" and "COVID2019," while the Boolean operator AND was used to limit the results to studies related to air pollution or air quality topics. The first search was conducted in September 2020 and updated biweekly through October 30, 2020. We further limited the search results to papers that had undergone peer review, were accepted by September 30, 2020, and were published in English.

Each of the 219 papers that met the above criteria was examined by at least one coauthor to determine its overall relevance to the goals of this study. The papers were then added to our database and all pertinent information was manually cataloged. This included the author list, journal

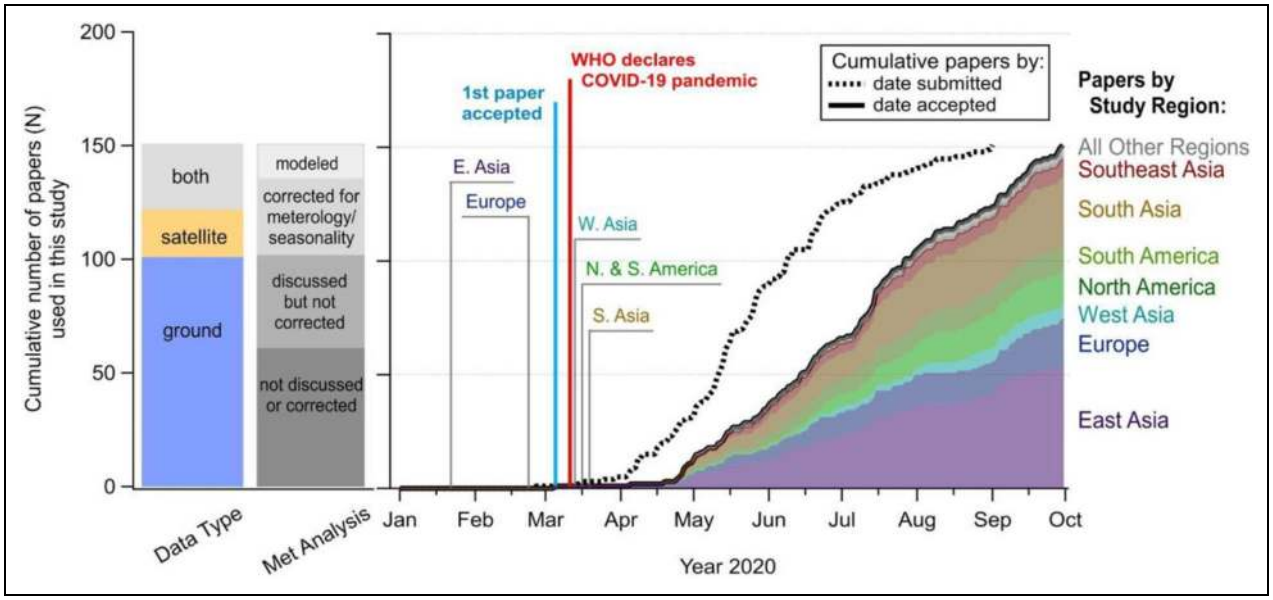

Figure 2. The cumulative number of papers for which we digitized data for this analysis. The papers are grouped by data type, treatment of meteorology/seasonality, and study region as a function of the manuscript acceptance date (also see **Tables 2**–4). The dates that the first country within each geographic region to undergo a strict lockdown (stringency index > 70) are included, starting with China on January 22, 2020. DOI: https://doi.org/10.1525/elementa.2021.00176.f2

name, dates of submission and acceptance, the region and time frames studied, the type of data set used (ground-based, satellite, or both), and whether the authors accounted for the effects of seasonality/meteorology and the year-to-year variability in atmospheric concentrations.

Furthermore, we manually digitized the findings from 150 papers relating to the observed percentage change and/or concentrations of the pollutants discussed in each study (see Table S1 for the nondigitized yet reviewed papers). **Figure 2** shows the cumulative number of papers by sample type, methodology, and region of study. This subset of our database comprises manuscripts published in 37 different scientific journals with a median submission to acceptance peer-review period of 35 days. There were 10 different geographic study regions, led by East Asia ($N = 54$ papers) and South Asia ($N = 28$ papers). These two regions were dominated by air quality studies in China ($N = 46$ papers) and India ($N = 27$ papers), respectively. The first COVID-related air quality manuscript was accepted on March 5, 2020 (Wang et al., 2020c) before the WHO declared COVID-19 a global pandemic on March 11, 2020.

Portions of our analysis rely on the stringency index (SI), a metric used to quantitatively compare lockdown measures for each country over time (Hale et al., 2020). The SI ranges from 0 (no lockdown) to 100 (strictest lockdown) based on a variety of measures meant to slow the spread of COVID-19 (see Section 3.2). We have not made explicit use of other common metrics of economic activity changes found in other papers, such as sector-specific mobility indices provided by Google or Apple (Forster et al., 2020) or traffic counts. The SI is convenient for the purpose of this article since its focus is appropriate for the continental and regional scales considered in the data synthesis presented here.

All data digitized for analysis in this review are available on the website https://covid-aqs.fz-juelich.de. This includes the observed percentage change in species concentration for NO_2, NO_x, CO, $PM_{2.5}$, PM_{10}, O_3, SO_2, NH_3, speciated nonmethane volatile organic compound (NMVOCs), aerosol optical depth (AOD), BC, and the AQI. Also, the absolute concentrations of NO_2, $PM_{2.5}$, O_3, and CO during the lockdown and reference periods are provided. Each data set is linked with the digital object identifier of the original publication, information on the corresponding author, region, country, city (where applicable), and the observational start and end times. This website is designed as a living version of this review, that is, as new literature emerges, authors of published papers are encouraged to upload their data to the database, thus complementing the data coverage in space, time, and compound dimensions. The data sets from the website are provided with free and unrestricted access for scientific (noncommercial) use including the option to generate targeted reference lists. Users of the database are requested to acknowledge the data source and reference this review in publications utilizing the data set.

2.2. Platforms used to measure pollutant concentrations

2.2.1. Ground-based

Figure 2 shows that ground-based measurements comprise the largest fraction of the data used in the analysis of COVID-19 lockdowns to date. These data normally come from local, regional, or national air quality monitoring networks in various regions, as discussed in Section S1.1. Air quality monitoring networks include the U.S. Environmental Protection Agency (2020), the European Environment Agency EAA together with the European Monitoring

and Evaluation Programme (2020), the China National Environmental Monitoring Center established by the Ministry of Ecology and Environment of China (Chu et al., 2021), and the Central Pollution Control Board in India managed by the Ministry of Environment, Forests, and Climate Change (Pant et al., 2020).

All these networks or infrastructures such as the Aerosols, Clouds and Trace gases Research Infrastructure and In-service Aircraft for a Global Observing System (Petzold et al., 2015) provide preliminary data in near real time, with final, quality-assured data updated either quarterly or biannually. Other data sources such as the OPEN-AQ data source (https://openaq.org/) compile network data into readily accessible, larger databases. However, the data quality assurance process is not always made clear in a given publication. For example, the OPEN-AQ platform explicitly makes no guarantee of quality assurance or assessment of accuracy. Data are uploaded in real time and not necessarily updated when quality assured (final) data are made available from a given air quality network. Papers published to date on COVID-19 lockdown effects using ground-based monitors generally specify the source of their data but commonly do not specify whether those data are preliminary or final. Given the speed with which these manuscripts were prepared, it is possible that many are based on data with no final quality control.

2.2.2. Satellites

Roughly one-third of the publications discussed in this review make use of satellite observations. A large number of satellite data sets have been used, including:

- Sentinel-5P TROPOspheric Monitoring Instrument (TROPOMI) NO_2, CO, SO_2, and HCHO;
- AURA-OMI (Ozone Monitoring Instrument) NO_2, SO_2, and AOD;
- Terra and Aqua MODIS AOD, PM, and fire products; and
- Terra MOPITT CO and Aqua AIRS CO.

By far, the most used data set is the TROPOMI NO_2 tropospheric column product of Sentinel-5P, used in 41% of cases (calculated as the number of papers using TROPOMI NO_2 divided by the total number of satellite data sets used in the papers). The second most used data set is AURA-OMI NO_2, used in 27% of cases, followed by MODIS AOD, used in 14% of cases. All other data sets have been used sporadically (1–3 times). Of the papers reviewed herein that use satellite data, 61% used TROPOMI NO_2, 40% used OMI NO_2, and 21% used MODIS AOD (note that several papers used multiple satellite data sets for their analysis, on average 1.5 satellite data sets per paper). Taking the NO_2 data sets from OMI and TROPOMI together, 68% of the published satellite results on the COVID-19 impact on air quality were generated using these two data sets.

Note that satellite instruments like TROPOMI and OMI measure at one given overpass time (e.g., 13:30 local). As the diurnal profile of the emissions may have changed during the lockdowns, observed changes at a given overpass time may not be fully representative of the total changes. Also, TROPOMI and OMI tropospheric column NO_2 retrieval products contain detailed uncertainty estimates for each observation separately, typically ranging between 20% and 60% for polluted scenes. The use of averaging kernels in the data products is advised to remove the dependency on the retrieval a priori and reduce the associated uncertainties (see Section S1.2).

2.3. Methods used to determine lockdown effects on pollutants

The atmospheric abundance of trace compounds is determined through the interplay of emissions, atmospheric chemistry, transport, and loss processes. To quantify the effect of changes in any of these, an analysis must isolate the influence of confounding parameters. The main focus of the literature reviewed here is the effect of emission changes on ambient mixing ratios of criteria pollutants. In general, three types of approaches are used: a comparison of observed concentrations to a reference period during which "business as usual" emissions prevailed (see Section 2.3.1), an analysis of observed concentrations when accounting for meteorological influences or atmospheric chemistry (e.g., photolysis frequencies, humidity, and temperature dependencies; Section 2.3.2), and a comparison of observed concentrations with the output of CTMs run to derive "business as usual" expected values (Section 2.3.3).

2.3.1. Direct comparison to a reference period

Nearly two-thirds of the studies summarized here were a direct comparison of lockdown periods to a reference measurement period (**Table 2**). Two main approaches were used: (1) a comparison of pollutant concentrations directly before and/or after a lockdown, that is, data sets covering a relatively short time period or (2) a comparison of pollutant concentrations from seasonally similar time periods, that is, data sets that included 2019, and often several other previous years, for the same period of time as the 2020 lockdown. The main advantage of these approaches is the simplicity in identifying relative changes. For the first approach, uncertainties arise due to the unquantified effects of seasonality, meteorology, and atmospheric chemistry. Although the second approach generally covers meteorological effects, uncertainty may still arise from other processes that affect the abundance of atmospheric trace compounds, such as climatological variability and exceptional events. It is not possible to conclude generally whether the use of direct comparisons to reference periods bias the derived changes low or high, as this will be determined by the specific conditions prevailing in each studied region. Unambiguous quantification of emission changes is, therefore, not possible, although the correlation of observed changes with indicators of emission activity (e.g., traffic counts, fuel sales, mobility, electric power consumption) can be explored. Various studies included in this work highlight the importance of identifying the effects of meteorology, atmospheric chemistry, and emission trends in the observed

Table 2. Summary of studies that perform a direct comparison of the lockdown period to a reference period. DOI: https://doi.org/10.1525/elementa.2021.00176.t2

Direct Comparison Publications	
East Asia	**China:** (Agarwal et al., 2020; Chauhan and Singh, 2020; Chen et al., 2020a; Chen et al., 2020c; Chen et al., 2020d; Fan et al., 2020; G Huang and Sun, 2020; Lian et al., 2020; Liu et al., 2020c; Miyazaki et al., 2020; Nichol et al., 2020; Pei et al., 2020; Shakoor et al., 2020; Shi and Brasseur, 2020; Silver et al., 2020; Wan et al., 2020; Wang et al., 2020a; Wang et al., 2020b; Wang et al., 2020f; Xu et al., 2020c; Zhang et al., 2020a; Yuan et al., 2021)
	Other: (Ghahremanloo et al., 2020; Han et al., 2020; Ju et al., 2020; Ma and Kang, 2020; Zhang et al., 2020b)
South Asia	**India:** (Bedi et al., 2020; Beig et al., 2020; Biswal et al., 2020; Chatterjee et al., 2020; Gautam et al., 2020; Harshita and Vivek, 2020; Jain and Sharma, 2020; Kant et al., 2020; Kumari and Toshniwal, 2020; Kumari et al., 2020; Mahato and Ghosh, 2020; Mahato et al., 2020; Panda et al., 2020; Ranjan et al., 2020; Selvam et al., 2020; Sharma et al., 2020a; Siddiqui et al., 2020; Singh and Chauhan, 2020; Singh et al., 2020; Vadrevu et al., 2020)
	Other: (Masum and Pal, 2020; Rodríguez-Urrego and Rodríguez-Urrego, 2020)
Southeast Asia	**Malaysia:** (Abdullah et al., 2020; Ash'aari et al., 2020; Kanniah et al., 2020; Mohd Nadzir et al., 2020; Suhaimi et al., 2020)
	Other: (Jiayu and Federico, 2020; Stratoulias and Nuthammachot, 2020)
West Asia	**Turkey:** (Aydın et al., 2020; Şahin, 2020)
	Iran: (Broomandi et al., 2020; Faridi et al., 2020)
	Other: (Anil and Alagha, 2020; Hashim et al., 2020)
North America	**United States:** (Bauwens et al., 2020; Berman and Ebisu, 2020; Chen et al., 2020b; Hudda et al., 2020; Pan et al., 2020; Son et al., 2020; Zangari et al., 2020; Zhang et al., 2020d; Liu et al., 2021b)
South America	**Brazil:** (Dantas et al., 2020; Krecl et al., 2020; Nakada and Urban, 2020; Siciliano et al., 2020a)
	Other: (Mendez-Espinosa et al., 2020; Pacheco et al., 2020; Zalakeviciute et al., 2020; Zambrano-Monserrate and Ruano, 2020)
Europe	**Multiple countries:** (Baldasano, 2020; Collivignarelli et al., 2020; Filippini et al., 2020; Gautam, 2020a; Giani et al., 2020; Gualtieri et al., 2020; Higham et al., 2020; Ljubenkov et al., 2020; Sicard et al., 2020; Tobías et al., 2020; Martorell-Marugán et al., 2021)
Oceania	**Australia:** (Fu et al., 2020)
	New Zealand: (Patel et al., 2020)
Africa	**Morocco:** (Ass et al., 2020; Otmani et al., 2020)

This includes the "discussed but not corrected" and "not discussed or corrected" categories in **Figure 2.**

percentage emission changes and are discussed in the following section.

2.3.2. Accounting for effects of meteorology and emission trends

Meteorological factors have an important effect on atmospheric pollution levels (Shenfeld, 1970). Wind velocity, stability, and turbulence affect the dilution, transport, and dispersion of pollutants. Sunshine triggers the photochemical production of oxidants that form smog, whereas rainfall has a scavenging effect that washes out particles and some gases from the atmosphere. Furthermore, concentrations of various atmospheric pollutants can change due to decreasing trends of emissions in urban environments around the world (e.g., Warneke et al., 2012; Sun et al., 2018; Zheng et al., 2018). Changing pollutant concentrations can influence atmospheric chemistry by affecting the pollutant's chemical sources and sinks and therefore its lifetime (e.g., Shah et al., 2020). With atmospheric chemistry and pollutant distribution changing with season and location (e.g., summer vs. winter, urban vs. remote locations), all the above highlight the need to quantify the effects of meteorology, atmospheric chemistry, and emission trends on atmospheric pollutant concentrations when describing pollutant changes during the pandemic.

Several studies quantified the effects of meteorology and emission trends on the observed pollutant changes, as summarized in **Table 3.** Of the 32 studies listed, 16 studies focused on East Asia, six on Europe, six on North America, three on South Asia, two on South America, and two were global studies. Over 98% of the measurements presented in publications that were included in this review were from urban environments. Different statistical approaches were used to account for the above effects, which are summarized below.

2.3.2.1. Statistical tools used for pollutant source apportionment

Two approaches were utilized to apportion pollutant concentrations to different sectors and to elucidate the role of atmospheric chemistry and/or meteorology. One commonly used approach was positive matrix factorization

Table 3. Summary of studies controlling for effects of meteorology, atmospheric chemistry, and emission trends on air quality analysis. DOI: https://doi.org/10.1525/elementa.2021.00176.t3

Type	Region	Study Period	Baseline Year(s)	Species	Meteorological Variables	Reference
Dilution corrected	East Asia	January 26–February 17	2016–2020	NO_2, SO_2, CO, and $PM_{2.5}$	PBLH	(Su et al., 2020)
Dilution corrected	North America	January 1–April 30	2019–2020	NO_2	SZA, WS, and WD	(Goldberg et al., 2020)
Dilution corrected with CO	East Asia	January 14–March 4	2020	NR-PM_1	—	(Xu et al., 2020a)
Tracer–tracer ratios	East Asia	January 1–March 31	2012–2019	$PM_{2.5}$	—	(Sun et al., 2020)
Benchmarking	North America	March 14–April 30	2019–2020	CO, NO_2, and $PM_{2.5}$	T and precip.	(Tanzer-Gruener et al., 2020)
Deseasonalize	North America	January 1–April 27	2015–2020	$PM_{2.5}$, NO_2, NO_x, and O_3	—	(Adams, 2020)
Deseasonalize	East Asia	January 1–May 31	2005–2020	NO_2 and AOD	—	(Diamond and Wood, 2020)
Deseasonalize	South Asia and East Asia	January 1–April 30	2016–2019	NO_2, SO_2, and CO	—	(Metya et al., 2020)
Dispersion indices	East Asia	January 26–February 25	2013–2020	$PM_{.2.5}$, PM_{10}, SO_2, CO, NO_2, and O_3	WS, wind shear, potential T, and RH	(Wang and Zhang, 2020)
Back-trajectory	East Asia	January 1–February 26	2019–2020	$PM_{2.5}$	HYSPLIT	(Chang et al., 2020)
Back-trajectory and PMF	East Asia	January 12–April 2	2020	$PM_{2.5}$	GDAS	(Cui et al., 2020)
Back-trajectory	South America	March 1–April 16	2020	CO, NO_2, O_3, VOC, and PM_{10}	HYSPLIT	(Siciliano et al., 2020b)
Back-trajectory and cluster analysis	East Asia	January 23–April 8	2020	$PM_{2.5}$, SO_2, NO_2, CO, and O_3	HYSPLIT	(Zhao et al., 2020a)
Back-trajectory analysis	East Asia	January 24–February 29	2000–2020	AOD	HYSPLIT	(Shen et al., 2021)
Machine learning and PMF	East Asia	January 23–February 22	2019	$PM_{2.5}$	T, P, WS, RH, PBLH, and radiation	(Zheng et al., 2020)
Dispersion-normalized PMF	East Asia	January 1–February 15	2020	$PM_{2.5}$	T, WS, PBLH, and radiation	(Dai et al., 2020)
Cluster analysis	South Asia	March 25–May 15	2017–2020	CO, NO_2, SO_2, O_3, PM_{10}, and $PM_{2.5}$	T	(Bera et al., 2020)
Multivariate regression	East Asia	January 23–March 21	2019–2020	SO_2, $PM_{2.5}$, PM_{10}, NO_2, and CO	WS, rain, and snow	(Bao and Zhang, 2020)
Multivariate regression	North America	March 25–May 4	2017–2020	$PM_{2.5}$, NO_2, and O_3	WS, T, and precip.	(Jia et al., 2020a)
Multivariate regression	Europe	January 1–March 27	2017–2020	NO_2 and PM_{10}	T, WS, and precip.	(Cameletti, 2020)

(continued)

TABLE 3. *(continued)*

Type	Region	Study Period	Baseline Year(s)	Species	Meteorological Variables	Reference
Multivariate regression	South America, North America, and Europe	March 1–March 31	2015–2020	$PM_{2.5}$, CO, NO_2, and O_3	T, RH, WS, and precip.	(Connerton et al., 2020)
Multivariate regression and machine learning	East Asia	February 5–February 20	2013–2018	$PM_{2.5}$ and O_3	Geopotential height, T, RH, dew point, stability, WS, and precip.	(Lei et al., 2020)
Multivariate regression	Global	January 1–May 15	2017–2020	NO_2, $PM_{2.5}$, and O_3	T, RH, precip., and WS	(Venter et al., 2020)
Multivariate regression	North America	February 17–May 31	2020	BC, $PM_{2.5}$, NO, NO_2, NO_x, CO, and UFP	T, RH, precip., WS, and WD	(Xiang et al., 2020)
Machine learning	Europe	January 1–April 23	2013–2020	NO_2	T2, WS, U10, V10, P, cloud cover, radiation, UV, and PBLH	(Petetin et al., 2020)
Machine learning	East Asia	January 1–April 26	2020	NO_2, $PM_{2.5}$, and O_3	WS, WD, T, RH, and P	(Wang et al., 2020e)
Machine learning	Europe	March 1–May 31	2015–2019	NO_2, O_3, PM_{10}, and $PM_{2.5}$	WS, WD, P, RH, T, and radiation	(Wyche et al., 2020)
Difference-in-difference method	Global	January 1–July 7	2020	NO_2, PM_{10}, SO_2, $PM_{2.5}$, CO, and O_3	T, WS, and RH	(Liu et al., 2021a)
Difference-in-difference method	South Asia	March 25–May 3	2019–2020	$PM_{2.5}$, PM_{10}, NO_2, CO, and SO_2	T, WS, and RH	(Navinya et al., 2020)
Difference-in-difference method	East Asia	January 1–March 1	2019–2020	Air quality index, $PM_{2.5}$, CO, NO_2, PM_{10}, SO_2, and O_3	T, precip., and snow	(He et al., 2020)
Generalized additive model	Europe	March 15–April 30	2015–2019	NO_2 and O_3	T2, U10, V10, Z500, specific humidity, radiation, and precip.	(Ordóñez et al., 2020)
Generalized additive model	Europe	March 10–June 30	2015–2019	NO, NO_2, NO_x, O_3, PM_{10}, and $PM_{2.5}$	WS, WD, and T	(Ropkins and Tate, 2020)

This includes the "corrected for meteorology/seasonality" category in **Figure 2.** PMF = positive matrix factorization; AOD = aerosol optical depth; BC = black carbon; VOC = volatile organic compound; NO_2 = nitrogen dioxide; SO_2 = sulfur dioxide; O_3 = ozone; PM = particulate matter; CO = carbon monoxide; NO_x = nitrogen oxide.

(PMF), a widely used receptor model to resolve pollution sources and quantify the source contributions. Studies using PMF focused on the $PM_{2.5}$ chemical composition, and the sources of organic particulate pollution, in Beijing (Cui et al., 2020), Wuhan (Zheng et al., 2020), and Tianjin (Dai et al., 2020), China. Conventional PMF analysis may suffer from information loss due to nonlinear dilution variations. Dai et al. (2020) incorporated the ventilation coefficient into their dispersion-normalized PMF, which reduced the dilution effect. The advantages of using PMF were highlighted in all studies, and their findings supported the substantial contribution of secondary sources, as well as the influence of local primary sources, to PM pollution. Finally, a hierarchical cluster analysis and principal component analysis were used in one study in India to investigate the impact of changing temperatures on pollutant concentrations (Bera et al., 2020). However, although these approaches will more reliably quantify observed changes in the atmospheric abundance of pollutants as a response to emission changes, the effects of meteorology and atmospheric chemistry are not always fully disentangled.

2.3.2.2. Statistical tools to account for the influence of meteorology and emission trends

Several approaches were used to reduce the effects of meteorology on the interpretation of air quality. One approach is to examine tracer-tracer ratios (Homan et al., 2010; Borbon et al., 2013), for example, normalizing pollutants relative to a relatively long-lived species like CO. These ratios provide a simple way to account for dilution and are typically used to isolate the effects of secondary chemistry. A confounding factor is that many of the commonly used tracers in the denominator (e.g., CO) also changed significantly due to emission reductions related to COVID-19. Other studies performed dilution corrections by normalizing to meteorological variables such as planetary boundary layer height (Su et al., 2020) or satellite column data with solar zenith angle, wind speed, and wind direction (Goldberg et al., 2020). Another approach is to benchmark periods of similar meteorology in past years with meteorology experienced during lockdown periods (Tanzer-Gruener et al., 2020). Methods to deseasonalize lockdown periods with prelockdown periods or past years were also employed (Adams, 2020; Diamond and Wood, 2020; Metya et al., 2020). Finally, other approaches identified metrics to assess synoptic meteorological conditions conducive to air pollution episodes (Wang and Zhang, 2020) or performed back trajectory analysis, such as with the Hybrid Single-Particle Lagrangian Integrated Trajectory (HYSPLIT) model, to assess the origin of pollutants and long-range transport (Chang et al., 2020; Cui et al., 2020; Siciliano et al., 2020b; Zhao et al., 2020a; Shen et al., 2021).

A variety of more complex statistical approaches were also used to quantify the effects of meteorology, atmospheric chemistry, and emission trends. This included the following:

1. multivariate regression analysis methods, where two main data sets were used: the dependent/outcome variables describing the pollutant concentrations and the independent/exposure variables that adjusted for weather conditions (Bao and Zhang, 2020; Cameletti, 2020; Connerton et al., 2020; Jia et al., 2020a; Lei et al., 2020; Venter et al., 2020; Xiang et al., 2020);
2. machine-learning methods, where algorithms were trained on measurements of pollutants and meteorological parameters from previous years to predict the "business as usual" emission estimates for 2020 (Petetin et al., 2020; Wang et al., 2020e; Wyche et al., 2020; Zheng et al., 2020);
3. difference-in-difference methods, where the impact of lockdown measures on air quality were quantified through a fixed-effects ordinary least squares (OLS) approach with the key explanatory variable being the lockdown measures and weather variables used as vectors (Navinya et al., 2020; Liu et al., 2021a); and
4. generalized additive models that accounted for the additive effect of meteorology on the pollutant concentrations and their nonlinear relationships using the meteorological parameters as a model predictor input to derive the pollutant concentration (Ordóñez et al., 2020; Ropkins and Tate, 2020).

The majority of these studies included data sets from multiple years, thereby accounting not only for meteorological effects but also emission trends. Although each of these statistical tools has uncertainties associated with the representativeness of the input data sets, they constitute the best up-to-date published methods to quantify the effects of meteorology, and/or atmospheric chemistry, and/or long-range transport on pollutant concentrations.

2.3.3. Air quality modeling and emission inventories constrained by observed changes

Chemical transport modeling provides a means for disentangling the effects of changes in emissions, chemistry, and meteorology on observed changes in air quality due to changing emissions. **Table 4** provides a summary of air quality or climate modeling studies published in the literature assessing the impacts of COVID-19. Of the 16 modeling studies listed, 14 are regional modeling studies: 12 of East Asia, one of Europe, and one of Europe and East Asia and two are global climate modeling studies. These modeling studies focused on lockdown measures in China and Europe, and the time period of study is limited to the winter of 2020. Studies of North America, South America,

Table 4. Summary of modeling studies assessing COVID-19 and air quality or climate impacts. DOI: https://doi.org/10.1525/elementa.2021.00176.t4

Model	Type	Resolution	Baseline Inventory	Region	Emission Sectors Adjusted	Simulation Period	Lockdown Impact	Reference
WRF-CMAQ	Forward CTM	27 · 27 km, 9 · 9 km, and 3 · 3 km	MICS-Asia + TEDS	East Asia	50% reduction of all sectors	January 28, 2020–February 2, 2020	$PM_{2.5}$ ↓	(Griffith et al., 2020)
WRF-Chem	Forward CTM	60 · 60 km and 20 · 20 km	MEIC	East Asia	Adjust mobile, power, and industry	December 1, 2019–March 5, 2020	$PM_{2.5}$ ↑ and O_3 ↑	(Huang et al., 2020)
WRF-Chem	Forward CTM	12 · 12 km	INTEX-B	East Asia	80% reduction of NO_x	January 21, 2020–February 16, 2020	$PM_{2.5}$ ↑ and O_3 ↑	(Le et al., 2020a)
WRF-CAMx	Forward CTM	36 · 36 km, 12 · 12 km, and 4 · 4 km	MEIC + MIX	East Asia	Adjust mobile, industry, dust, solvent, cooking, residential, and biomass burning	January 1, 2020–March 31, 2020	$PM_{2.5}$ ↓, NO_2 ↓, SO_2 ↓, and O_3 ↑	(Li et al., 2020a)
GEOS-GMI	Forward CTM	0.25 · 0.25	RCP 6.0 + EDGAR	East Asia	Constant emissions (to assess meteorology)	January 1, 2020–February 29, 2020	NO_2 ↓	(Liu et al., 2020a)
WRF-CMAQ	Forward CTM	36 · 36 km	MEIC + MIX	East Asia	Adjust mobile, industry, and residential	January 1, 2020–February 12, 2020	$PM_{2.5}$ ↓	(Wang et al., 2020c)
WRF-GC	Top-down	27 · 27 km	MEIC	East Asia	Derive NO_x emissions from TROPOMI NO_2	January 1, 2020–March 12, 2020	NO_x ↓	(Zhang et al., 2020c)
WRF-CMAQ	Forward	36 · 36 km	AiMa	East Asia	Constant emissions (to assess meteorology)	January 8, 2020–February 6, 2020	NO_2 ↓, SO_2 ↓, CO ↓, $PM_{2.5}$ ↓, and O_3 ↑	(Zhao et al., 2020b)
WRF-CMAQ	Forward CTM	4 · 4 km	SAES	East Asia	Adjust mobile, power, and industry	December 29, 2019–February 29, 2020	$PM_{2.5}$ ↓ and O_3 ↑	(Liu et al., 2020b)
GEOS-Chem	Top-down	0.5 · 0.625	MIX + EDGAR	East Asia	Derive NO_x emissions from TROPOMI NO_2	January–March 2019 January–March 2020	NO_x ↓, $PM_{2.5}$ ↓, and O_3 ↑	(Zhang et al., 2021)
GEOS-Chem	Forward CTM	0.25 · 0.31	MEIC	East Asia	60% reduction of NO_x and 30% reduction of VOC	January 1, 2020–February 15, 2020	PAN ↑	(Qiu et al., 2020)
CHIMERE	Top-down	0.25 · 0.25	Satellite-derived	East Asia	DESCO Inverse Algorithm	January 24, 2020–March 20, 2020	NO_2 ↓	(Ding et al., 2020)
WRF-Chem	Gaussian	27 · 27 km	EDGAR	East Asia and Europe	Model 2016 to get spatial $PM_{2.5}$ gradient	2016	$PM_{2.5}$ ↓	(Giani et al., 2020)
WRF-CHIMERE	Forward CTM	60 · 60 km and 20 · 20 km	CAMS	Europe	Adjust mobile and industry	March 1, 2020–March 31, 2020	NO_2 ↓, O_3 ↑↓, and $PM_{2.5}$ ↓	(Menut et al., 2020)
CAM5	Climate	1.9 · 2.5	CMIP6 + MEIC	Global	Adjust mobile, power, and industry	2020	T ↑	(Yang et al., 2020)
FaIR	Climate	–	EDGAR	Global	Adjust mobile, industry, and buildings	2020	T ↓	(Forster et al., 2020)

This includes the "modeling" category in **Figure 2.** WRF-CMAQ = Weather Research Forecasting and Community Multiscale Air Quality; WRF-Chem = Weather Research Forecasting with Chemistry; WRF-CAMx = Weather Research Forecast with Comprehensive air quality model with extensions; GMI = Global Modeling Initiative; WRF-GC = Weather Research Forecast with GEOS-Chem; WRF-CHIMERE = Weather Research Forecast with CHIMERE chemistry-transport model; GEOS-Chem = Goddard Earth Observing System with Chemistry; CTM = chemical transport model; EDGAR = Emissions Database for Global Atmospheric Research; MEIC = Multi-resolution Emission Inventory for China; CAMS = Copernicus Atmosphere Monitoring Service; VOC = volatile organic compound; NO_2 = nitrogen dioxide; SO_2 = sulfur dioxide; O_3 = ozone; PM = particulate matter; CO = carbon monoxide; PAN = peroxyacetyl nitrate; NO_x = nitrogen oxide.

and Africa are notably missing, although it is anticipated that modeling studies will be published in the future for these regions.

Most of the modeling studies listed in **Table 4** used a traditional forward Eulerian CTM, such as the Weather Research Forecasting and Community Multiscale Air Quality (Wong et al., 2012), Weather Research Forecasting with Chemistry (Grell et al., 2005), or Goddard Earth Observing System with Chemistry (Henze et al., 2007) models. All of the studies simulate business-as-usual conditions with a baseline emissions inventory. A variety of baseline inventories were used (**Table 4**), the most common being the global Emissions Database for Global Atmospheric Research (EDGAR) inventory (Crippa et al., 2020) and the Multi-resolution Emission Inventory for China (He, 2012). Many of the modeling studies adjusted their input emission inventories by scaling all emission sectors relative to changes in ambient or satellite observations (Griffith et al., 2020; Le et al., 2020a; Qiu et al., 2020; Zhang et al., 2020c; Zhang et al., 2021). Others have taken a sector-by-sector approach to scaling emission inventories (Forster et al., 2020; Huang et al., 2020; Le Quéré et al., 2020; Li et al., 2020a; Liu et al., 2020b; Menut et al., 2020; Wang et al., 2020d; Yang et al., 2020). For example, Forster et al. (2020) scaled mobile source emissions based on mobility and traffic count data, Huang et al. (2020) scaled industrial emissions based on economic and industrial activity data, and Le Quéré et al. (2020) scaled power generation emissions using energy statistics. Forster et al. have made publicly available a lockdown-adjusted daily inventory based on EDGAR emissions of CO_2, CH_4, N_2O, SO_2, BC, OC, CO, NMVOC, NH_3, and NO_x for each country throughout the COVID-19 lockdown period.

In general, by modeling both baseline and COVID-19-perturbed emissions scenarios, the effects of meteorology can be isolated from those related to changes in emissions and can then be used to quantitatively assess the impacts of emission changes on the formation of secondary pollutants, such as O_3 and $PM_{2.5}$. Other studies have modeled constant or prepandemic emissions during the lockdown period to quantify the expected changes in atmospheric concentrations due to meteorology alone and thereby deduce the fraction of observed changes in air quality that are due to emission changes. Additionally, TROPOMI NO_2 vertical column densities were used to derive top-down scaling factors of NO_x emission inventories (Zhang et al., 2020c; Zhang et al., 2021), which were then used to assess impacts on O_3 and $PM_{2.5}$ formation (Zhang et al., 2021). Ding et al. (2020) use an inverse modeling algorithm to derive top-down NO_x emissions in China. Finally, climate models were used in some studies to assess COVID-19 perturbations in bottom-up emission inventories and their impacts on global radiative forcing (Forster et al., 2020; Yang et al., 2020). Although the number of modeling studies comprises <10% of the total number of studies analyzed here (**Figure 2**), they provide an explicit means by which to control the effects of meteorology on observed changes in primary and secondary pollutants.

3. Results and discussion

3.1. "Business as usual" emission inventory

Worldwide lockdown measures strongly impacted the transportation sector (Forster et al., 2020; Le Quéré et al., 2020). To assess the impact that the transportation sector typically has on pollutant emissions for each country, a "business as usual" emission scenario was investigated using the 2015 EDGAR v5 (Crippa et al., 2020), which is the most recent year for which data are publicly available. **Figure 3** shows a world map colored by the largest source of NO_x emissions for each country as well as characteristic examples of the contribution of different sectors to the NO_x, CO, and $PM_{2.5}$ emissions for various countries around the world. Emission sectors are separated into transportation, energy and manufacturing, industrial and other processes, building and miscellaneous, and agriculture by lumping IPCC emission categories (see Table S2). Following the IPCC guidelines, energy and manufacturing (IPCC 1.A.1, 1.A.2, 1.B.1, 1.B.2) is classified as fuel combustion activities associated with energy production and industry. All other industrial emissions are included under industrial and other processes. In the following, the contribution of the different sectors to NO_x, $PM_{2.5}$, and CO emissions is discussed and detailed differences for countries around the world are provided in Section S2. Pie charts in **Figure 3** are used to highlight differences in the contribution of the various pollutant sectors for countries representative of different regions of the world, with an emphasis on the countries listed in **Tables 5**–**10.** The category "building emissions" includes residential, commercial, and institutional combustion as well as other combustion sources, whereas "miscellaneous emissions" apply to all remaining emissions from fuel combustion that are not specified elsewhere. Note that agricultural and land-use change emissions, for example, of NO_x from soil are not included in the EDGAR emission inventory, which likely results in an underestimation of the agricultural NO_x emissions. Global annual NO_x emissions based on the 2015 EDGAR inventory were 40 Tg of nitrogen with agriculture accounting for less than 1%. However, global soil NO_x emissions are estimated to be around 5 Tg/year (Yan et al., 2005).

The global EDGAR inventory provides context for expected changes in air pollutant species due to the COVID-19 pandemic, especially those related to the transportation, energy, manufacturing, and industrial sectors. Globally, the median transportation contribution was 36% (15%–51%), 8% (3%–19%), and 30% (5%–70%) for the NO_x, primary $PM_{2.5}$, and CO emissions, respectively.

Countries were further divided into developed (Annex I) and developing (Annex II) categories based on the United Nations (2020) Climate Change framework to examine the contribution differences of the various emission sectors. The median transportation contribution for Annex I countries was 44% (36%–56%), 14% (8%–19%), and 25% (17%–44%) for the NO_x, primary $PM_{2.5}$, and CO emissions, respectively, whereas for Annex II countries, it was 29% (5%–49%), 9% (2%–42%), and 35% (1%–75%). Although the contribution of transportation emissions varied for the above pollutants, it is evident that

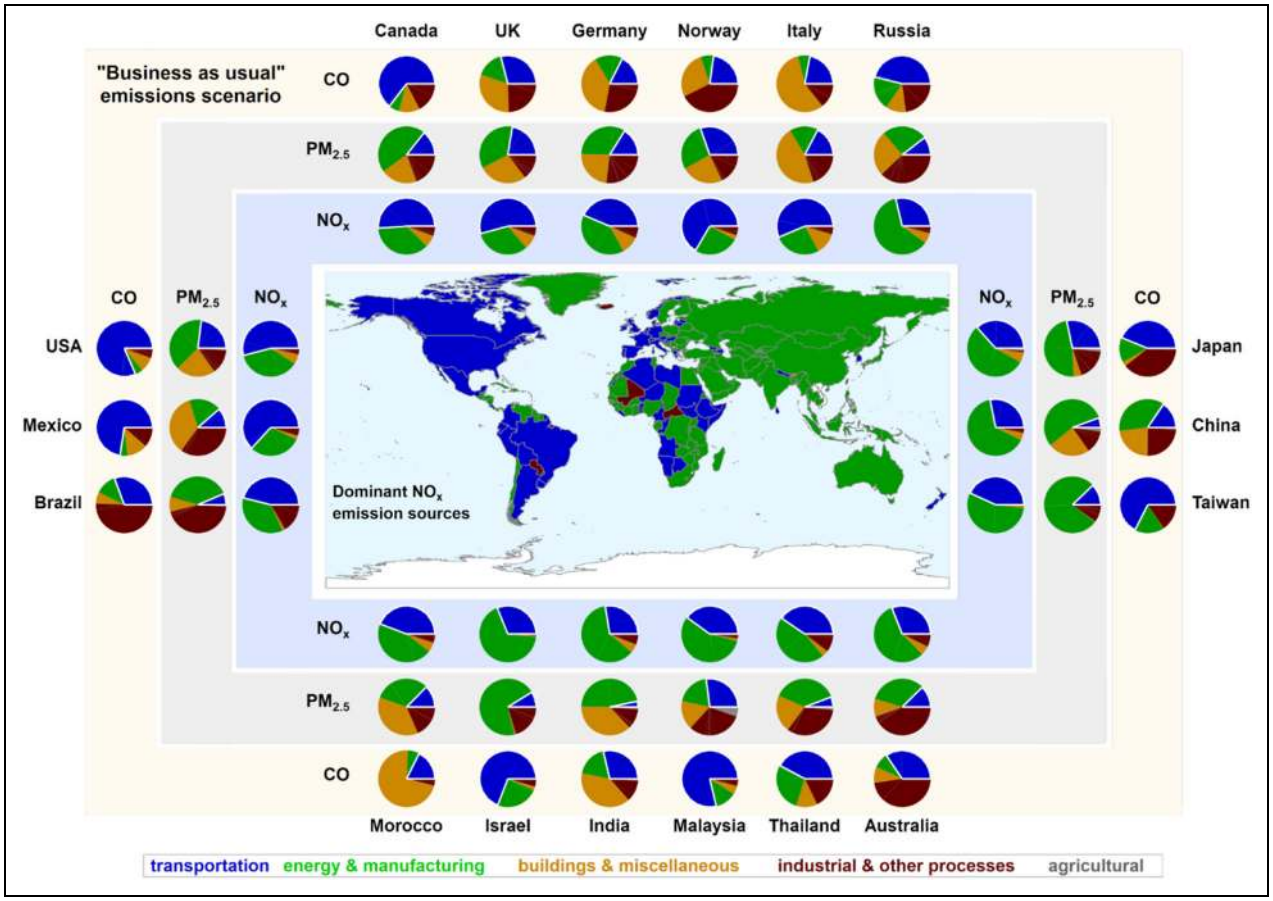

Figure 3. Distribution of emissions among different sectors (pie charts) based on the "business as usual" scenario using the 2015 Emissions Database for Global Atmospheric Research (EDGAR v5) for nitrogen oxide (NO_x), primary $PM_{2.5}$, and CO. Countries in the world map are colored by the dominant source of NO_x emissions for each country. DOI: https://doi.org/10.1525/elementa.2021.00176.f3

Table 5. Nitrogen dioxide (NO_2) publications for the percentage change analysis and the absolute concentration change analysis. DOI: https://doi.org/10.1525/elementa.2021.00176.t5

NO_2	Country	Publications
East Asia	China	(Agarwal et al., 2020), (Bao and Zhang, 2020),[a] (Bauwens et al., 2020), (Chen et al., 2020c), (Diamond and Wood, 2020), (Forster et al., 2020), (Gautam, 2020a), (Griffith et al., 2020), (X Huang et al., 2020), (Le et al., 2020a),[a] (Lian et al., 2020)[a], (Liu et al., 2020a), (Ma and Kang, 2020),[a] (Metya et al., 2020), (Nichol et al., 2020),[a] (Pei et al., 2020),[a] (Shakoor et al., 2020),[a] (Shi and Brasseur, 2020),[a] (Silver et al., 2020), (Venter et al., 2020), (Wang et al., 2020b),[a] (Xu et al., 2020c),[a] (Zhang et al., 2020a),[a] (Zhang et al., 2020c), (Zhao et al., 2020b),[a] (Zheng et al., 2020), (Wang et al., 2020e),[a] (Fu et al., 2020), (Wang et al., 2020f),[a] (Wang et al., 2020a),[a] (Ding et al., 2020), (Chen et al., 2020d),[a] (Ghahremanloo et al., 2020), (Zhang et al., 2020d), (Fan et al., 2020),[a] (Wan et al., 2020),[a] (Xu et al., 2020c),[a] (Yuan et al., 2021),[a] (Zhang et al., 2021), (Liu et al., 2020b), (Liu et al., 2020c), (Wang et al., 2021),[a] (Su et al., 2020), (Miyazaki et al., 2020), (Huang and Sun, 2020), (Wang and Zhang, 2020), (Xu et al., 2020b),[a] (Park et al., 2020)
	Japan	(Ghahremanloo et al., 2020), (Ma and Kang, 2020),[a] (Fu et al., 2020)
	South Korea	(Fu et al., 2020), (Han et al., 2020),[a] (Ju et al., 2020),[a] (Bauwens et al., 2020), (Ma and Kang, 2020),[a] (Ghahremanloo et al., 2020)
	Taiwan	(Forster et al., 2020)

(continued)

TABLE 5. *(continued)*

NO_2	Country	Publications
South Asia	India	(Agarwal et al., 2020), (Bera et al., 2020),[a] (Dhaka et al., 2020), (Forster et al., 2020), (Gautam, 2020a), (Jain and Sharma, 2020),[a] (Kumari and Toshniwal, 2020),[a] (Mahato et al., 2020),[a] (Metya et al., 2020), (Navinya et al., 2020), (Resmi et al., 2020),[a] (Selvam et al., 2020),[a] (Sharma et al., 2020b),[a] (Siddiqui et al., 2020), (Venter et al., 2020), (Fu et al., 2020), (Gautam et al., 2020),[a] (Biswal et al., 2020), (Mahato and Ghosh, 2020),[a] (Kant et al., 2020), (Zhang et al., 2020d), (Sharma et al., 2020a),[a] (Harshita and Vivek, 2020), (Singh et al., 2020),[a] (Kumari et al., 2020),[a] (Bedi et al., 2020),[a] (Beig et al., 2020),[a] (Naqvi et al., 2020), (Vadrevu et al., 2020)
	Nepal	(Venter et al., 2020)
	Bangladesh	(Masum and Pal, 2020)[a]
Southeast Asia	Malaysia	(Kanniah et al., 2020),[a] (Suhaimi et al., 2020), (Ash'aari et al., 2020)[a]
	Thailand	(Venter et al., 2020), (Stratoulias and Nuthammachot, 2020)[a]
	Singapore	(Jiayu and Federico, 2020)[a]
Central Asia	Kazakhstan	(Kerimray et al., 2020)[a]
West Asia	Turkey	(Fu et al., 2020), (Şahin, 2020)[a]
	Iran	(Bauwens et al., 2020), (Broomandi et al., 2020)[a]
	Iraq	(Hashim et al., 2020)[a]
	Saudi Arabia	(Anil and Alagha, 2020)[a]
North America	United States	(Bauwens et al., 2020), (Berman and Ebisu, 2020),[a] (Connerton et al., 2020),[a] (Forster et al., 2020), (Goldberg et al., 2020), (Jia et al., 2020a),[a] (Shakoor et al., 2020),[a] (Tanzer-Gruener et al., 2020),[a] (Venter et al., 2020), (Zangari et al., 2020),[a] (Fu et al., 2020), (Chen et al., 2020b), (Zhang et al., 2020d), (Hudda et al., 2020),[a] (Xiang et al., 2020), (Liu et al., 2021b), (Naeger and Murphy, 2020)
	Canada	(Adams, 2020),[a] (Forster et al., 2020), (Venter et al., 2020)
	Mexico	(Venter et al., 2020), (Fu et al., 2020)
South America	Brazil	(Connerton et al., 2020),[a] (Dantas et al., 2020),[a] (Nakada and Urban, 2020),[a] (Siciliano et al., 2020a),[a] (Fu et al., 2020), (Krecl et al., 2020), (Siciliano et al., 2020b)
	Ecuador	(Forster et al., 2020), (Zalakeviciute et al., 2020),[a] (Zambrano-Monserrate and Ruano, 2020),[a] (Parra and Espinoza, 2020),[a] (Pacheco et al., 2020)
	Chile	(Forster et al., 2020), (Venter et al., 2020)
	Peru	(Venter et al., 2020), (Fu et al., 2020)
	Colombia	(Mendez-Espinosa et al., 2020),[a] (Forster et al., 2020)
Europe	Multiple countries	(Baldasano, 2020),[a] (Bauwens et al., 2020), (Cameletti, 2020),[a] (Collivignarelli et al., 2020),[a] (Connerton et al., 2020),[a] (Forster et al., 2020), (Gautam, 2020a), (Menut et al., 2020), (Sicard et al., 2020),[a] (Tobías et al., 2020),[a] (Venter et al., 2020), (Higham et al., 2020),[a] (Fu et al., 2020), (Petetin et al., 2020), (Martorell-Marugán et al., 2021),[a] (Filippini et al., 2020), (Zhang et al., 2020d), (Gualtieri et al., 2020),[a] (Ordóñez et al., 2020), (Ropkins and Tate, 2020), (Wyche et al., 2020), (Ljubenkov et al., 2020), (Jakovljević et al., 2020)[a]
Oceania	Australia	(Forster et al., 2020), (Venter et al., 2020), (Fu et al., 2020)
	New Zealand	(Patel et al., 2020)[a]
Africa	Morocco	(Otmani et al., 2020),[a] (Ass et al., 2020)[a]

[a]Publications that include absolute concentrations and relative changes.

transportation reduction measures during lockdowns are expected to consistently have a greater impact on CO and NO_x emissions than for primary $PM_{2.5}$ worldwide.

3.2. Worldwide lockdown measures

Next, we discuss the impact of policy actions designed to mitigate the COVID-19 pandemic and relate the stringency of lockdown measures with observed changes in the atmosphere. The onset and temporal evolution of SARS-CoV-2 infection rates have varied globally, as have the respective lockdown periods, resulting in emission reductions that are distributed over time and space. Although the onset of lockdown measures is well-defined on national or state levels, the transition to the

Table 6. $PM_{2.5}$ publications for the percentage change analysis and the absolute concentration change analysis. DOI: https://doi.org/10.1525/elementa.2021.00176.t6

$PM_{2.5}$	Country	Publications
East Asia	China	(Agarwal et al., 2020), (Bao and Zhang, 2020),[a] (Chauhan and Singh, 2020),[a] (Chen et al., 2020c),[a] (Huang et al., 2020), (Le et al., 2020a),[a] (Li et al., 2020a), (Li et al., 2020b),[a] (Lian et al., 2020),[a] (Ma and Kang, 2020),[a] (Nichol et al., 2020),[a] (Rodríguez-Urrego and Rodríguez-Urrego, 2020),[a] (Shakoor et al., 2020),[a] (Shi and Brasseur, 2020),[a] (Silver et al., 2020), (Venter et al., 2020), (Wang et al., 2020b),[a] (Wang et al., 2020c), (Xu et al., 2020c),[a] (Zhang et al., 2020a),[a] (Zhao et al., 2020b),[a] (Zheng et al., 2020),[a] (Wang et al., 2020e),[a] (Fu et al., 2020), (Wang et al., 2020f),[a] (Wang et al., 2020a),[a] (Chen et al., 2020a),[a] (Chen et al., 2020d),[a] (Zhang et al., 2020d), (Wan et al., 2020),[a] (Lei et al., 2020),[a] (Xu et al., 2020c),[a] (Giani et al., 2020), (Yuan et al., 2021),[a] (Zhang et al., 2021), (Liu et al., 2020b),[a] (Liu et al., 2020c),[a] (Su et al., 2020), (Xu et al., 2020a),[a] (Jia et al., 2020b)
	Japan	(Ma and Kang, 2020),[a] (Fu et al., 2020), (Rodríguez-Urrego and Rodríguez-Urrego, 2020),[a] (Wang and Zhang, 2020), (Xu et al., 2020b)[a]
	South Korea	(Ma and Kang, 2020),[a] (Fu et al., 2020), (Han et al., 2020),[a] (Ju et al., 2020)[a]
	Nepal, Mongolia	(Rodríguez-Urrego and Rodríguez-Urrego, 2020)[a]
	Taiwan	(Griffith et al., 2020)
South Asia	India	(Agarwal et al., 2020), (Bera et al., 2020),[a] (Chauhan and Singh, 2020),[a] (Jain and Sharma, 2020),[a] (Kumari and Toshniwal, 2020),[a] (Mahato et al., 2020),[a] (Navinya et al., 2020), (Resmi et al., 2020),[a] (Selvam et al., 2020),[a] (Sharma et al., 2020b),[a] (Singh and Chauhan, 2020), (Venter et al., 2020), (Fu et al., 2020), (Gautam et al., 2020),[a] (Mahato and Ghosh, 2020),[a] (Kant et al., 2020), (Zhang et al., 2020d), (Sharma et al., 2020a),[a] (Harshita and Vivek, 2020), (Singh et al., 2020),[a] (Kumari et al., 2020),[a] (Bedi et al., 2020),[a] (Rodríguez-Urrego and Rodríguez-Urrego, 2020),[a] (Beig et al., 2020)[a]
	Sri Lanka	(Rodríguez-Urrego and Rodríguez-Urrego, 2020)[a]
	Nepal	(Venter et al., 2020)
	Bangladesh	(Masum and Pal, 2020),[a] (Rodríguez-Urrego and Rodríguez-Urrego, 2020)[a]
Southeast Asia	Malaysia	(Abdullah et al., 2020),[a] (Kanniah et al., 2020),[a] (Mohd Nadzir et al., 2020),[a] (Suhaimi et al., 2020),[a] (Mohd Nadzir et al., 2020),[a] (Ash'aari et al., 2020)[a]
	Vietnam	(Rodríguez-Urrego and Rodríguez-Urrego, 2020)[a]
	Indonesia	(Rodríguez-Urrego and Rodríguez-Urrego, 2020),[a] (Venter et al., 2020)
	Thailand	(Rodríguez-Urrego and Rodríguez-Urrego, 2020),[a] (Stratoulias and Nuthammachot, 2020)[a]
	Singapore	(Rodríguez-Urrego and Rodríguez-Urrego, 2020),[a] (Jiayu and Federico, 2020)[a]
Central Asia	Kazakhstan	(Kerimray et al., 2020),[a] (Rodríguez-Urrego and Rodríguez-Urrego, 2020)[a]
	Uzbekistan	(Rodríguez-Urrego and Rodríguez-Urrego, 2020)[a]
	Afghanistan	(Rodríguez-Urrego and Rodríguez-Urrego, 2020)[a]
West Asia	Turkey	(Fu et al., 2020), (Aydın et al., 2020), (Şahin, 2020),[a] (Rodríguez-Urrego and Rodríguez-Urrego, 2020)[a]
	Iran	(Broomandi et al., 2020),[a] (Faridi et al., 2020),[a] (Rodríguez-Urrego and Rodríguez-Urrego, 2020)[a]
	Iraq	(Hashim et al., 2020)[a]
	United Arab Emirates	(Venter et al., 2020)
	Israel, and Kuwait	(Rodríguez-Urrego and Rodríguez-Urrego, 2020)[a]
North America	United States	(Berman and Ebisu, 2020),[a] (Bekbulat et al., 2021),[a] (Chauhan and Singh, 2020),[a] (Connerton et al., 2020),[a] (Jia et al., 2020a),[a] (Shakoor et al., 2020),[a] (Tanzer-Gruener et al., 2020),[a] (Venter et al., 2020), (Zangari et al., 2020),[a] (Fu et al., 2020), (Chen et al., 2020b), (Zhang et al., 2020d), (Pan et al., 2020),[a] (Son et al., 2020),[a] (Hudda et al., 2020),[a] (Xiang et al., 2020), (Liu et al., 2021b)
	Canada	(Adams, 2020),[a] (Venter et al., 2020)
	Mexico	(Rodríguez-Urrego and Rodríguez-Urrego, 2020),[a] (Venter et al., 2020), (Fu et al., 2020)

(continued)

TABLE 6. *(continued)*

$PM_{2.5}$	Country	Publications
South America	Brazil	(Connerton et al., 2020),[a] (Nakada and Urban, 2020),[a] (Nakada and Urban, 2020),[a] (Fu et al., 2020)
	Ecuador	(Zalakeviciute et al., 2020),[a] (Zambrano-Monserrate and Ruano, 2020),[a] (Parra and Espinoza, 2020)[a]
	Chile	(Rodríguez-Urrego and Rodríguez-Urrego, 2020),[a] (Venter et al., 2020)
	Peru	(Rodríguez-Urrego and Rodríguez-Urrego, 2020),[a] (Venter et al., 2020), (Fu et al., 2020)
	Colombia	(Rodríguez-Urrego and Rodríguez-Urrego, 2020),[a] (Mendez-Espinosa et al., 2020)[a]
Europe	Multiple countries	(Cameletti, 2020), (Chauhan and Singh, 2020),[a] (Collivignarelli et al., 2020),[a] (Connerton et al., 2020),[a] (Menut et al., 2020), (Rodríguez-Urrego and Rodríguez-Urrego, 2020),[a] (Sicard et al., 2020),[a] (Venter et al., 2020), (Zoran et al., 2020),[a] (Higham et al., 2020),[a] (Fu et al., 2020), (Martorell-Marugán et al., 2021),[a] (Zhang et al., 2020d), (Giani et al., 2020), (Gualtieri et al., 2020),[a] (Ropkins and Tate, 2020), (Wyche et al., 2020), (Ljubenkov et al., 2020)
Oceania	Australia	(Venter et al., 2020), (Fu et al., 2020)
	New Zealand	(Patel et al., 2020)[a]
Africa	Uganda	(Rodríguez-Urrego and Rodríguez-Urrego, 2020)[a]

PM = particulate matter.

[a]Publications that include absolute concentrations and relative changes.

Table 7. Ozone (O_3) publications for the percentage change analysis and the absolute concentration change analysis. DOI: https://doi.org/10.1525/elementa.2021.00176.t7

O_3	Country	Publications
East Asia	China	(Chen et al., 2020c), (Huang et al., 2020), (Le et al., 2020a),[a] (Li et al., 2020b),[a] (Lian et al., 2020),[a] (Shi and Brasseur, 2020), (Silver et al., 2020), (Venter et al., 2020), (Wang et al., 2020b),[a] (Xu et al., 2020c), (Zhang et al., 2020a),[a] (Zhao et al., 2020b),[a] (Wang et al., 2020e),[a] (Fu et al., 2020), (Wang et al., 2020f),[a] (Wang et al., 2020a),[a] (Zhang et al., 2020d), (Wan et al., 2020),[a] (Lei et al., 2020),[a] (Xu et al., 2020c),[a] (Yuan et al., 2021),[a] (Zhang et al., 2021), (Liu et al., 2020b),[a] (Liu et al., 2020c),[a] (Wang and Zhang, 2020), (Xu et al., 2020b)[a]
	Japan	(Fu et al., 2020)
	South Korea	(Han et al., 2020),[a] (Ju et al., 2020),[a] (Fu et al., 2020)
South Asia	India	(Bera et al., 2020),[a] (Jain and Sharma, 2020),[a] (Mahato et al., 2020),[a] (Resmi et al., 2020),[a] (Selvam et al., 2020),[a] (Sharma et al., 2020b),[a] (Venter et al., 2020), (Fu et al., 2020), (Gautam et al., 2020),[a] (Chatterjee et al., 2020),[a] (Mahato and Ghosh, 2020),[a] (Zhang et al., 2020d), (Panda et al., 2020),[a] (Sharma et al., 2020a),[a] (Harshita and Vivek, 2020), (Singh et al., 2020),[a] (Kumari et al., 2020),[a] (Bedi et al., 2020),[a] (Beig et al., 2020),[a] (Naqvi et al., 2020)
	Nepal	(Venter et al., 2020)
Southeast Asia	Thailand	(Venter et al., 2020), (Stratoulias and Nuthammachot, 2020)[a]
	Singapore	(Jiayu and Federico, 2020)[a]
Central Asia	Kazakhstan	(Kerimray et al., 2020)[a]
West Asia	Turkey	(Fu et al., 2020), (Aydın et al., 2020)
	Iran	(Broomandi et al., 2020)[a]
	Iraq	(Hashim et al., 2020)[a]
	United Arab Emirates	(Venter et al., 2020)
	Saudi Arabia	(Anil and Alagha, 2020)[a]
North America	United States	(Bekbulat et al., 2021),[a] (Jia et al., 2020a),[a] (Venter et al., 2020), (Fu et al., 2020), (Chen et al., 2020b), (Zhang et al., 2020d), (Pan et al., 2020),[a] (Liu et al., 2021b)

(continued)

TABLE 7. *(continued)*

O_3	Country	Publications
	Canada	(Adams, 2020),[a] (Venter et al., 2020)
	Mexico	(Venter et al., 2020), (Fu et al., 2020)
South America	Brazil	(Dantas et al., 2020),[a] (Fu et al., 2020), (Nakada and Urban, 2020),[a] (Siciliano et al., 2020b)
	Ecuador	(Zambrano-Monserrate and Ruano, 2020),[a] (Parra and Espinoza, 2020)[a]
	Chile	(Venter et al., 2020)
	Peru	(Venter et al., 2020), (Fu et al., 2020)
Europe	Multiple countries	(Collivignarelli et al., 2020),[a] (Menut et al., 2020), (Sicard et al., 2020),[a] (Tobías et al., 2020),[a] (Venter et al., 2020), (Higham et al., 2020),[a] (Fu et al., 2020), (Martorell-Marugán et al., 2021),[a] (Zhang et al., 2020d), (Gualtieri et al., 2020),[a] (Ordóñez et al., 2020), (Ropkins and Tate, 2020), (Wyche et al., 2020)
Oceania	Australia	(Venter et al., 2020), (Fu et al., 2020)
	New Zealand	(Patel et al., 2020)[a]
Africa	Morocco	(Ass et al., 2020)[a]

[a]Publications that include absolute concentrations and relative changes.

Table 8. Carbon monoxide (CO) publications for the percentage change analysis and the absolute concentration change analysis. DOI: https://doi.org/10.1525/elementa.2021.00176.t8

CO	Country	Publications
East Asia	China	(Bao and Zhang, 2020),[a] (Chen et al., 2020c), (Lian et al., 2020), (Metya et al., 2020), (Shakoor et al., 2020), (Silver et al., 2020), (Wang et al., 2020b),[a] (Xu et al., 2020c),[a] (Zhang et al., 2020a),[a] (Zhao et al., 2020b),[a] (Wang et al., 2020e),[a] (Fu et al., 2020), (Wang et al., 2020f),[a] (Wang et al., 2020a),[a] (Chen et al., 2020a), (Chen et al., 2020d), (Ghahremanloo et al., 2020), (Zhang et al., 2020d), (Wan et al., 2020),[a] (Xu et al., 2020c),[a] (Yuan et al., 2021),[a] (Liu et al., 2020b), (Liu et al., 2020c), (Su et al., 2020), (Xu et al., 2020a), (Wang and Zhang, 2020), (Xu et al., 2020b),[a] (Park et al., 2020)
	Japan	(Fu et al., 2020), (Ghahremanloo et al., 2020)
	South Korea	(Han et al., 2020),[a] (Ju et al., 2020),[a] (Fu et al., 2020), (Ghahremanloo et al., 2020)
South Asia	India	(Bera et al., 2020),[a] (Jain and Sharma, 2020),[a] (Mahato et al., 2020),[a] (Navinya et al., 2020), (Resmi et al., 2020), (Selvam et al., 2020),[a] (Sharma et al., 2020b),[a] (Fu et al., 2020), (Gautam et al., 2020),[a] (Mahato and Ghosh, 2020),[a] (Zhang et al., 2020d), (Panda et al., 2020),[a] (Harshita and Vivek, 2020), (V Singh et al., 2020),[a] (Kumari et al., 2020),[a] (Bedi et al., 2020),[a] (Beig et al., 2020)[a]
Southeast Asia	Malaysia	(Kanniah et al., 2020),[a] (Mohd Nadzir et al., 2020),[a] (Suhaimi et al., 2020),[a] (Mohd Nadzir et al., 2020),[a] (Ash'aari et al., 2020)[a]
	Singapore	(Jiayu and Federico, 2020)[a]
Central Asia	Kazakhstan	(Kerimray et al., 2020)[a]
West Asia	Turkey	(Fu et al., 2020), (Şahin, 2020)[a]
	Iran	(Broomandi et al., 2020)[a]
	Saudi Arabia	(Anil and Alagha, 2020)
North America	United States	(Connerton et al., 2020),[a] (Shakoor et al., 2020), (Tanzer-Gruener et al., 2020),[a] (Fu et al., 2020), (Chen et al., 2020b), (Zhang et al., 2020d), (Xiang et al., 2020), (Liu et al., 2021b)
	Mexico	(Fu et al., 2020)
South America	Brazil	(Connerton et al., 2020),[a] (Dantas et al., 2020),[a] (Nakada and Urban, 2020),[a] (Siciliano et al., 2020a),[a] (Siciliano et al., 2020a),[a] (Fu et al., 2020), (Siciliano et al., 2020b)
	Ecuador	(Zalakeviciute et al., 2020),[a] (Parra and Espinoza, 2020)[a]
	Peru	(Fu et al., 2020)
Europe	Multiple countries	Italy: (Collivignarelli et al., 2020),[a] France: (Connerton et al., 2020),[a] Russia: (Fu et al., 2020), UK: (Fu et al., 2020), Spain: (Martorell-Marugán et al., 2021)[a]
Oceania	Australia	(Fu et al., 2020)
Africa	—	—

[a]Publications that include absolute concentrations and relative changes.

Table 9. PM_{10} publications for the percentage change analysis. DOI: https://doi.org/10.1525/elementa.2021.00176.t9

PM_{10}	Country	Publications
East Asia	China	(Bao and Zhang, 2020; Chen et al., 2020c; Chen et al., 2020d; Fu et al., 2020; Shakoor et al., 2020; Silver et al., 2020; Wan et al., 2020; Wang et al., 2020a; Wang et al., 2020b; Wang et al., 2020f; Xu et al., 2020a; Xu et al., 2020c; Zhang et al., 2020a; Zhao et al., 2020b; Zheng et al., 2020; Yuan et al., 2021), (Wang and Zhang, 2020), (Xu et al., 2020b)
	Japan	(Fu et al., 2020)
	South Korea	(Fu et al., 2020; Han et al., 2020; Ju et al., 2020)
South Asia	India	(Bedi et al., 2020; Bera et al., 2020; Fu et al., 2020; Gautam et al., 2020; Harshita and Vivek, 2020; Jain and Sharma, 2020; Kant et al., 2020; Kumari and Toshniwal, 2020; Kumari et al., 2020; Mahato and Ghosh, 2020; Mahato et al., 2020; Navinya et al., 2020; Resmi et al., 2020; Selvam et al., 2020; Sharma et al., 2020a; Sharma et al., 2020b; Singh et al., 2020)
	Bangladesh	(Masum and Pal, 2020)
Southeast Asia	Malaysia	(Kanniah et al., 2020; Mohd Nadzir et al., 2020)
	Thailand	(Stratoulias and Nuthammachot, 2020)
	Singapore	(Jiayu and Federico, 2020)
Central Asia	—	—
West Asia	Turkey	(Fu et al., 2020; Şahin, 2020)
	Iran	(Broomandi et al., 2020; Faridi et al., 2020; Hashim et al., 2020)
	Iraq	
	Saudi Arabia	(Anil and Alagha, 2020)
North America	United States	(Chen et al., 2020b; Fu et al., 2020; Shakoor et al., 2020; Liu et al., 2021b)
	Mexico	(Fu et al., 2020)
South America	Brazil	(Dantas et al., 2020; Fu et al., 2020; Nakada and Urban, 2020; Siciliano et al., 2020a), (Siciliano et al., 2020b)
	Peru	(Fu et al., 2020)
	Colombia	(Mendez-Espinosa et al., 2020)
Europe	Multiple countries	Italy: (Collivignarelli et al., 2020; Fu et al., 2020; Gualtieri et al., 2020; Sicard et al., 2020; Zoran et al., 2020), France: (Fu et al., 2020: Sicard et al., 2020, #5), Spain: (Fu et al., 2020; Tobías et al., 2020; Martorell-Marugán et al., 2021), United Kingdom: (Fu et al., 2020; Ropkins and Tate, 2020; Wyche et al., 2020), Germany, and Russia (Fu et al., 2020)
Oceania	Australia	(Fu et al., 2020)
	New Zealand	(Patel et al., 2020)
Africa	Morocco	(Otmani et al., 2020), (Ass et al., 2020)

PM = particulate matter.

"new normal" after the initial containment of the disease still implies ongoing changes to anthropogenic emission sectors such as transportation. Emissions thus dropped rapidly at the beginning of the lockdown, but the increases after the initial lockdown are often much slower, and emissions may not return to their prepandemic levels, for example, due to changes in corporate policies for telecommuting, reduced business travel, and so on.

To better compare observations from different regions worldwide and at different times and stages of the pandemic, the government SI (Cameron-Blake et al., 2020; Petherick et al., 2020) is used. This index varies from 0 to 100 and takes into account available information on ordinal indicators of government responses to limit the spread of COVID-19. The index is available on national scales at a 1-day time resolution. The index provides a comparative measure only and is not designed to evaluate the effectiveness of a country's response. Categories that are included in the index are (1) the implementation and extent of school closures, (2) implementation and extent of workplace closures, (3) restrictions on public events, (4) restrictions on gatherings, (5) closure of public transport, (6) method of public information campaigns, for example, public officials urging caution or coordinated campaigns across traditional and social media, (7) extent of measures to enforce the lockdown, (8) restrictions on internal movement, (9) restrictions on international travel, (10) COVID-19 testing policy, and (11) contact tracing. As such, the index includes both measures that impact emissions and measures with no obvious consequence for emissions.

Table 10. Sulfur dioxide (SO_2) and other pollutant publications for the percentage change analysis. DOI: https://doi.org/10.1525/elementa.2021.00176.t10

SO_2	Country	Publications
East Asia	China	(Chen et al., 2020a; Chen et al., 2020c; Chen et al., 2020d; Fan et al., 2020; Fu et al., 2020; Ghahremanloo et al., 2020; Li et al., 2020a; Li et al., 2020b; Lian et al., 2020; Liu et al., 2020b; Liu et al., 2020c; Su et al., 2020; Wan et al., 2020; Wang et al., 2020a; Wang et al., 2020b; Wang et al., 2020f; Xu et al., 2020a; Xu et al., 2020c; Zhang et al., 2020a; Zhang et al., 2020d; Zhao et al., 2020b; Zheng et al., 2020; Yuan et al., 2021), (Wang and Zhang, 2020), (Xu et al., 2020b)
	Japan	(Fu et al., 2020; Ghahremanloo et al., 2020)
	South Korea	(Fu et al., 2020; Ghahremanloo et al., 2020; Han et al., 2020; Ju et al., 2020)
South Asia	India	(Bedi et al., 2020; Bera et al., 2020; Fu et al., 2020; Gautam et al., 2020; Harshita and Vivek, 2020; Kumari and Toshniwal, 2020; Kumari et al., 2020; Mahato et al., 2020; Metya et al., 2020; Navinya et al., 2020; Resmi et al., 2020; Selvam et al., 2020; Sharma et al., 2020a; Sharma et al., 2020b; Singh et al., 2020; Zhang et al., 2020d)
Southeast Asia	Malaysia	(Ash'aari et al., 2020; Kanniah et al., 2020; Suhaimi et al., 2020)
	Singapore	(Jiayu and Federico, 2020)
Central Asia	Kazakhstan	
West Asia	Turkey	(Fu et al., 2020; Şahin, 2020)
	Saudi Arabia	(Anil and Alagha, 2020)
North America	United States	(Zhang et al., 2020d)
	Mexico	(Fu et al., 2020)
South America	Brazil	(Nakada and Urban, 2020), (Fu et al., 2020)
	Ecuador	(Zalakeviciute et al., 2020)
Europe	Multiple countries	Italy: (Collivignarelli et al., 2020), (Zhang et al., 2020d), United Kingdom: (Higham et al., 2020), (Fu et al., 2020; Zhang et al., 2020d), Russia: (Fu et al., 2020), Italy: (Fu et al., 2020), France: (Fu et al., 2020), (Zhang et al., 2020d), Spain: (Fu et al., 2020), (Martorell-Marugán et al., 2021), (Zhang et al., 2020d), and Germany: (Zhang et al., 2020d)
Oceania	—	—
Africa	Morocco	(Otmani et al., 2020)
Other pollutants		
NO_x	China: (Chen et al., 2020a; Chen et al., 2020d; Jia et al., 2020b; Li et al., 2020a; Li et al., 2020b; Liu et al., 2020c; Qiu et al., 2020; Yuan et al., 2021), India: (Chatterjee et al., 2020; Panda et al., 2020), Italy: (Collivignarelli et al., 2020), United Kingdom: (Ropkins and Tate, 2020), Canada: (Adams, 2020), United States: (Xiang et al., 2020), and Brazil: (Nakada and Urban, 2020; Siciliano et al., 2020b)	
AOD	India: (Gautam, 2020b; Mahato and Ghosh, 2020; Ranjan et al., 2020; Zhang et al., 2020d), China (Diamond and Wood, 2020; Ghahremanloo et al., 2020; Zhang et al., 2020d; Shen et al., 2021), South Korea, and Japan (Ghahremanloo et al., 2020), North America, and Europe (Zhang et al., 2020d)	
NMVOCs	China: (Ghahremanloo et al., 2020; Jia et al., 2020b; Li et al., 2020a; Qiu et al., 2020), South Korea: (Ghahremanloo et al., 2020), Japan: (Ghahremanloo et al., 2020; Zhang et al., 2020b), India: (Beig et al., 2020; Resmi et al., 2020), Kazakhstan (Kerimray et al., 2020), Italy (Collivignarelli et al., 2020), Brazil (Siciliano et al., 2020b)	
NH_3	India: (Bedi et al., 2020; Beig et al., 2020; Gautam et al., 2020; Mahato and Ghosh, 2020; Mahato et al., 2020)	
BC	India: (Panda et al., 2020), China: (Liu et al., 2020c; Wang et al., 2020a), Italy: (Collivignarelli et al., 2020), New Zealand: (Patel et al., 2020), United States: (Hudda et al., 2020; Xiang et al., 2020)	
AQI	Iraq: (Hashim et al., 2020), China: (Bao and Zhang, 2020; Chen et al., 2020c; He et al., 2020; Lian et al., 2020; Wan et al., 2020; Xu et al., 2020b; Xu et al., 2020c; Zhang et al., 2020a), India: (Gautam et al., 2020; Mahato and Ghosh, 2020; Mahato et al., 2020; Naqvi et al., 2020; Selvam et al., 2020; Sharma et al., 2020b; Siddiqui et al., 2020), Bangladesh: (Masum and Pal, 2020)	

AOD = aerosol optical depth; BC = black carbon; NMVOC = nonmethane volatile organic compound; NH_3 = ammonia; AQI = air quality index; NO_x = nitrogen oxide.

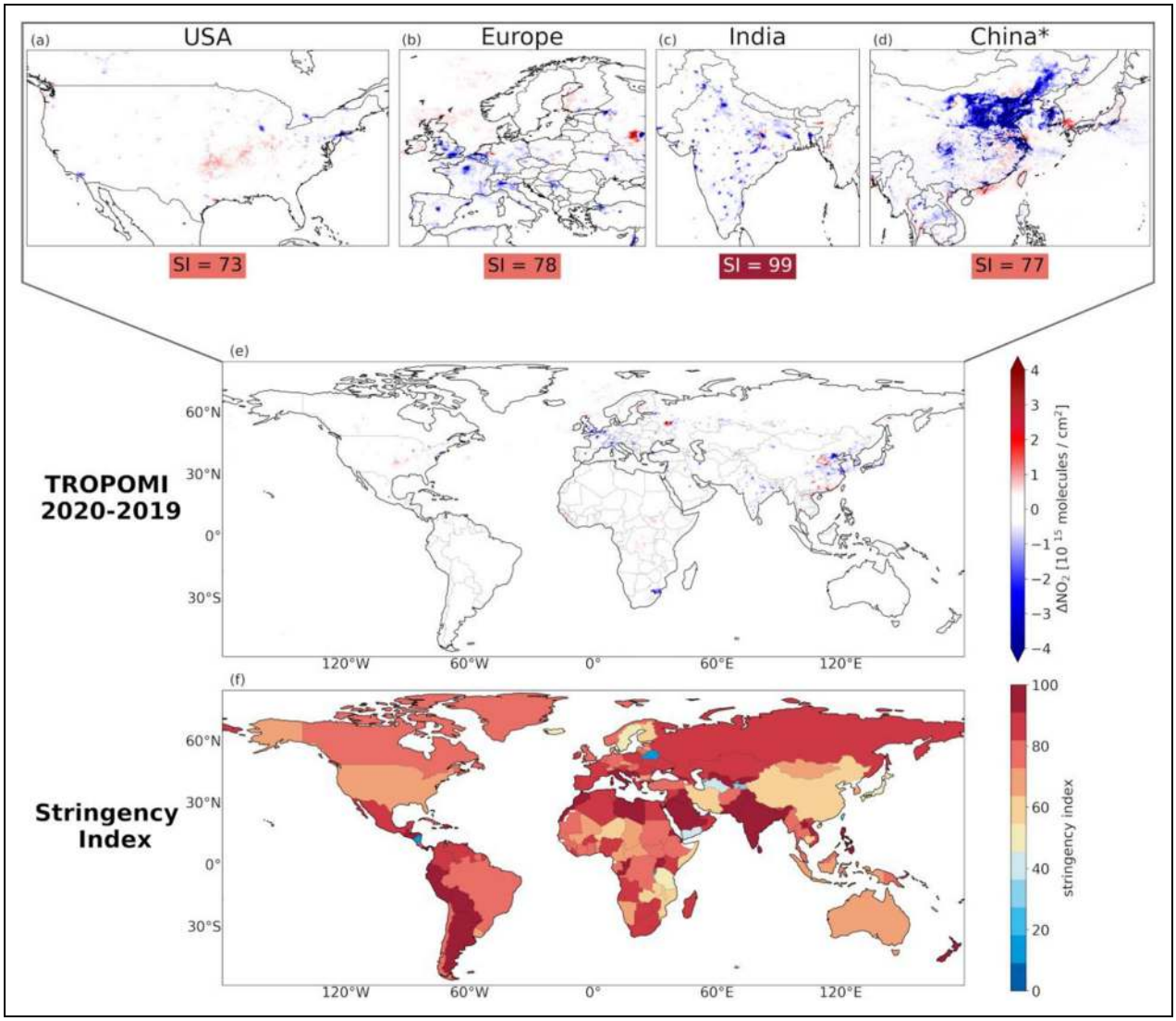

Figure 4. Meteorologically corrected TROPOMI NO_2 column difference between April 2020 and 2019 using the global Copernicus Atmosphere Monitoring Service-Integrated Forecasting System reanalysis in (a) the United States, (b) Europe, and (c) India at 0.1 × 0.1 resolution, as well as (d*) for the three post-Chinese New Year weeks in 2020 and 2019 in China at a 2 × 2 km resolution, (e) globally between April 2020 and 2019 at 0.4 × 0.4 resolution, and (f) the national stringency index as an indicator for the severity of lockdown averaged over April 2020. The corresponding stringency indices of the regions (a)–(d) are provided below the individual panels. DOI: https://doi.org/10.1525/elementa.2021.00176.f4

Here, we test the use of the government SI as an indicator for atmospheric composition change, with the data set (Cameron-Blake et al., 2020) as downloaded from the SI web page (Stringency Index, 2020). **Figure 4** shows the country-based SI averaged over April as a representative month for the most stringent conditions globally. China is an exception where lockdown measures were implemented in February–March and relaxed in April. Also shown is the April difference in NO_2 column concentrations based on TROPOMI measurements for 2020 compared to 2019. The high spatial resolution of TROPOMI is highlighted for the United States, Canada, Europe, India, and East Asia. Since China was the first country to undergo a lockdown at a time that coincided with the celebration of the Chinese New Year, the 3 post-Chinese New Year weeks in 2020 are compared to 2019 for the high spatial resolution map of China. Results in **Figure 4** are generated based on analysis performed as part of this work. The TROPOMI comparisons are only used qualitatively to show the effects of lockdowns in urban and industrialized environments around the world, and detailed analysis of emission reduction comparisons to stringency indices are the focus of future studies. The Copernicus Atmosphere Monitoring Service (CAMS) reanalysis results (Inness et al., 2019) were used to correct for variability of meteorology between the months of April 2019 and April 2020. The emissions used in the CAMS reanalysis were based on "business as usual" scenarios, unaffected by COVID-19 reductions. The CAMS 3-D NO_2 fields were interpolated to the location and time of all the individual TROPOMI observations used to construct the monthly mean. The averaging kernels were applied to obtain CAMS simulations of

the TROPOMI observations. These data were averaged over the month of April, and the ratio 2020/2019 was applied to the TROPOMI monthly mean to correct for the expected meteorological impact on NO_2 between the 2 years.

Overall, densely populated regions around the world experienced NO_2 reductions, suggesting that the lockdowns and their consequent reduction in transportation and industrial activities influenced global NO_2 emissions. Specifically, various megacities shown in **Figure 4** had detectable NO_2 reductions including New Delhi, India; Beijing, China; New York City and Los Angeles, United States; Paris, France; and Sao Paulo, Brazil. A notable example highlighting the effect of lockdowns on emission reductions is India, the country with the most severe restrictions during April (SI = 98.6), which experienced NO_2 column concentration reductions for urban, industrial, and even remote regions across the country. Less densely populated regions around the world had no change, or sporadic increases, in NO_2 column densities (up to 10^{15} molecules cm^{-2}). Although measurements at remote sites are reported in this review, they represent the minority of the collected literature values (fewer than 5% of the reviewed data sets) because most studies focused on measurements observed predominantly in urban environments where emissions reductions were more evident.

3.3. Relative pollutant changes in different regions and their correlations with the SI

Figure 5 shows the relative changes in pollutant concentrations during the lockdown compared to reference periods for different continents and regions of the world. Pollutants include NO_2, NO_x, and CO, which have the largest expected contribution from transportation (see Section 3.1); $PM_{2.5}$ and O_3, secondary pollutants and the two most important pollutants for health impacts (Anderson et al., 2004); SO_2, NH_3, and NMVOCs, which are mostly related to primary gas-phase emissions; and PM_{10}, AOD, BC, and the AQI. For each region, ground-based measurements, satellite measurements, or modeling studies were performed for multiple countries, and often multiple cities within each country, using the different approaches discussed in the Methods section to determine the lockdown effects on pollutant concentrations. All results from these studies are combined in **Figure 5** to determine the broader impacts of lockdown measures and establish the variability of changes in atmospheric composition. Numbers in parentheses show the number of publications and the number of data sets considered to produce the respective distributions. A higher spatial resolution analysis is presented in the following sections. An overview of the literature associated with the respective compounds and regions is provided in **Tables 5**–**10**, and relative changes on a national level are further discussed in the Supplement (Section S3). All data are downloadable from the database (see Section 2.1).

NO_2 decreased for all continents and regions during lockdowns. The median reductions ranged from 20% to 54% (see **Figure 5**), except for Africa, where a 70% reduction was found based on two studies in Morocco (see **Table 5**, Section S3.1). The median reduction in NO_x ranged from 26% to 67% (see Table 10 and Section S3.2). Note that the set of studies reporting NO_x is considerably smaller than the literature on NO_2. The median reduction in CO ranged from 16% to 49%. Within one region, India had the largest variability of reported CO changes, ranging from decreases of 80% to increases of 60% (see **Table 8** and Section S3.3). Median reductions in $PM_{2.5}$ and PM_{10} for all continents and regions ranged from 10% to 40% and 8% to 40%, respectively (see **Tables 6** and **9** and Sections S3.4 and S3.5). $PM_{2.5}$ measurements were widely used, whereas PM_{10} measurements were limited to fewer studies. The median change in O_3 ranged from a decrease of 15% to an increase of 18% (see **Table 7** and Section S3.6). O_3 was the only pollutant that increased on a regional scale during the lockdowns, with a positive median change of 6.4% ($\pm$11%). The response of O_3 is complex and varies by season and region, as described further in Section 3.3.5. The median reduction in SO_2 for all continents and regions ranged from 5% to 49% (see **Table 10**and Section S3.7). For other pollutants, including AOD, NMVOCs, NH_3, BC, and the AQI, a much smaller number of publications for only a few regions were reported (see **Table 10** and Section S3.8).

3.3.1. Importance of accounting for the effects of meteorology and emission trends

The literature summarized in this section lacks consistency in the analysis methodology or degree of meteorological normalization, which can confound the attribution of changes in ambient pollutant concentration changes to emissions reductions associated with COVID-19 lockdowns. Here, we compare reported changes, sorted by those that either do or do not correct for meteorology, to the SI in order to assess whether the changes in pollutant concentration correlate with metrics of lockdown intensity across a global scale. **Figure 6** shows box-and-whisker plots of NO_2, $PM_{2.5}$, and O_3 when combining data from all the countries around the globe and grouping them into different SI bins ranging from 20–40, 40–60, 60–80, and 80–100 (all bin ranges herein are defined as $\geq$ the lower number and < the higher number). Measurements were further separated into direct comparisons of lockdown to reference periods as discussed in Section 2.3.1 and comparisons that were quantified and corrected for meteorological effects (see Sections 2.3.2 and 2.3.3).

For studies that performed a direct comparison of lockdown to reference periods without a meteorological correction, no significant trend in the median with increasing SI was found for NO_2, $PM_{2.5}$, or O_3. Rather, the changes were similar across SI bins, with average pollutant changes ($\pm$standard deviation) of −36% ($\pm$5%), −20% ($\pm$7%), and +6% ($\pm$ 1), respectively (**Figure 6**). Conversely, the binned SI did correlate with the change in NO_2 and $PM_{2.5}$ for studies that accounted for the effects of meteorology. The median change in NO_2 decreased from −13% to −48% and in $PM_{2.5}$ decreased from −10% to −33%, whereas the median change in O_3 increased from 0% to 4% with increasing SI. Studies performed in the 40–100 SI range were statistically significant for all pollutants, and

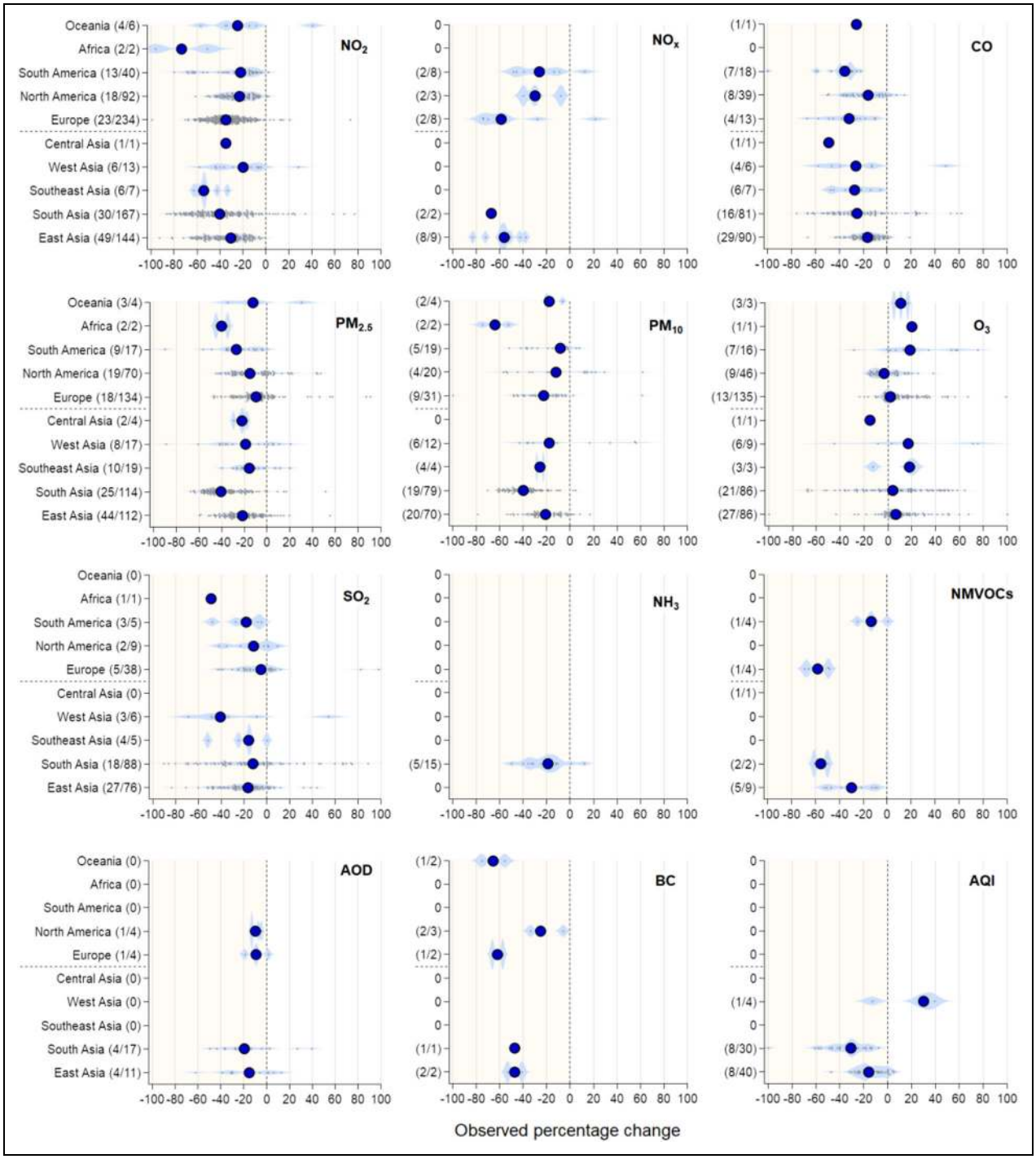

Figure 5. Distribution of the observed changes of pollutants as percentage difference during the lockdown for different regions of the world. Circle markers indicate the median values, and gray dots individual data sets averaged for periods ranging from days to several weeks. Numbers in parenthesis correspond to the number of publications and the number of measurements performed at each region/continent. DOI: https://doi.org/10.1525/elementa.2021.00176.f5

for both methods, with 19 or more data points per SI bin. Measurements were sparse for the 20–40 SI bin and statistically significant only for NO_2 (14). The same analysis was done for compounds less studied in the literature: CO, SO_2, and PM_{10} (Figure S2). The change of these three pollutants did not correlate with the SI when at least three bins were populated, although dependencies on SI may become apparent for CO, SO_2, and PM_{10} as more studies are published. Although there were only 44, 33, and 33 data sets in total that accounted for meteorology when reporting a change in concentration for CO, SO_2 and PM_{10}, respectively, stronger reductions were evident for all pollutants with increasing SI.

With the emissions of primary pollutants expected to decrease as the lockdown measures become stricter, these results highlight the importance of accounting and

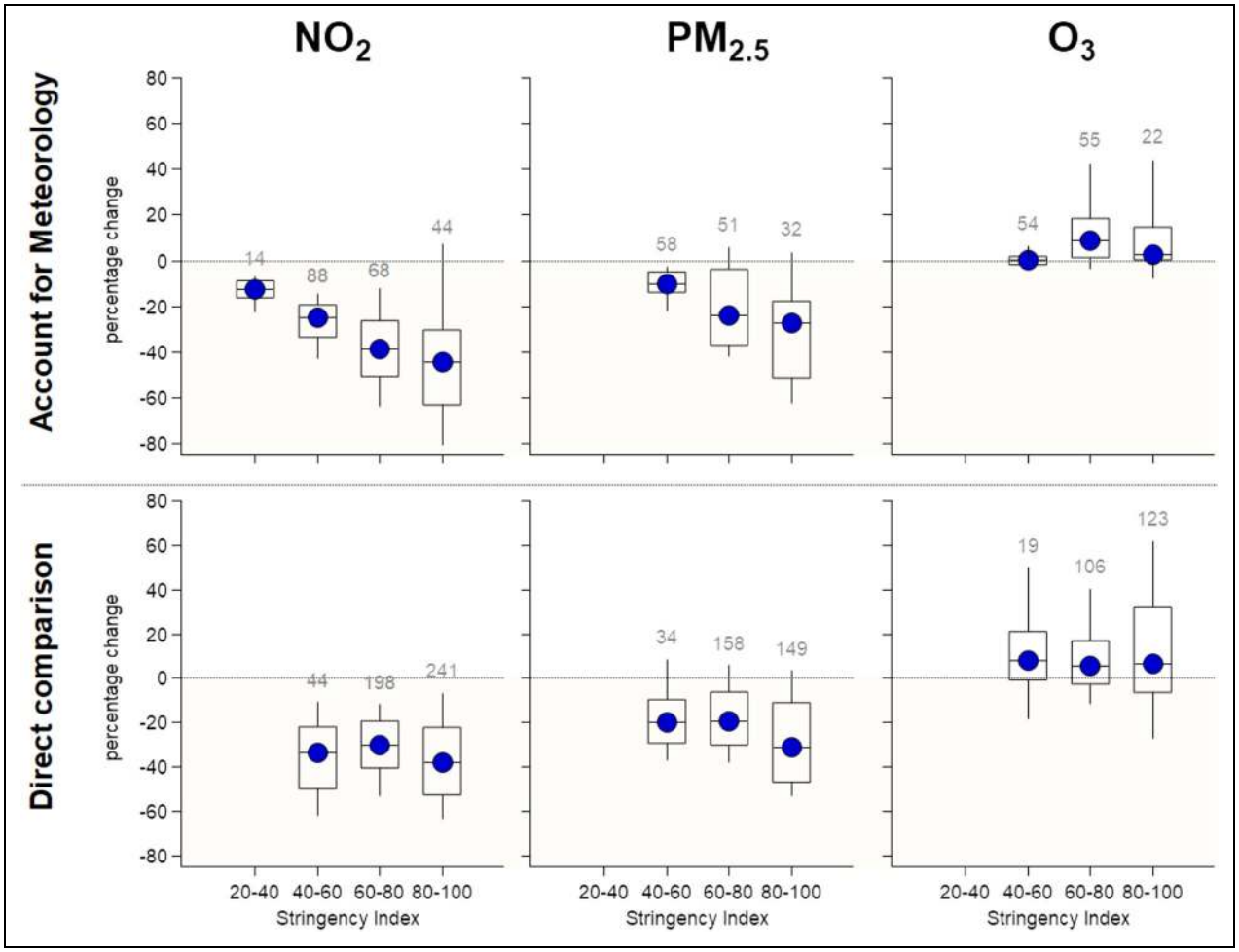

Figure 6. Pollutant changes during lockdowns are binned into intervals of the stringency index. Box and whiskers (10th, 25th, 50th, 75th, and 90th percentiles) are separated into studies that compared pollutant concentrations without accounting for meteorology in the bottom row and studies that accounted for the effects of meteorology in the top row. The number of studies per bin is provided above the whisker. DOI: https://doi.org/10.1525/elementa.2021.00176.f6

quantifying the effects of meteorology in order to quantitatively link changes in atmospheric abundance with changes in emissions. Although a direct comparison of reference to lockdown periods is valuable for identifying air-quality exceedances, its representativeness depends on the similarity of the meteorology during the reference period to the lockdown period. Furthermore, pollutants such as CO and NO_x arise from direct emissions, while $PM_{2.5}$ is often largely from secondary processes and O_3 has both local secondary production and destruction superimposed on a large background. Meteorology influences both the dilution and deposition of primary emissions, as well as the production and destruction of secondary species through the availability of oxidants and the rates of atmospheric chemical processes (see **Figure 1**). It should be stressed that data sets included in this work were from northern hemisphere springtime (Figure S1). Although an O_3 increase with other pollutant reductions was evident for this period, such increases can have different NO_x-VOC sensitivities than do summertime O_3 changes. Although an O_3 increase is evident in the existing literature, more analysis is required as more papers are published throughout the year to assess the effects of emission reductions on summer O_3 formation.

In the following, each pollutant will be further investigated on a per country basis using all available data sets including studies that do and do not correct for the effects of meteorology. Although this introduces higher uncertainties, it improves the global data coverage and provides better statistics for comparisons to emission inventories. The distribution of studies that makes direct comparisons and those that correct for meteorological effects will be discussed for each pollutant, and a comparison to emission inventories will be performed when available.

3.3.2. Observed changes in NO_2 compared with estimates based on the EDGAR emission inventory

Figure 7 shows the median decrease in NO_2 concentration (circles) during lockdowns for each country colored by the SI. Included in this calculation are studies using both the direct comparison approach (67%) and studies that correct for meteorological effects (33%). An overview of the measurements grouped by observation type as ground-based only (48%), satellite only (12%), or both

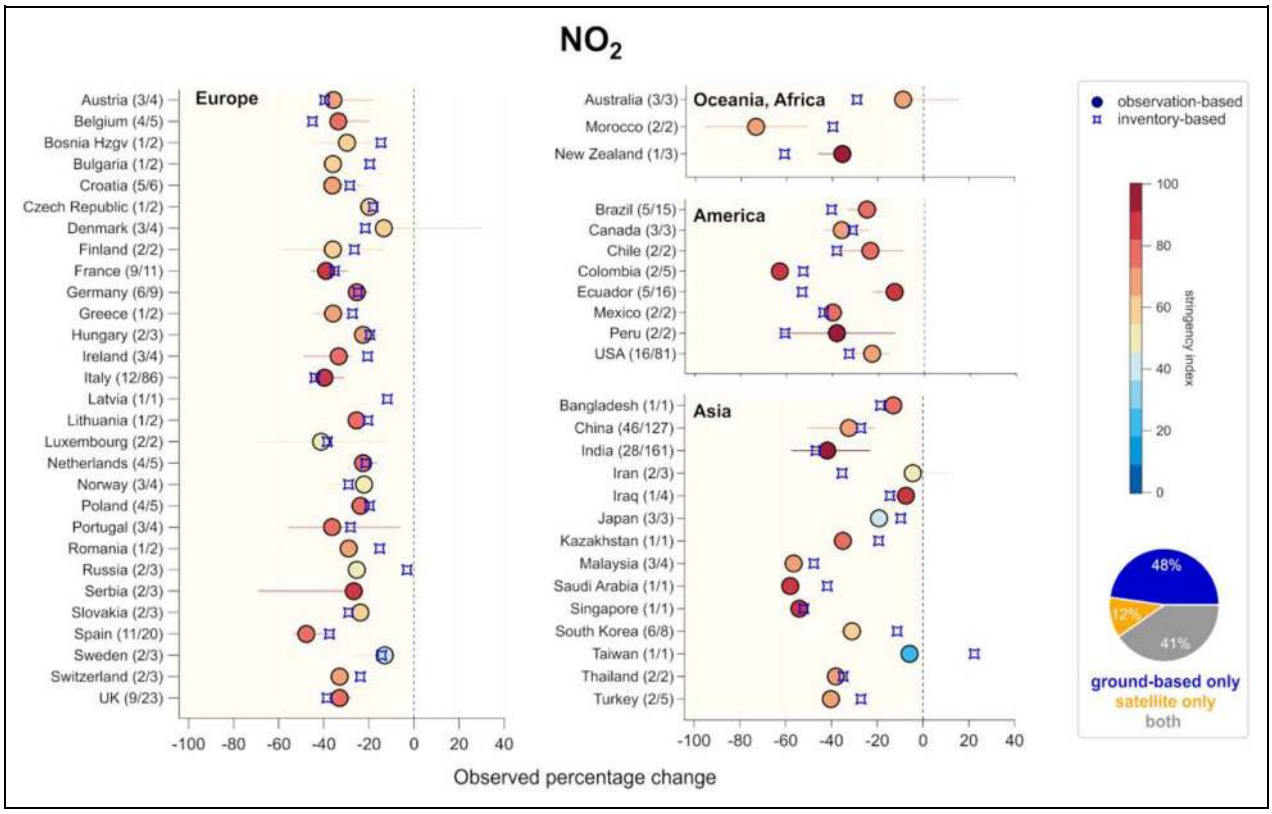

Figure 7. Observed median percentage decrease of NO_2 (circle markers) for each country. Error bars indicate the 25th and 75th percentiles of the distribution. The markers are colored by the median stringency index based on all measurements associated with each country. Numbers in parenthesis correspond to the number of publications and the number of data sets collected at each region/continent. Also shown as star squares is the Emissions Database for Global Atmospheric Research inventory NO_x emissions decrease calculated by Forster et al. (2020). The pie chart indicates the platforms used for the measurements. DOI: https://doi.org/10.1525/elementa.2021.00176.f7

(41%), is also provided. Also plotted is the adapted EDGAR inventory median decrease in emissions during lockdowns based on Forster et al. (2020; star squares). It should be noted here that Forster et al. (2020) implement the reductions in the emission inventory by scaling individual emission sectors. Studies mostly report data from lockdowns when stringency indices are greater than 50. Both observations and inventory-based reductions are reported as percentage difference.

Figure 8 plots the observed median decrease of NO_2 for each studied country against that country's inventory decrease (Forster et al., 2020). The observed decrease for each country is further binned by percentage decrease (<20%, 20%–30%, 30%–40%, 40%–50%, and >50%), and the median inventory decreases for each observation-based bin are calculated. The bin ranges were chosen arbitrarily to ensure more than five data points per bin. These binned data are then colored by the median SI. For most countries, the observations and emission inventory agree within a factor of 2 (shaded area in **Figure 8**). The NO_2 decrease is driven for both atmospheric observations and the emission inventory by the stringency of the lockdown measures, with larger NO_2 decreases observed for higher stringency indices. Overall, despite the NO_2 observation-based uncertainties associated with instrument limitations (Section 2.2.1), satellite measurement uncertainties (Section 2.2.2), meteorological dependencies in determining the effects of shutdown (Section 2.3), and the uncertainties associated with inventory estimation reductions (Forster et al., 2020), the two approaches result in consistent emissions decreases, in line with the SI. This suggests that the stringency of lockdown measures has a strong influence on emissions from transportation, as exhibited by mobility data sets used to adjust global emission inventories (Forster et al., 2020). The similarity between changes in the emissions inventory and changes in atmospheric observations due to lockdown measures further confirms the importance of traffic as a source of NO_x in cities around the world. A more detailed analysis of the differences between the two approaches is beyond the scope of this review.

3.3.3. Observed changes in SO_2 compared with estimates based on the EDGAR emission inventory

Figure 9 shows the median decrease in SO_2 concentration during the lockdown for each country colored by the SI (circles). Studies examining changes in SO_2 mostly used the direct comparison approach (80%), but 20% of studies corrected for meteorological effects. Also shown is the adapted EDGAR inventory median percentage drop in

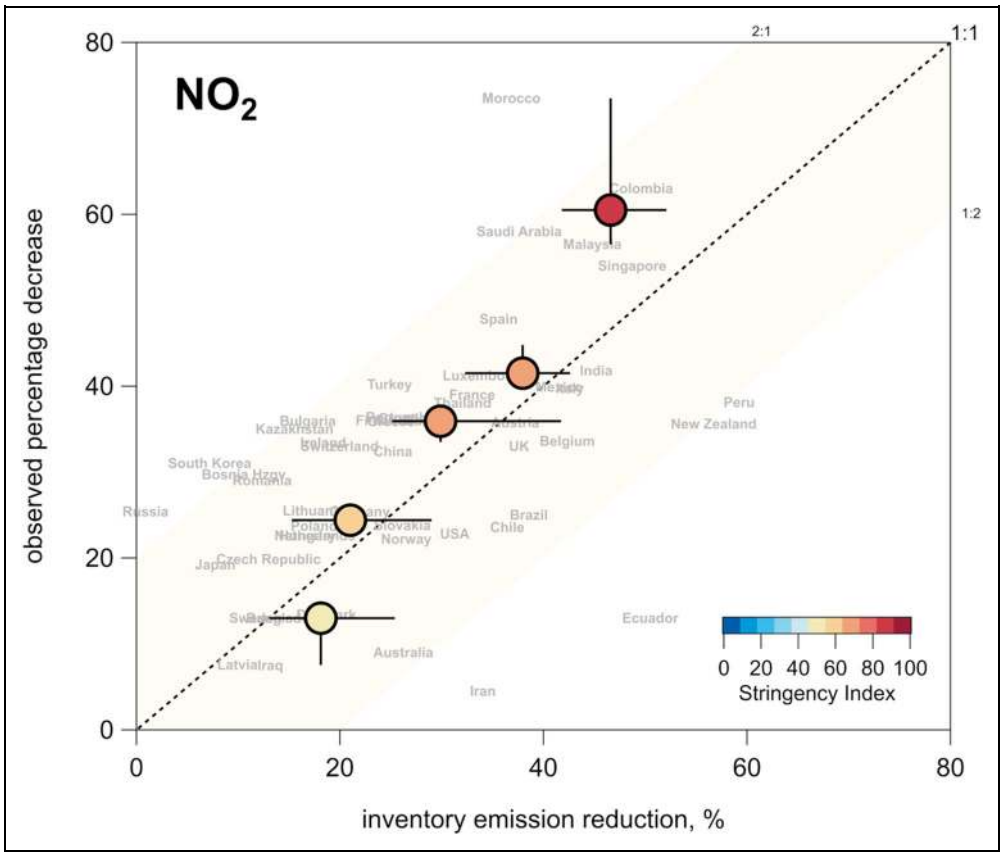

Figure 8. Observed percentage change of NO_2 during the lockdown based on literature (*y*-axis) compared to the Emissions Database for Global Atmospheric Research inventory reductions based on Forster et al. (2020). The median decrease for each country is shown in gray. Markers indicate the observed median decrease binned for all countries by <20%, 20%–30%, 30%–40%, 40%–50%, and >50%, with the inventory-based medians, colored by the median stringency index. Horizontal and vertical lines indicate the 25th and 75th percentiles of the distribution within each bin. DOI: https://doi.org/10.1525/elementa.2021.00176.f8

SO_2 emissions during the lockdown based on Forster et al. (2020; star squares). The pie charts show the breakdown by study measurement type, that is, ground-based, satellite, or both, for China (91%, 5%, and 5%, respectively), India (80%, 0%, and 20%, respectively), and for all other countries (76%, 8%, and 16%, respectively). All studies reported measurements from lockdown periods with an SI greater than 50. The majority of the studies were performed in China (25) and India (17), while three or fewer studies were performed for the remaining 18 countries.

Qualitatively, the inventory SO_2 emissions decreased with increasing SI, but the observed SO_2 changes were poorly correlated with either (**Figure 10**). Countries expected to account for the majority of SO_2 emissions globally based on the 2015 EDGAR inventory were China, India, and the United States, plus international shipping emissions (Figure S3). Observed SO_2 decreases and the Forster inventory reduction estimates showed discrepancies for China (16% vs. 26%), India (14% vs. 41%), and the United States (7% vs. 21%), suggesting that discrepancies on global scale emission estimates may also be expected. All but two studies were done in urban environments, and the average time period per study was greater than 50 days, resulting in urban-dominated SO_2 statistics for a long time period. The inventory SO_2 emission reductions are greater for the energy and manufacturing sources than from transportation. A lack of consistency in predicted versus observed SO_2 reductions (**Figure 10**) may therefore point toward uncertainties in the SO_2 inventory. NO_2, by contrast, arises primarily from transportation and shows better agreement between observation and inventory reduction estimates (**Figure 8**). However, there are fewer SO_2 observations and substantially fewer with meteorological normalization. There are also larger uncertainties associated with its measurement from ground-based and satellite-borne instruments. Further assessment of SO_2, a major precursor for $PM_{2.5}$, is an important topic for further study as more high-quality results from the COVID-19 period become available.

3.3.4. Observed changes in PM compared with estimates based on the EDGAR emission inventory

Figure 11 shows the median decrease in $PM_{2.5}$ concentration during lockdowns for each country colored by the SI (circles). Included in this calculation are studies using the direct comparison approach (i.e., no meteorological correction, 70%) and studies that correct for meteorological effects (30%). Effectively all analysis available to date considers $PM_{2.5}$ mass, and there is only limited information available on the changes in aerosol composition in

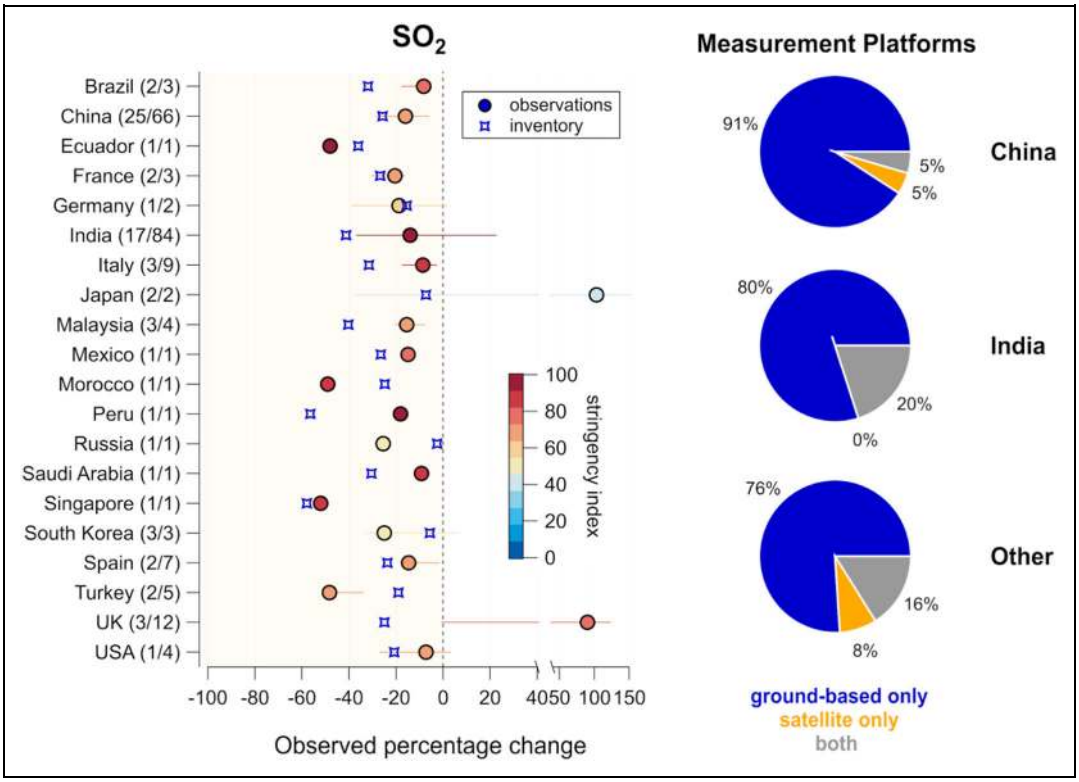

Figure 9. Observed median percentage decrease of SO_2 (circle markers) for each country. Error bars indicate the 25th and 75th percentiles of the distribution. The color of the markers indicates the median stringency index based on all studies associated with each country. Numbers in parentheses correspond to the number of publications and the number of measurements performed at each region/continent. Also, shown as star squares is the Emissions Database for Global Atmospheric Research inventory SO_2 emissions decrease calculated by Forster et al. (2020). The pie charts indicate the measurement platforms used by the studies for China, India, and all other countries. DOI: https://doi.org/10.1525/elementa.2021.00176.f9

response to lockdown measures. Also shown is the inventory median decrease in $PM_{2.5}$ emissions during the lockdowns approximated by both the organic and BC emission reductions based on the adjusted EDGAR inventory (Forster et al., 2020; star squares). We note that global inventories typically do not include speciated fractions of $PM_{2.5}$, which can be significant and reported by national-scale inventories (e.g., road dust, brake wear, tire wear). An inventory prediction of $PM_{2.5}$, which has both primary and secondary sources, is complicated by secondary PM formation, as discussed further below. $PM_{2.5}$ studies mostly report data from lockdowns when stringency indices are greater than 50.

Figure 12 further highlights the challenges associated with the comparison of $PM_{2.5}$ observations to the adapted EDGAR inventory based on Forster et al. (2020). The observed decreases for each country are further binned into percentage decrease ranges as in **Figure 8**. As the SI increased, the observed $PM_{2.5}$ median decreased; however, the inventory $PM_{2.5}$ emission reductions were poorly correlated. $PM_{2.5}$ can either be directly emitted or formed via secondary chemistry from a wide variety of other primary emissions (NO_x, SO_2, NH_3, NMVOCs, etc.). Therefore, a direct comparison of emission inventories and observations is challenging if the primary and secondary sources are not disentangled.

By the literature cutoff time of this review (September 30, 2020), only a few studies had been published that investigated the effects of secondary chemistry and local primary emissions on PM levels and composition in China (Chang et al., 2020; Chen et al., 2020a; Cui et al., 2020; Dai et al., 2020; Li et al., 2020b; Sun et al., 2020; Zheng et al., 2020), Bangladesh (Masum and Pal, 2020), and South Africa (Williams et al., 2020). More studies will be essential to understand the complexity of $PM_{2.5}$ pollution. For example, studies that address the possible effects of long-range transport that affect background PM levels are needed. Furthermore, changing atmospheric chemistry regimes can change secondary PM production rates. Characteristic examples that highlight this complexity are (1) the effects of NO_x reductions on organic peroxy radical (RO_2) chemistry affecting dimer formation and highly oxygenated molecules (e.g., McFiggans et al., 2019), (2) changes in organic and inorganic equilibrium partitioning, due to changes in particle acidity and the associated shifts between nitrate and sulfate formation in the particle-phase (e.g., Guo et al., 2016; Wang et al., 2016; Wang et al., 2020d), (3) changes in production rates of organic and inorganic pollutants due to increased availability of oxidants when emissions are reduced (e.g., Nault et al., 2018; Shah et al., 2018; Laughner and Cohen, 2019; Womack et al., 2019), and (4) changes in the rate of nighttime

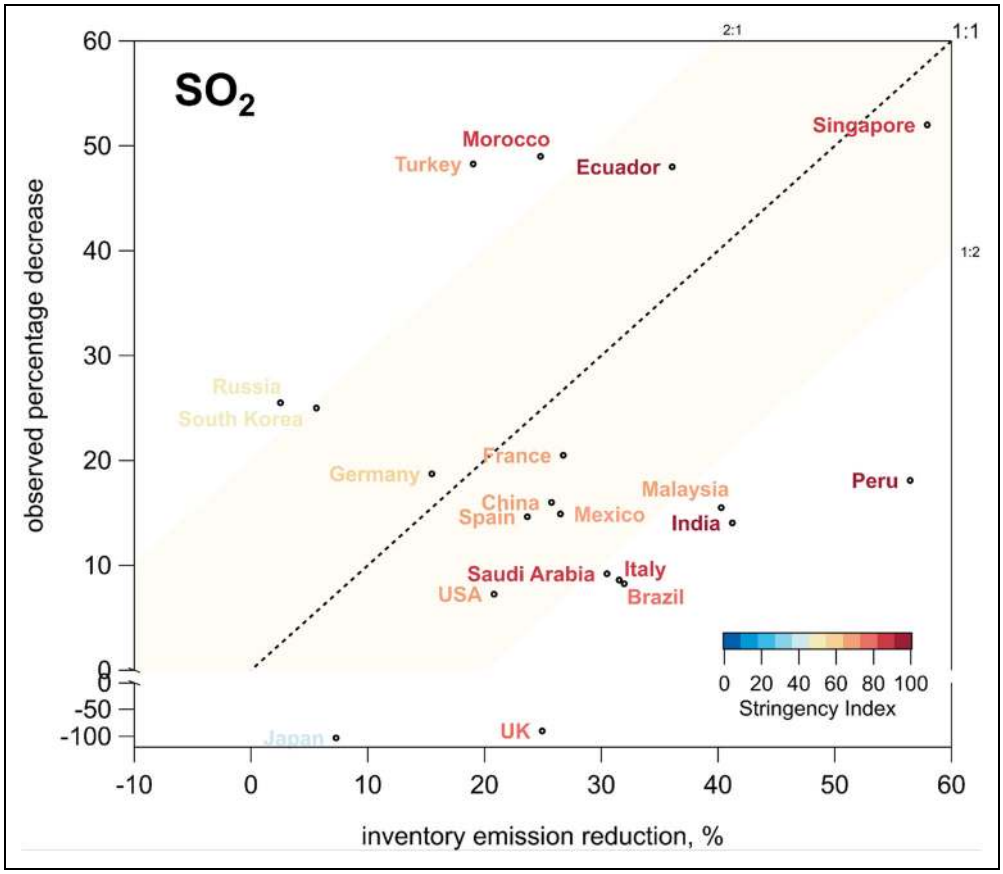

Figure 10. Observed percentage decrease in SO_2 during the lockdown based on literature (*y*-axis) compared to the Emissions Database for Global Atmospheric Research inventory emission reductions (Forster et al., 2020). The color of the country indicates the stringency index and the circle markers the percentage changes. Measurements were predominantly from studies that did not account for the effects of meteorology (80%). Due to the limited number of measurements, no additional binning of the data is performed as in **Figure 9.** DOI: https://doi.org/10.1525/elementa.2021.00176.f10

chemical processes (e.g., Kiendler-Scharr et al., 2016). PM composition measurements in addition to PM mass will be essential to assess these and other effects in order to elucidate changes in PM pollution arising from the COVID-19 emission reductions.

3.3.5. Changes in O_3

Figure 13 shows the observed median change in O_3 concentration from ground-based measurements during the lockdown for each country colored by the SI (circles). Included in this calculation are studies using the direct comparison approach without meteorological normalization (69%) and studies that correct for meteorological effects (31%). A violin plot shows the overall distribution of O_3 changes. Studies for most countries had SI values above 50 and either showed minor median O_3 decreases or increases in the 5%–20% range. O_3 increases greater than 50% were observed for Milan, Italy (reflected by the high 75th percentile values; Collivignarelli et al., 2020), as well as studies in Peru (Venter et al., 2020), Ecuador (Parra and Espinoza, 2020; Zambrano-Monserrate and Ruano, 2020), and Iraq (Hashim et al., 2020). To assess whether the changes in O_3 were driven by changes in emissions, the change in observed O_3 was plotted against the SI for each country together with the medians binned as done for **Figures 8** and **12** (**Figure 13**, right panel). As the lockdown measures became more stringent, the percentage change in O_3 increased, suggesting that significant changes in O_3 formation were driven by emission reductions.

O_3 is a secondary pollutant whose formation results from the interplay of NO_x, VOC emissions, and meteorology (Sillman, 1999). Most regions have a significant background O_3 concentration, and local emissions may either deplete O_3 from this background or produce it photochemically. Although NO_x emission reductions were evident during the lockdown, changes in VOC concentrations and composition have not been well investigated (see **Figure 5**). Furthermore, the literature covered in this review was predominantly focused on February, March, and April (Figure S1). Studies were also weighted toward the northern hemisphere, representing late winter and early spring. During these months, O_3 concentrations are expected to be low due to reduced wintertime photochemistry (Khoder, 2009). For the studied periods, it is therefore expected that an increase in O_3 could be more sensitive to NO emission reductions that would reduce O_3 titration. However, summertime measurements of O_3,

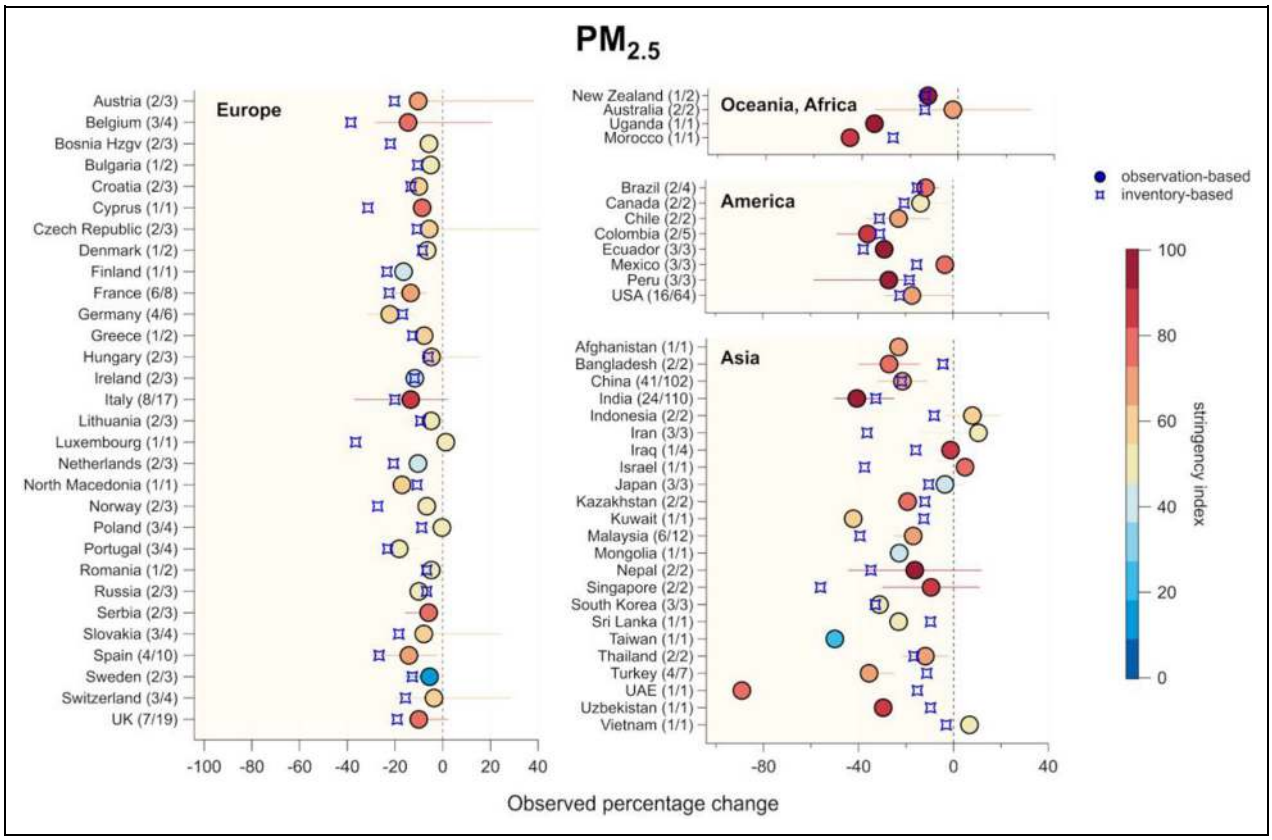

Figure 11. Observed median percentage decrease in $PM_{2.5}$ (circle markers) for each country. Error bars indicate the 25th and 75th percentiles of the distribution. The color of the markers indicates the median stringency index based on all measurements associated with each country. Numbers in parentheses correspond to the number of publications and the number of data sets collected at each region/continent. Also, shown are the Emissions Database for Global Atmospheric Research inventory emission reductions calculated by Forster et al. (2020; star squares). DOI: https://doi.org/10.1525/elementa.2021.00176.f11

NO_x, and VOCs are essential to investigate how changes in emissions affect O_3 formation when photochemistry is at its peak. Greater biogenic VOC and wildfire biomass burning emissions during the summer significantly alter VOC speciation and abundance. It is therefore evident that although reduced emissions increased O_3 concentrations in late winter and early spring, more studies will be necessary to address COVID-19-related shifts in summertime O_3, which is sensitive both to the local chemical environment and broad-scale changes in the ozone background.

3.3.6. Changes in other pollutants

Figure 14 shows the median change in pollutant concentrations for PM_{10}, NH_3, NO_x, AOD, BC, AQI, NMVOCs, and CO during the lockdown for each country colored by the SI. Note that for AQI, no unique definition exists, and it is used to assess the simultaneous presence of multiple pollutants. For example, in the United States, AQI is calculated based on the concentration of PM, O_3, SO_2, and CO (Bishoi et al., 2009), whereas in China, AQI is determined by the concentrations of the above four pollutants plus NO_2 (Fareed et al., 2020). Studies using the direct comparison approach accounted for 80%, 100%, 56%, 57%, 86%, 82%, 50%, and 72% of the data sets for PM_{10}, NH_3, NO_x, AOD, BC, AQI, NMVOCs, and CO, respectively. For the majority of countries, a decrease in pollutant concentrations was evident during the lockdowns compared to reference periods (see also **Table 8**). On average, decreases of 22% (±19%), 9% (±13%), 43% (±25%), 9% (±20%), 51% (±13%), 11% (±28%), 59% (±64%), and 27% (±18%) were observed for PM_{10}, NH_3, NO_x, AOD, BC, AQI, NMVOCs, and CO, respectively. More studies are needed to better understand the effects of the lockdowns on the above pollutant concentrations. With most of the current literature failing to account for the possible effects of meteorology, these results suggest a need for future studies in this area. Furthermore, NMVOCs and NH_3 can contribute to PM pollution through atmospheric chemical processes, and BC has direct impacts on climate forcing, which highlights the need to better monitor their concentrations.

3.4. Progress toward compliance with air quality standards during COVID-19

An interesting question is to what degree emissions reductions during the COVID-19 pandemic brought regions into compliance with air quality standards. **Table 1** lists the WHO exposure guidelines for a series of common air pollutants. Assessment of compliance with these standards requires comparison to absolute pollutant

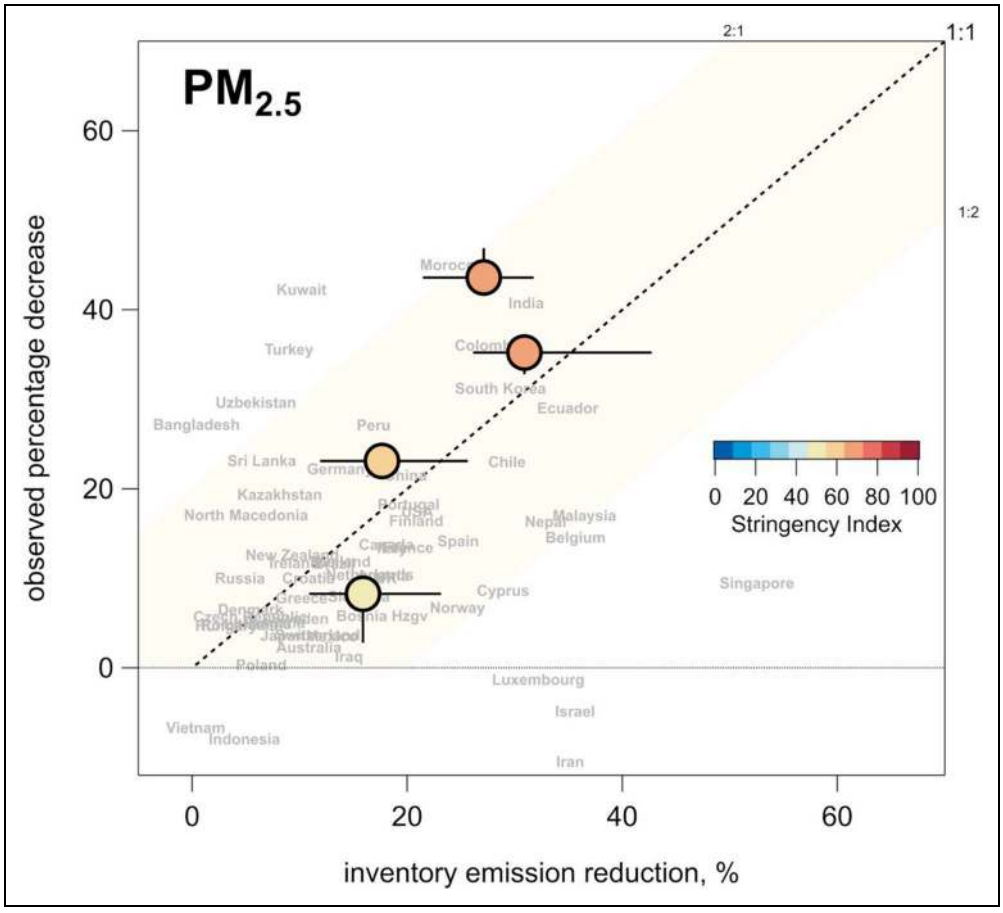

Figure 12. Observed percentage decrease in $PM_{2.5}$ during lockdowns based on literature (*y*-axis) compared to the Emissions Database for Global Atmospheric Research inventory percentage decrease in emissions (Forster et al., 2020). The median decrease for each country is shown in gray. Markers indicate the observed median decrease binned for all countries by <20%, 20%–30%, 30%–40%, 40%–50%, and >50%, with the inventory-based medians, colored by the median stringency index. Horizontal and vertical lines indicate the 25th and 75th percentiles of the distribution within each bin. DOI: https://doi.org/10.1525/elementa.2021.00176.f12

concentrations. Only a subset of the literature reviewed here reports data in absolute units, with the majority reporting relative changes without providing the underlying concentration values. This section therefore summarizes literature that reported the concentration of NO_2, $PM_{2.5}$, O_3, and CO using the direct comparison approach.

Figure 15 shows the mean concentrations of these four pollutants during lockdowns (circle markers) and reference periods (star markers) reported by 96 publications across different continents. Asia, the largest and most populous continent, is further separated into different geographical regions. Violin plots show the distribution of concentrations reported within each region. Circle markers are colored by the percentage change of the mean lockdown concentration with respect to mean reference period concentrations per region/continent. Also shown are the WHO guideline values for NO_2, $PM_{2.5}$ and O_3 for different exposure times, including 1 year, 24 h, and 8 h. Finally, the number of publications and the number of collected measurements (from different sites and/or times) are provided in parentheses per region/pollutant. Although the WHO guideline values are limited to multiple-hour or annually averaged exposure times for the different pollutants, observation-based concentration averages range from 1 week to 5 months. A direct comparison of observations to the WHO guideline values is therefore challenging. However, the WHO guideline values for hourly and annual means provide a range of concentrations that put the observed means into perspective. For example, if monthly measurements of a pollutant are greater than the hourly WHO guideline values, then exceedances by definition occurred during the studied period; if observations are greater than the annual guideline values, then exceedances could also occur if high concentrations were to persist beyond the observation period. In the following, each pollutant is examined separately, and the literature corresponding to each pollutant is provided in **Tables 5**–**8.** Concentration changes on a national level are further discussed in Section S4 and downloadable from the database (See Section 2.1).

The mean NO_2 concentration reported by all studies for lockdown conditions was 22 $\pm$ 18 μg m^{-3} (1 standard deviation) and lower than the reported mean, 31 $\pm$ 15 μg m^{-3}, for the respective reference periods. The lockdown and reference concentrations from 100% ground-based measurements were below the WHO annual guideline

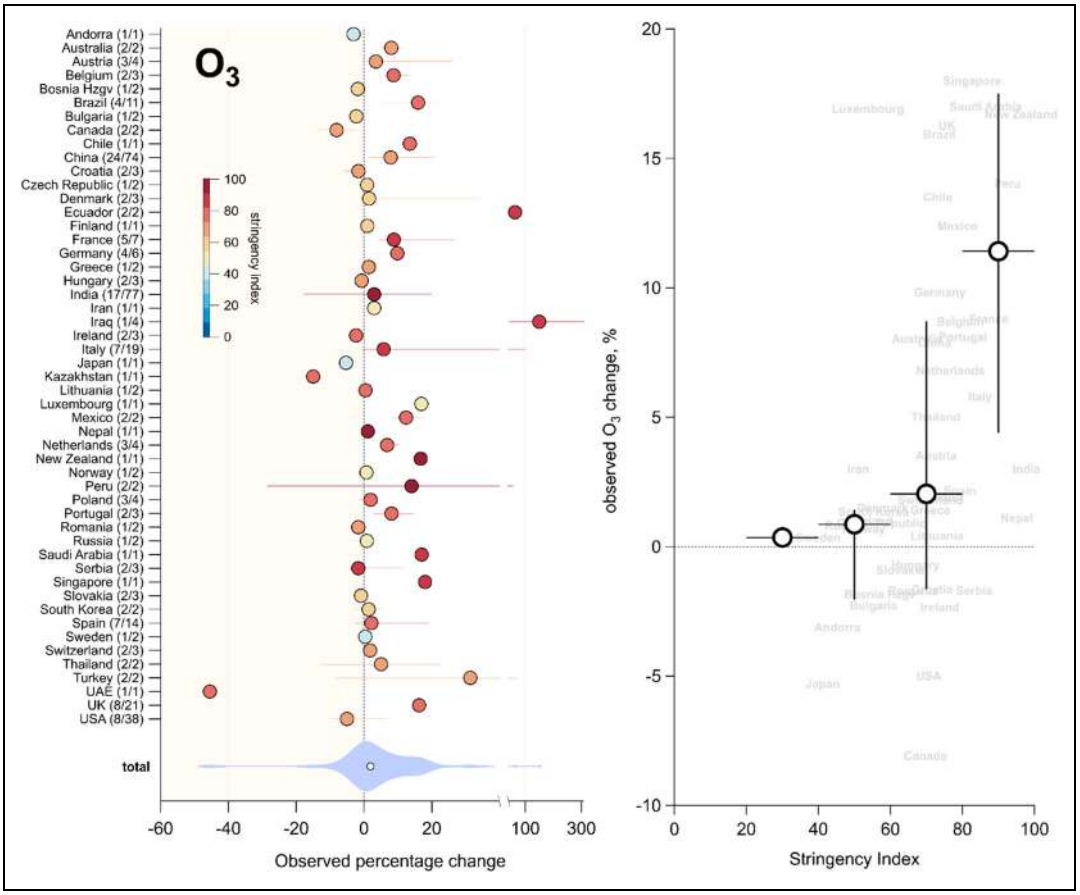

Figure 13. Observed median percentage change of O_3 (circle markers) for each country. Error bars indicate the 25th and 75th percentiles of the distribution. The color of the markers indicates the median stringency index based on all studies for each country. Numbers in parenthesis correspond to the number of publications and the number of measurements performed at each region/continent. The violin plot at the bottom left shows the distribution of all observed O_3 changes. In the right panel, the change in observed O_3 is plotted against the stringency index for each country together with the medians binned as done for **Figures 9** and **13.** DOI: https://doi.org/10.1525/elementa.2021.00176.f13

values, and NO_2 concentrations decreased during the lockdown compared to the reference period for all regions except West Asia. Literature corresponding to these measurements is provided in **Table 5.**

The mean $PM_{2.5}$ concentration reported for lockdown conditions was 24 $\pm$ 14 μg m^{-3} and lower than the reported mean, 32 $\pm$ 22 μg m^{-3}, for the respective reference periods. The lockdown and reference concentrations (80% ground-based, 2% satellite, 18% both) were above the WHO mean annual guideline value of 10 μg m^{-3} for nearly all regions, and mean values in Asia often exceeded the 24-h guideline value of 25 μg m^{-3}. $PM_{2.5}$ decreased during the lockdown compared to the reference periods for all regions except West Asia. However, this decrease was not sufficient to reduce concentrations below the WHO guideline values during the lockdown, especially for regions in Asia. This variability in $PM_{2.5}$ concentrations may reflect the much wider variety of $PM_{2.5}$ sources with secondary $PM_{2.5}$ responding to the changes in NO_x, VOCs, SO_2, and NH_3 as well as many other sources. Literature corresponding to these measurements is provided in **Table 6.**

The mean O_3 concentration reported by all studies for lockdown conditions was 43 $\pm$ 21 μg m^{-3} and higher than the reported mean, 36 $\pm$ 19 μg m^{-3}, for the respective reference periods. The lockdown and reference concentrations from 100% ground-based measurements were below the 8-h mean WHO guideline value (100 μg m^{-3}, approximately 50 ppb) for all regions. However, the ground-based mean values were calculated as averages for multiple weeks/months, including nighttime measurements, allowing for the possibility that midday O_3 might still have exceeded the 8-h guideline value. O_3 increased during the lockdowns compared to the reference periods for all regions except South Asia. An overview of the literature corresponding to these measurements is provided in **Table 7** and is dominated by urban measurements (>98%).

The mean CO concentration reported by all studies for lockdown conditions was 580 $\pm$ 310 μg m^{-3} and lower than the reported mean, 630 $\pm$ 440 μg m^{-3}, for the respective reference periods. There are currently no WHO guideline values for CO to compare to; however, the U.S., European, and Chinese guidelines shown in **Table 1** are

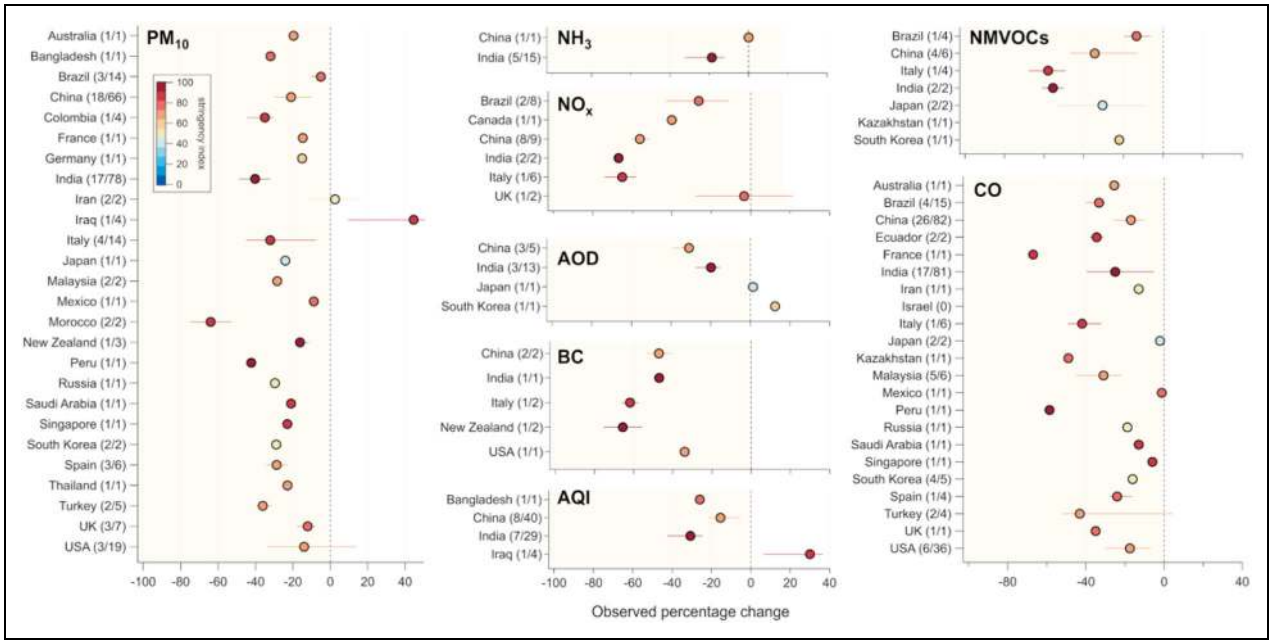

Figure 14. Observed median percentage change of all other pollutants (circle markers) for each country. Error bars indicate the 25th and 75th percentiles of the distribution. The color of the markers indicates the median stringency index based on all studies for each country. Numbers in parentheses indicate the number of publications and the number of data sets collected at each region/continent. DOI: https://doi.org/10.1525/elementa.2021.00176.f14

significantly greater than the observed CO concentrations. CO decreased during the lockdowns compared to the reference periods for all regions. An overview of the literature corresponding to these measurements is provided in **Table 8.**

4. Conclusions and outlook

Analysis of emissions changes and their resulting influence on air quality worldwide during the COVID-19 pandemic is a rapidly evolving topic of intense public and scientific interest. This review provides a summary of the current literature that has examined mainly the stringent, early lockdown periods in February–May 2020. Despite the short duration of the observational time period and the limited time since that period to this writing, the number of papers and the depth of the analysis is substantial. Already, there are several initial conclusions, recommendations for careful consideration and best use of the observations, and a list of suggestions for further analysis. This review synthesizes these reported changes in air pollutants during the COVID-19 lockdowns and further provides context for these changes using the SI, a unified, globally consistent measure of the policy response to confining the pandemic. All data digitized for analysis in this review are available on the website in https://covid-aqs.fz-juelich.de. This website is designed as a living version of this review, that is, as new literature emerges, authors of published papers are encouraged to upload their data to the database, thus complementing the data coverage in space, time, and compound dimensions.

Much of the COVID-19 air quality literature surveyed for this review does not explicitly account for the effect that the year-to-year variability, largely driven by meteorology, has on observed atmospheric concentration changes. The dependence of concentration changes on the SI are readily apparent in the meteorologically corrected data but not in the uncorrected data. We recommend that all future analyses take explicit account of meteorology and specify the method for doing so, for example, as outlined in Section 2.3.2, or perform chemical transport modeling (Section 2.3.3) since disregarding this consideration largely increases the associated uncertainties.

Two of the main species arising from primary emissions analyzed to date are NO_2 and SO_2, both of which have readily available ground-based monitoring networks and satellite remote sensing data sets. They also arise from different emission sectors, with NO_x (for which NO_2 is a proxy) having its largest contribution from transportation and SO_2 from power generation and certain industrial sources. For NO_2, the observed changes correspond within uncertainties with the estimated emission inventory reductions when accounting for COVID-19 lockdowns. The analysis of NO_2 also encompasses the largest number of publications and the largest number that explicitly account for meteorological effects. Analysis of SO_2, by contrast, shows distinct evidence for reductions during the lockdown periods, but those emissions reductions are not as clearly associated with predictions from inventories. This difference may be due to incomplete information of the impacts of COVID-19 on industrial activity and the more limited publication database of SO_2 changes during COVID-19, especially for papers that account for meteorology, or uncertainties in the measurement database for SO_2. We recommend further investigation of the SO_2 reductions, especially since this has the potential to inform inventories for this critical $PM_{2.5}$ precursor.

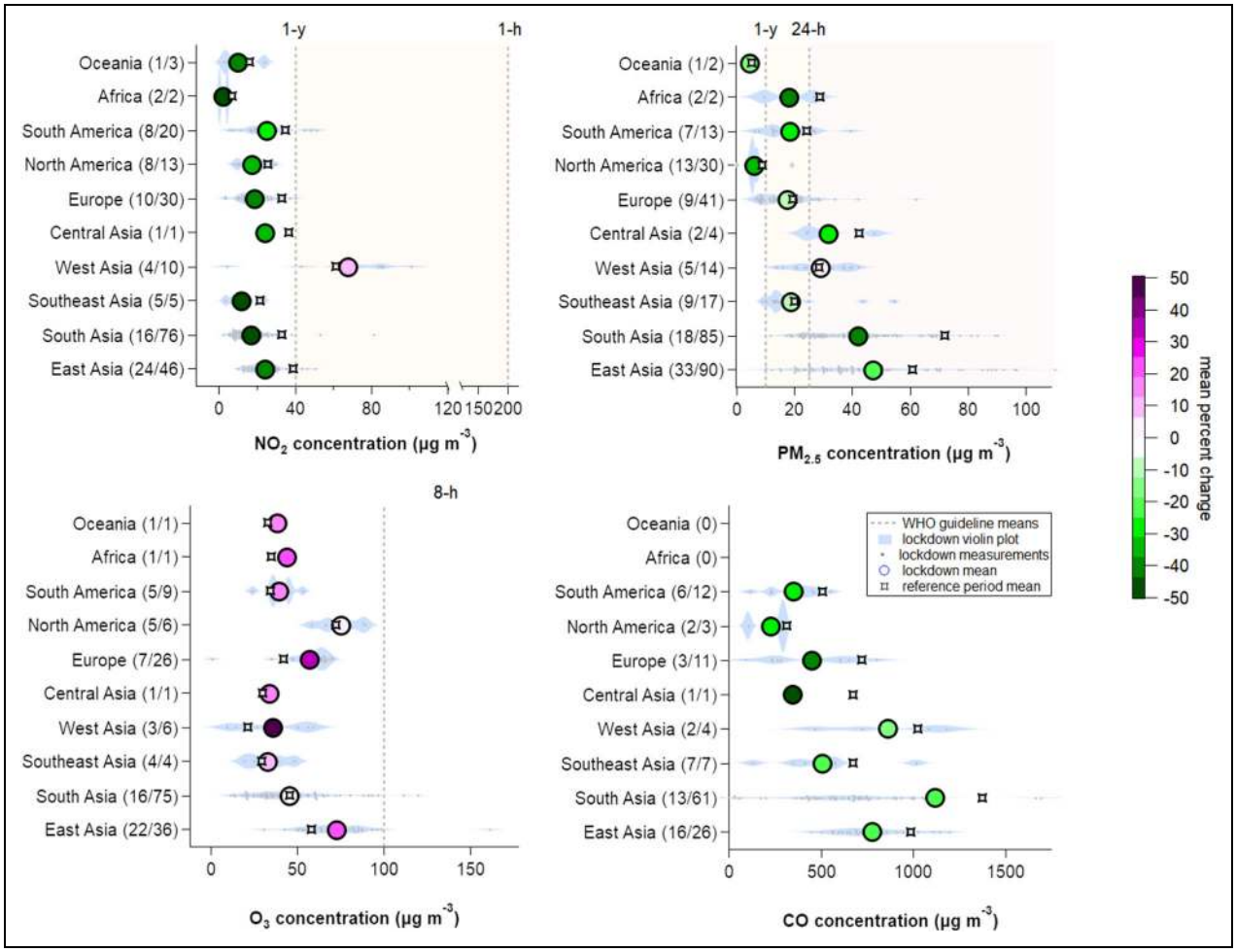

Figure 15. Distributions of the absolute concentration of pollutants, shown as violin plots, around the world during the lockdown period and the reference period (star square markers indicate the mean) for each study. Blue shaded area shows the density of samples at each concentration, and gray dots show the individual data sets averaged for periods ranging from days to several weeks. The hour/year mean World Health Organization guideline values are shown as vertical dashed lines. Numbers in parentheses indicate the number of publications and the number of data sets collected at each region/continent. DOI: https://doi.org/10.1525/elementa.2021.00176.f15

Analysis of changes on primary emissions of other species, such as CO, NMVOCs, BC, and NH_3, is more limited. CO is covered in the literature by 67 publications, albeit predominantly without explicitly accounting for meteorological impacts on pollutant abundance. BC, NH_3, and NMVOCs are covered by seven, five, and 10 publications, respectively, far from providing a global overview at this stage. This reflects the frequency with which these compounds are typically measured by air quality monitoring networks. However, considering the important role of SO_2 and VOCs in secondary aerosol formation and of CO and VOCs in ozone chemistry, further analysis of available COVID-19 changes is needed for these species.

Both $PM_{2.5}$ and O_3 have large secondary sources arising from complex atmospheric chemical cycles, and together they are responsible for the majority of adverse health outcomes associated with air pollution. Total $PM_{2.5}$ mass and O_3 are covered comparatively widely in the literature, although there is little information on speciated $PM_{2.5}$ composition. The COVID-19 literature shows that $PM_{2.5}$ decreases with increasing SI, whereas O_3 increases with SI. Key uncertainties in the understanding of these changes should be addressed through the combined use of observational and atmospheric chemistry modeling approaches. With the chemistry leading to ozone and secondary aerosol (both organic and inorganic) formation being nonlinearly dependent on NO_x levels, the lockdown periods and seasonality of its effect on pollutants offers unique possibilities to assess model abilities in capturing changes on local to global scales. Further analysis of photochemically active periods with reduced emissions in the northern hemisphere in forthcoming literature may be particularly informative.

More use can be made of the high-resolution capabilities of the TROPOMI sensor, in particular for NO_2. Analyses of the data at high resolution may provide COVID-19 emission impact estimates of different sources and source sectors such as individual power plants, highways, shipping, urban areas, industrial complexes, and airports. The influence of the day-to-day changes in weather is, however, substantial on such local scales, and we recommend that such high-resolution satellite-based studies make use

of high-quality weather analyses and chemical modeling. When using satellite NO_2 measurements, we advise that the averaging kernels remove the dependency on the retrieval a priori profile shape, which can always be done when three-dimensional CTMs are involved in the analysis. Satellite instruments like TROPOMI and OMI measure at one given overpass time (e.g., 13:30), but it should be considered that the diurnal profile of the emissions may have changed during the lockdowns. Satellite retrievals often suffer from systematic uncertainties. In the case of TROPOMI NO_2, we mention a negative bias compared to surface remote sensing observations, with an apparent linear scaling with the tropospheric column amount over polluted regions. This scaling suggests that relative changes, for example, the percentage reduction compared to a reference time period, are not so sensitive to the negative bias, and we recommend reporting such relative differences, which is done in most of the papers studied in this review.

As the atmospheric chemistry community makes continued efforts toward observational coverage of the pandemic influences on atmospheric composition, we anticipate that additional data sets will become available for further analysis. We recommend attention to the following issues, although this list is certainly far from comprehensive.

First, changes in O_3 associated with COVID-19 emissions reductions, particularly during photochemically active seasons, may be informative for assessing the sensitivity of this photochemistry to NO_x and VOCs in different regions. The northern hemisphere late winter and early spring period that dominates this review reflects O_3 data that are not particularly sensitive to photochemistry. However, careful comparisons of meteorologically normalized O_3 to detailed photochemical models may elucidate NO_x and VOC sensitivities that can inform regional O_3 mitigation strategies across the world.

Second, changes in $PM_{2.5}$ may enable similar sensitivity analyses to primary emissions. As $PM_{2.5}$ composition depends on a number of emission sources and chemical cycles, a broader analysis of chemically speciated $PM_{2.5}$ data, where available, will be especially informative.

Third, but related to both of the above, the seasonality of O_3 and $PM_{2.5}$ may be addressed if there are sufficient observations of emissions reductions across different hemispheres or times of year. Given the trajectory of the COVID-19 pandemic at the time of this writing, such an analysis may be feasible even within the northern hemisphere. Particularly for $PM_{2.5}$, there is a well-known seasonality, with severe effects arising from distinct cycles and emissions that occur in midlatitude summer and winter.

Fourth, expansion of the available analyses to include a larger number of species would help to constrain and inform emissions inventories. This review has provided an initial analysis of the difference between NO_2 and SO_2. Further analysis, to include detailed analysis of CO, BC, NH_3, and especially speciated NMVOCs, where available, would provide unprecedented tests of the current understanding of emissions inventories across an array of sectors.

Fifth, analysis of the radiative forcing associated with short-lived climate forcers is a priority. For example, regional emissions changes should lead to both local and hemispheric effects on O_3. The influence on this broader scale, or background O_3, needs to be evaluated through both modeling and observational efforts. Remote sensing O_3 products and vertical profiles from, for example, O_3 LIDAR networks will be particularly informative. Similarly, changes in $PM_{2.5}$ affect both regional air quality and global climate. Widespread global reductions in primary emissions and $PM_{2.5}$ precursors must similarly be evaluated in terms of their short-term climate forcing in 2020.

Finally, changes in the oxidative capacity of the global atmosphere arising from COVID-19 may also have occurred with changes in NO_x and other species, but those changes have yet to be evaluated. Such changes have the potential to influence the lifetime of methane, an important greenhouse gas. Model evaluations will be informative in this regard since we anticipate few, if any, observations of the influence lockdowns have on oxidants such as HO_x radicals.

We note that this review has been limited in scope to air pollutants that are of importance as short-lived climate forcers. However, to our knowledge, no information is currently available on short-lived climate forcers such as methane and halogenated compounds. N_2O and CO_2 are beyond the scope of this review with the latter evaluated elsewhere (Le Quéré et al., 2020). The developing analysis of the COVID-19 emission reductions will certainly address these topics.

Data accessibility statement

The review compiles data published in the peer-reviewed literature. All data are accessible through https://covid-aqs.fz-juelich.de designed as a living version of this review. The data sets from the website are provided with free and unrestricted access for scientific (noncommercial) use including the option to generate targeted reference lists. Users of the database are requested to acknowledge the data source and reference this review in publications utilizing the data set. As new literature emerges, authors of published papers can upload their data to the database, thus complementing the data coverage in space, time, and compound dimensions.

Supplemental files

The supplemental files for this article can be found as follows:

Text S1–S4. Figure S1–S4. Table S1–S2. Docx.

Acknowledgments

The authors acknowledge discussions with Pieternel Levelt and Pepijn Veefkind on the satellite measurements, as well as the support from John Douros of Royal Netherlands Meteorological Institute in computing the Copernicus Atmosphere Monitoring Service (CAMS) global reanalysis simulations of the TROPOMI NO_2 observations. This article contains modified CAMS Information (2020).

They also acknowledge Alina Zimmermann and Michael Decker for support on the database operation and Kenneth C. Aikin for IGOR programming support for the figures. Finally, they acknowledge and appreciate the fast response from the editor and reviewers for this timely publication.

Funding

The authors acknowledge institutional funding from the Earth and Environment research field of the Helmholtz Association (FZ Jülich), the NOAA Atmospheric Chemistry Carbon Cycle and Climate (AC4) Program, and the ESA Impacts of COVID-19 lockdown measures on Air quality and Climate project.

Competing interests

The authors declare no competing interests.

Author contributions

Performed the literature review and categorized the papers: GIG, JBG, SB, BCM, AKS.

Extracted data from the reviewed literature and performed analyses: GIG, JBG.

Provided Figure 1: CT.

Provided Figure 4: HE, ACL.

Designed the database and web page: ARG, AP.

All authors contributed to the interpretation of data, drafted and/or revised this article, and approved the final version for submission.

References

Abdullah, S, Mansor, AA, Napi, NNLM, Mansor, WNW, Ahmed, AN, Ismail, M, Ramly, ZTA. 2020. Air quality status during 2020 Malaysia Movement Control Order (MCO) due to 2019 novel coronavirus (2019-nCoV) pandemic. *Science of the Total Environment* **729**. DOI: http://dx.doi.org/10.1016/j.scitotenv.2020.139022.

Adams, MD. 2020. Air pollution in Ontario, Canada during the COVID-19 state of emergency. *Science of the Total Environment* **742**. DOI: http://dx.doi.org/10.1016/j.scitotenv.2020.140516.

Agarwal, A, Kaushik, A, Kumar, S, Mishra, RK. 2020. Comparative study on air quality status in Indian and Chinese cities before and during the COVID-19 lockdown period. *Air Quality, Atmosphere & Health*. DOI: http://dx.doi.org/10.1007/s11869-020-00881-z.

Anderson, HR, Atkinson, RW, Peacock, JL, Marston, L, Konstantinou, K. 2004. *Meta-analysis of time-series studies and panel studies of particulate matter (PM) and ozone (O_3): Report of a WHO task group*. Copenhagen, Denmark: WHO Regional Office for Europe.

Anil, I, Alagha, O. 2020. The impact of COVID-19 lockdown on the air quality of Eastern Province, Saudi Arabia. *Air Quality, Atmosphere & Health*. DOI: http://dx.doi.org/10.1007/s11869-020-00918-3.

Ash'aari, ZH, Aris, AZ, Ezani, E, Ahmad Kamal, NI, Jaafar, N, Jahaya, JN, Manan, SA, Umar, Saifuddin, MF. 2020. Spatiotemporal variations and contributing factors of air pollutant concentrations in Malaysia during movement control order due to pandemic COVID-19. *Aerosol and Air Quality Research* **20**. DOI: http://dx.doi.org/10.4209/aaqr.2020.06.0334.

Ass, KE, Eddaif, A, Radey, O, Aitzaouit, O, Yakoubi, ME, Chelhaoui, Y. 2020. Effect of restricted emissions during Covid-19 lockdown on air quality in Rabat—Morocco. *Global NEST Journal* **22**. DOI: http://dx.doi.org/10.30955/gnj.003431.

Aydın, S, Nakiyingi, BA, Esmen, C, Güneysu, S, Ejjada, M. 2020. Environmental impact of coronavirus (COVID-19) from Turkish perceptive. *Environment, Development and Sustainability*. DOI: http://dx.doi.org/10.1007/s10668-020-00933-5.

Baldasano, JM. 2020. COVID-19 lockdown effects on air quality by NO_2 in the cities of Barcelona and Madrid (Spain). *Science of the Total Environment* **741**. DOI: http://dx.doi.org/10.1016/j.scitotenv.2020.140353.

Bao, R, Zhang, A. 2020. Does lockdown reduce air pollution? Evidence from 44 cities in northern China. *Science of the Total Environment* **731**. DOI: http://dx.doi.org/10.1016/j.scitotenv.2020.139052.

Bauwens, M, Compernolle, S, Stavrakou, T, Müller, JF, van Gent, J, Eskes, H, Levelt, PF, van der, AR, Veefkind, JP, Vlietinck, J, Yu, H, Zehner, C. 2020. Impact of Coronavirus outbreak on NO_2 pollution assessed using TROPOMI and OMI observations. *Geophysical Research Letters* **47**(11). DOI: http://dx.doi.org/10.1029/2020GL087978.

Beckett, FM, Witham, CS, Leadbetter, SJ, Crocker, R, Webster, HN, Hort, MC, Jones, AR, Devenish, BJ, Thomson, DJ. 2020. Atmospheric dispersion modelling at the London VAAC: A review of developments since the 2010 Eyjafjallajökull Volcano ash cloud. *Atmosphere* **11**(4). DOI: http://dx.doi.org/10.3390/atmos11040352.

Bedi, JS, Dhaka, P, Vijay, D, Aulakh, RS, Gill, JPS. 2020. Assessment of air quality changes in the four metropolitan cities of India during COVID-19 pandemic lockdown. *Aerosol and Air Quality Research* **20**. DOI: http://dx.doi.org/10.4209/aaqr.2020.05.0209.

Beig, G, George, MP, Sahu, SK, Rathod, A, Singh, S, Dole, S, Murthy, BS, Latha, R, Tikle, S, Trimbake, HK, Shinde, R. 2020. Towards baseline air pollution under COVID-19: Implication for chronic health and policy research for Delhi, India. *Current Science* **119**(7). DOI: http://dx.doi.org/ 10.18520/cs/v119/i7/1178-1184.

Beirle, S, Platt, U, Wenig, M, Wagner, T. 2003. Weekly cycle of NO_2 by GOME measurements: A signature of anthropogenic sources. *Atmospheric Chemistry and Physics* **3**(6): 2225–2232. DOI: http://dx.doi.org/10.5194/acp-3-2225-2003.

Bekbulat, B, Apte, JS, Millet, DB, Robinson, AL, Wells, KC, Presto, AA, Marshall, JD. 2021. Changes in criteria air pollution levels in the US before, during, and after Covid-19 stay-at-home orders: Evidence from regulatory monitors. *Science of the Total*

Environment **769**. DOI: http://dx.doi.org/ https://doi.org/10.1016/j.scitotenv.2020.144693.

Bera, B, Bhattacharjee, S, Shit, PK, Sengupta, N, Saha, S. 2020. Significant impacts of COVID-19 lockdown on urban air pollution in Kolkata (India) and amelioration of environmental health. *Environment, Development and Sustainability* 1–28. DOI: http://dx.doi.org/10.1007/s10668-020-00898-5.

Berman, JD, Ebisu, K. 2020. Changes in U.S. air pollution during the COVID-19 pandemic. *Science of the Total Environment* **739**. DOI: http://dx.doi.org/10.1016/j.scitotenv.2020.139864.

Bishoi, B, Prakash, A, Jain, VK. 2009. A comparative study of air quality index based on factor analysis and US-EPA methods for an urban environment. *Aerosol and Air Quality Research* **9**(1): 1–17. DOI: http://dx.doi.org/10.4209/aaqr.2008.02.0007.

Biswal, A, Singh, T, Singh, V, Ravindra, K, Mor, S. 2020. COVID-19 lockdown and its impact on tropospheric NO_2 concentrations over India using satellite-based data. *Heliyon* **6**(9). DOI: http://dx.doi.org/10.1016/j.heliyon.2020.e04764.

Borbon, A, Gilman, JB, Kuster, WC, Grand, N, Chevaillier, S, Colomb, A, Dolgorouky, C, Gros, V, Lopez, M, Sarda-Esteve, R, Holloway, J, Stutz, J, Petetin, H, McKeen, S, Beekmann, M, Warneke, C, Parrish, DD, de Gouw, JA. 2013. Emission ratios of anthropogenic volatile organic compounds in northern mid-latitude megacities: Observations versus emission inventories in Los Angeles and Paris. *Journal of Geophysical Research: Atmospheres* **118**(4): 2041–2057. DOI: http://dx.doi.org/10.1002/jgrd.50059.

Broomandi, P, Karaca, F, Nikfal, A, Jahanbakhshi, A, Tamjidi, M, Kim, JR. 2020. Impact of COVID-19 event on the air quality in Iran. *Aerosol and Air Quality Research* **20**(8): 1793–1804. DOI: http://dx.doi.org/10.4209/aaqr.2020.05.0205.

Cameletti, M. 2020. The effect of Corona Virus lockdown on air pollution: Evidence from the city of Brescia in Lombardia Region (Italy). *Atmospheric Environment* **239**. DOI: http://dx.doi.org/10.1016/j.atmosenv.2020.117794.

Cameron-Blake, E, Tatlow, H, Hallas, L, Majumdar, S. 2020. Corona virus government response tracker. Available at https://www.bsg.ox.ac.uk/research/research-projects/coronavirus-government-response-tracker. Accessed 1 October 2020.

Chang, Y, Huang, R-J, Ge, X, Huang, X, Hu, J, Duan, Y, Zou, Z, Liu, X, Lehmann, MF. 2020. Puzzling Haze events in China during the Coronavirus (COVID-19) shutdown. *Geophysical Research Letters* **47**(12). DOI: http://dx.doi.org/10.1029/2020GL088533.

Chatterjee, A, Mukherjee, S, Dutta, M, Ghosh, A, Ghosh, SK, Roy, A. 2020. High rise in carbonaceous aerosols under very low anthropogenic emissions over eastern Himalaya, India: Impact of lockdown for COVID-19 outbreak. *Atmospheric Environment* **244**. DOI: http://dx.doi.org/10.1016/j.atmosenv.2020.117947.

Chauhan, A, Singh, RP. 2020. Decline in $PM_{2.5}$ concentrations over major cities around the world associated with COVID-19. *Environmental Research* **187**. DOI: http://dx.doi.org/10.1016/j.envres.2020.109634.

Chen, H, Huo, J, Fu, Q, Duan, Y, Xiao, H, Chen, J. 2020a. Impact of quarantine measures on chemical compositions of $PM_{2.5}$ during the COVID-19 epidemic in Shanghai, China. *Science of the Total Environment* **743**. DOI: http://dx.doi.org/10.1016/j.scitotenv.2020.140758.

Chen, LWA, Chien, L-C, Li, Y, Lin, G. 2020b. Nonuniform impacts of COVID-19 lockdown on air quality over the United States. *Science of the Total Environment* **745**. DOI: http://dx.doi.org/10.1016/j.scitotenv.2020.141105.

Chen, Q-X, Huang, C-L, Yuan, Y, Tan, H-P. 2020c. Influence of COVID-19 event on air quality and their association in Mainland China. *Aerosol and Air Quality Research* **20**(7): 1541–1551. DOI: http://dx.doi.org/10.4209/aaqr.2020.05.0224.

Chen, Y, Zhang, S, Peng, C, Shi, G, Tian, M, Huang, R-J, Guo, D, Wang, H, Yao, X, Yang, F. 2020d. Impact of the COVID-19 pandemic and control measures on air quality and aerosol light absorption in Southwestern China. *Science of the Total Environment* **749**. DOI: http://dx.doi.org/10.1016/j.scitotenv.2020.141419.

Chu, B, Zhang, S, Liu, J, Ma, Q, He, H. 2021. Significant concurrent decrease in $PM_{2.5}$ and NO_2 concentrations in China during COVID-19 epidemic. *Journal of Environmental Sciences* **99**: 346–353. DOI: http://dx.doi.org/10.1016/j.jes.2020.06.031.

Churkina, G, Kuik, F, Bonn, B, Lauer, A, Grote, R, Tomiak, K, Butler, TM. 2017. Effect of VOC emissions from vegetation on air quality in Berlin during a Heatwave. *Environmental Science & Technology* **51**(11): 6120–6130. DOI: http://dx.doi.org/10.1021/acs.est.6b06514.

Collivignarelli, MC, Abba, A, Bertanza, G, Pedrazzani, R, Ricciardi, P, Carnevale Miino, M. 2020. Lockdown for CoViD-2019 in Milan: What are the effects on air quality? *Science of the Total Environment* **732**. DOI: http://dx.doi.org/10.1016/j.scitotenv.2020.139280.

Connerton, P, Vicente de Assunção, J, Maura de Miranda, R, Dorothée Slovic, A, José Pérez-Martínez, P, Ribeiro, H. 2020. Air quality during COVID-19 in four megacities: Lessons and challenges for public health. *International Journal of Environmental Research and Public Health* **17**(14). DOI: http://dx.doi.org/10.3390/ijerph17145067.

Crippa, M, Solazzo, E, Huang, G, Guizzardi, D, Koffi, E, Muntean, M, Schieberle, C, Friedrich, R, Janssens-Maenhout, G. 2020. High resolution temporal profiles in the emissions database for global atmospheric research. *Scientific Data* **7**(1): 121. DOI: http://dx.doi.org/10.1038/s41597-020-0462-2.

Cui, Y, Ji, D, Maenhaut, W, Gao, W, Zhang, R, Wang, Y. 2020. Levels and sources of hourly $PM_{2.5}$-related elements during the control period of the COVID-19 pandemic at a rural site between Beijing and Tianjin. *Science of the Total Environment* **744**. DOI: http://dx.doi.org/10.1016/j.scitotenv.2020.140840.

Dai, Q, Liu, B, Bi, X, Wu, J, Liang, D, Zhang, Y, Feng, Y, Hopke, PK. 2020. Dispersion normalized PMF provides insights into the significant changes in source contributions to $PM_{2.5}$ after the COVID-19 outbreak. *Environmental Science & Technology* **54**(16): 9917–9927. DOI: http://dx.doi.org/10.1021/acs.est.0c02776.

Dantas, G, Siciliano, B, França, BB, da Silva, CM, Arbilla, G. 2020. The impact of COVID-19 partial lockdown on the air quality of the city of Rio de Janeiro, Brazil. *Science of the Total Environment* **729**. DOI: http://dx.doi.org/10.1016/j.scitotenv.2020.139085.

Dhaka, SK, Chetna Kumar, V, Panwar, V, Dimri, AP, Singh, N, Patra, PK, Matsumi, Y, Takigawa, M, Nakayama, T, Yamaji, K, Kajino, M, Misra, P, Hayashida, S. 2020. $PM_{2.5}$ diminution and haze events over Delhi during the COVID-19 lockdown period: An interplay between the baseline pollution and meteorology. *Scientific Reports* **10**(1). DOI: http://dx.doi.org/10.1038/s41598-020-70179-8.

Diamond, MS, Wood, R. 2020. Limited regional aerosol and cloud microphysical changes despite unprecedented decline in Nitrogen Oxide pollution during the February 2020 COVID-19 shutdown in China. *Geophysical Research Letters* **47**(17): e2020GL088913. DOI: http://dx.doi.org/10.1029/2020GL088913.

Diffenbaugh, NS, Field, CB, Appel, EA, Azevedo, IL, Baldocchi, DD, Burke, M, Burney, JA, Ciais, P, Davis, SJ, Fiore, AM, Fletcher, SM, Hertel, TW, Horton, DE, Hsiang, SM, Jackson, RB, Jin, X, Levi, M, Lobell, DB, McKinley, GA, Moore, FC, Montgomery, A, Nadeau, KC, Pataki, DE, Randerson, JT, Reichstein, M, Schnell, JL, Seneviratne, SI, Singh, D, Steiner, AL, Wong-Parodi, G. 2020. The COVID-19 lockdowns: A window into the Earth System. *Nature Reviews Earth & Environment* **1**: 470–481. DOI: http://dx.doi.org/10.1038/s43017-020-0079-1.

Ding, J, van der, ARJ, Eskes, HJ, Mijling, B, Stavrakou, T, van Geffen, JHGM, Veefkind, JP. 2020. NO_x emissions reduction and rebound in China due to the COVID-19 crisis. *Geophysical Research Letters* **47**(19): e2020GL089912. DOI: http://dx.doi.org/10.1029/2020GL089912.

Environmental Protection Agency. 2020. Air data: Air quality data collected at outdoor monitors across the US. Available at https://www.epa.gov/outdoor-air-quality-data. Assessed 15 November 2020.

European Monitoring and Evaluation Programme. 2020. European database. DOI: http://dx.doi.org/http://ebas.nilu.no.

Fan, C, Li, Y, Guang, J, Li, Z, Elnashar, A, Allam, M, de Leeuw, G. 2020. The impact of the control measures during the COVID-19 outbreak on air pollution in China. *Remote Sensing* **12**(10). DOI: http://dx.doi.org/10.3390/rs12101613.

Fareed, Z, Iqbal, N, Shahzad, F, Shah, SGM, Zulfiqar, B, Shahzad, K, Hashmi, SH, Shahzad, U. 2020. Co-variance nexus between COVID-19 mortality, humidity, and air quality index in Wuhan, China: New insights from partial and multiple wavelet coherence. *Air Quality, Atmosphere & Health* **13**(6): 673–682. DOI: http://dx.doi.org/10.1007/s11869-020-00847-1.

Faridi, S, Yousefian, F, Niazi, S, Ghalhari, MR, Hassanvand, MS, Naddafi, K. 2020. Impact of SARS-CoV-2 on ambient air particulate matter in Tehran. *Aerosol and Air Quality Research* **20**(8): 1805–1811. DOI: http://dx.doi.org/10.4209/aaqr.2020.05.0225.

Filippini, T, Rothman, KJ, Goffi, A, Ferrari, F, Maffeis, G, Orsini, N, Vinceti, M. 2020. Satellite-detected tropospheric nitrogen dioxide and spread of SARS-CoV-2 infection in Northern Italy. *Science of the Total Environment* **739**. DOI: http://dx.doi.org/10.1016/j.scitotenv.2020.140278.

Forster, PM, Forster, HI, Evans, MJ, Gidden, MJ, Jones, CD, Keller, CA, Lamboll, RD, Quéré, CL, Rogelj, J, Rosen, D, Schleussner, C-F, Richardson, TB, Smith, CJ, Turnock, ST. 2020. Current and future global climate impacts resulting from COVID-19. *Nature Climate Change* **10**: 913–919. DOI: http://dx.doi.org/10.1038/s41558-020-0883-0.

Fu, F, Purvis-Roberts, KL, Williams, B. 2020. Impact of the COVID-19 pandemic lockdown on air pollution in 20 major cities around the world. *Atmosphere* **11**(11). DOI: http://dx.doi.org/10.3390/atmos11111189.

Gakidou, E, Afshin, A, Abajobir, AA, Abate, KH, Abbafati, C, Abbas, KM, Abd-Allah, F, Abdulle, AM, Abera, SF, Aboyans, V, Abu-Raddad, LJ, Abu-Rmeileh, NME, Abyu, GY, Adedeji, IA, Adetokunboh, O, Afarideh, M, Agrawal, A, Agrawal, S, Ahmadieh, H, Ahmed, MB, Aichour, MTE, Aichour, AN, Aichour, I, Akinyemi, RO, Akseer, N, Alahdab, F, Al-Aly, Z, Alam, K, Alam, N, Alam, T, Alasfoor, D, Alene, KA, Ali, K, Alizadeh-Navaei, R, Alkerwi, Aa, Alla, F, Allebeck, P, Al-Raddadi, R, Alsharif, U, Altirkawi, KA, Alvis-Guzman, N, Amare, AT, Amini, E, Ammar, W, Amoako, YA, Ansari, H, Antó JM, Antonio, CAT, Anwari, P, Arian, N, Ärnlöv, J, Artaman, A, Aryal, KK, Asayesh, H, Asgedom, SW, Atey, TM, Avila-Burgos, L, Avokpaho, EFGA, Awasthi, A, Azzopardi, P, Bacha, U, Badawi, A, Balakrishnan, K, Ballew, SH, Barac, A, Barber, RM, Barker-Collo, SL, Bärnighausen, T, Barquera, S, Barregard, L, Barrero, LH, Batis, C, Battle, KE, Baumgarner, BR, Baune, BT, Beardsley, J, Bedi, N, Beghi, E, Bell, ML, Bennett, DA, Bennett, JR, Bensenor, IM, Berhane, A, Berhe, DF, Bernabé E, Betsu, BD, Beuran, M, Beyene, AS, Bhansali, A, Bhutta, ZA, Bicer, BK, Bikbov, B, Birungi, C, Biryukov, S, Blosser, CD, Boneya, DJ, Bou-Orm, IR, Brauer, M,

Breitborde, NJK, Brenner, H, Brugha, TS, Bulto, LNB, Butt, ZA, Cahuana-Hurtado, L, Cárdenas, R, Carrero, JJ, Castañeda-Orjuela, CA, Catalá-López, F, Cercy, K, Chang, H-Y, Charlson, FJ, Chimed-Ochir, O, Chisumpa, VH, Chitheer, AA, Christensen, H, Christopher, DJ, Cirillo, M, Cohen, AJ, Comfort, H, Cooper, C, Coresh, J, Cornaby, L, Cortesi, PA, Criqui, MH, Crump, JA, Dandona, L, Dandona, R, das Neves, J, Davey, G, Davitoiu, DV, Davletov, K, de Courten, B, Defo, BK, Degenhardt, L, Deiparine, S, Dellavalle, RP, Deribe, K, Deshpande, A, Dharmaratne, SD, Ding, EL, Djalalinia, S, Do, HP, Dokova, K, Doku, DT, Donkelaar, Av, Dorsey, ER, Driscoll, TR, Dubey, M, Duncan, BB, Duncan, S, Ebrahimi, H, El-Khatib, ZZ, Enayati, A, Endries, AY, Ermakov, SP, Erskine, HE, Eshrati, B, Eskandarieh, S, Esteghamati, A, Estep, K, Faraon, EJA, Farinha, CSeS, Faro, A, Farzadfar, F, Fay, K, Feigin, VL, Fereshtehnejad, S-M, Fernandes, JC, Ferrari, AJ, Feyissa, TR, Filip, I, Fischer, F, Fitzmaurice, C, Flaxman, AD, Foigt, N, Foreman, KJ, Frostad, JJ, Fullman, N, Fürst, T, Furtado, JM, Ganji, M, Garcia-Basteiro, AL, Gebrehiwot, TT, Geleijnse, JM, Geleto, A, Gemechu, BL, Gesesew, HA, Gething, PW, Ghajar, A, Gibney, KB, Gill, PS, Gillum, RF, Giref, AZ, Gishu, MD, Giussani, G, Godwin, WW, Gona, PN, Goodridge, A, Gopalani, SV, Goryakin, Y, Goulart, AC, Graetz, N, Gugnani, HC, Guo, J, Gupta, R, Gupta, T, Gupta, V, Gutiérrez, RA, Hachinski, V, Hafezi-Nejad, N, Hailu, GB, Hamadeh, RR, Hamidi, S, Hammami, M, Handal, AJ, Hankey, GJ, Hanson, SW, Harb, HL, Hareri, HA, Hassanvand, MS, Havmoeller, R, Hawley, C, Hay, SI, Hedayati, MT, Hendrie, D, Heredia-Pi, IB, Hernandez, JCM, Hoek, HW, Horita, N, Hosgood, HD, Hostiuc, S, Hoy, DG, Hsairi, M, Hu, G, Huang, JJ, Huang, H, Ibrahim, NM, Iburg, KM, Ikeda, C, Inoue, M, Irvine, CMS, Jackson, MD, Jacobsen, KH, Jahanmehr, N, Jakovljevic, MB, Jauregui, A, Javanbakht, M, Jeemon, P, Johansson, LRK, Johnson, CO, Jonas, JB, Jürisson, M, Kabir, Z, Kadel, R, Kahsay, A, Kamal, R, Karch, A, Karema, CK, Kasaeian, A, Kassebaum, NJ, Kastor, A, Katikireddi, SV, Kawakami, N, Keiyoro, PN, Kelbore, SG, Kemmer, L, Kengne, AP, Kesavachandran, CN, Khader, YS, Khalil, IA, Khan, EA, Khang, Y-H, Khosravi, A, Khubchandani, J, Kiadaliri, AA, Kieling, C, Kim, JY, Kim, YJ, Kim, D, Kimokoti, RW, Kinfu, Y, Kisa, A, Kissimova-Skarbek, KA, Kivimaki, M, Knibbs, LD, Knudsen, AK, Kopec, JA, Kosen, S, Koul, PA, Koyanagi, A, Kravchenko, M, Krohn, KJ, Kromhout, H, Kumar, GA, Kutz, M, Kyu, HH, Lal, DK, Lalloo, R, Lallukka, T, Lan, Q, Lansingh, VC, Larsson, A, Lee, PH, Lee, A, Leigh, J, Leung, J, Levi, M, Levy, TS, Li, Y, Li, Y, Liang, X, Liben, ML, Linn, S, Liu, P, Lodha, R, Logroscino, G, Looker, KJ, Lopez, AD, Lorkowski, S, Lotufo, PA, Lozano, R, Lunevicius, R, Macarayan, ERK, Magdy Abd El Razek, H, Magdy Abd El Razek, M, Majdan, M, Majdzadeh, R, Majeed, A, Malekzadeh, R, Malhotra, R, Malta, DC, Mamun, AA, Manguerra, H, Mantovani, LG, Mapoma, CC, Martin, RV, Martinez-Raga, J, Martins-Melo, FR, Mathur, MR, Matsushita, K, Matzopoulos, R, Mazidi, M, McAlinden, C, McGrath, JJ, Mehata, S, Mehndiratta, MM, Meier, T, Melaku, YA, Memiah, P, Memish, ZA, Mendoza, W, Mengesha, MM, Mensah, GA, Mensink, GBM, Mereta, ST, Meretoja, TJ, Meretoja, A, Mezgebe, HB, Micha, R, Millear, A, Miller, TR, Minnig, S, Mirarefin, M, Mirrakhimov, EM, Misganaw, A, Mishra, SR, Mohammad, KA, Mohammed, KE, Mohammed, S, Mohan, MBV, Mokdad, AH, Monasta, L, Montico, M, Moradi-Lakeh, M, Moraga, P, Morawska, L, Morrison, SD, Mountjoy-Venning, C, Mueller, UO, Mullany, EC, Muller, K, Murthy, GVS, Musa, KI, Naghavi, M, Naheed, A, Nangia, V, Natarajan, G, Negoi, RI, Negoi, I, Nguyen, CT, Nguyen, QL, Nguyen, TH, Nguyen, G, Nguyen, M, Nichols, E, Ningrum, DNA, Nomura, M, Nong, VM, Norheim, OF, Norrving, B, Noubiap, JJN, Obermeyer, CM, Ogbo, FA, Oh, I-H, Oladimeji, O, Olagunju, AT, Olagunju, TO, Olivares, PR, Olsen, HE, Olusanya, BO, Olusanya, JO, Opio, JN, Oren, E, Ortiz, A, Ota, E, Owolabi, MO, Pa, M, Pacella, RE, Pana, A, Panda, BK, Panda-Jonas, S, Pandian, JD, Papachristou, C, Park, E-K, Parry, CD, Patten, SB, Patton, GC, Pereira, DM, Perico, N, Pesudovs, K, Petzold, M, Phillips, MR, Pillay, JD, Piradov, MA, Pishgar, F, Plass, D, Pletcher, MA, Polinder, S, Popova, S, Poulton, RG, Pourmalek, F, Prasad, N, Purcell, C, Qorbani, M, Radfar, A, Rafay, A, Rahimi-Movaghar, A, Rahimi-Movaghar, V, Rahman, MHU, Rahman, MA, Rahman, M, Rai, RK, Rajsic, S, Ram, U, Rawaf, S, Rehm, CD, Rehm, J, Reiner, RC, Reitsma, MB, Remuzzi, G, Renzaho, AMN, Resnikoff, S, Reynales-Shigematsu, LM, Rezaei, S, Ribeiro, AL, Rivera, JA, Roba, KT, Rojas-Rueda, D, Roman, Y, Room, R, Roshandel, G, Roth, GA, Rothenbacher, D, Rubagotti, E, Rushton, L, Sadat, N, Safdarian, M, Safi, S, Safiri, S, Sahathevan, R, Salama, J, Salomon, JA, Samy, AM, Sanabria, JR, Sanchez-Niño, MD, Sánchez-Pimienta, TG, Santomauro, D, Santos, IS, Santric, Milicevic, MM, Sartorius, B, Satpathy, M, Sawhney, M, Saxena, S, Schmidt, MI, Schneider, IJC, Schutte, AE, Schwebel, DC, Schwendicke, F, Seedat, S, Sepanlou, SG, Serdar, B, Servan-Mori, EE, Shaddick, G, Shaheen, A, Shahraz, S, Shaikh, MA, Shamsipour, M, Shamsizadeh, M, Shariful Islam, SM, Sharma, J, Sharma, R, She, J, Shen, J, Shi, P, Shibuya, K, Shields, C, Shiferaw, MS, Shigematsu, M, Shin, M-J, Shiri, R, Shirkoohi, R, Shishani, K, Shoman, H, Shrime, MG, Sigfusdottir, ID, Silva, DAS, Silva, JP, Silveira, DGA, Singh, JA, Singh, V, Sinha, DN, Skiadaresi, E, Slepak, EL, Smith, DL, Smith, M, Sobaih, BHA, Sobngwi, E,

Soneji, S, Sorensen, RJD, Sposato, LA, Sreeramareddy, CT, Srinivasan, V, Steel, N, Stein, DJ, Steiner, C, Steinke, S, Stokes, MA, Strub, B, Subart, M, Sufiyan, MB, Suliankatchi, RA, Sur, PJ, Swaminathan, S, Sykes, BL, Szoeke, CEI, Tabarés-Seisdedos, R, Tadakamadla, SK, Takahashi, K, Takala, JS, Tandon, N, Tanner, M, Tarekegn, YL, Tavakkoli, M, Tegegne, TK, Tehrani-Banihashemi, A, Terkawi, AS, Tesssema, B, Thakur, JS, Thamsuwan, O, Thankappan, KR, Theis, AM, Thomas, ML, Thomson, AJ, Thrift, AG, Tillmann, T, Tobe-Gai, R, Tobollik, M, Tollanes, MC, Tonelli, M, Topor-Madry, R, Torre, A, Tortajada, M, Touvier, M, Tran, BX, Truelsen, T, Tuem, KB, Tuzcu, EM, Tyrovolas, S, Ukwaja, KN, Uneke, CJ, Updike, R, Uthman, OA, van Boven, JFM, Varughese, S, Vasankari, T, Veerman, LJ, Venkateswaran, V, Venketasubramanian, N, Violante, FS, Vladimirov, SK, Vlassov, VV, Vollset, SE, Vos, T, Wadilo, F, Wakayo, T, Wallin, MT, Wang, Y-P, Weichenthal, S, Weiderpass, E, Weintraub, RG, Weiss, DJ, Werdecker, A, Westerman, R, Whiteford, HA, Wiysonge, CS, Woldeyes, BG, Wolfe, CDA, Woodbrook, R, Workicho, A, Xavier, D, Xu, G, Yadgir, S, Yakob, B, Yan, LL, Yaseri, M, Yimam, HH, Yip, P, Yonemoto, N, Yoon, S-J, Yotebieng, M, Younis, MZ, Zaidi, Z, Zaki, MES, Zavala-Arciniega, L, Zhang, X, Zimsen, SRM, Zipkin, B, Zodpey, S, Lim, SS, Murray, CJL. 2017. Global, regional, and national comparative risk assessment of 84 behavioural, environmental and occupational, and metabolic risks or clusters of risks, 1990–2016: A systematic analysis for the Global Burden of Disease Study 2016. *The Lancet* **390**(10100): 1345–1422. DOI: http://dx.doi.org/10.1016/S0140-6736(17)32366-8.

Gautam, AS, Dilwaliya, NK, Srivastava, A, Kumar, S, Bauddh, K, Siingh, D, Shah, MA, Singh, K, Gautam, S. 2020. Temporary reduction in air pollution due to anthropogenic activity switch-off during COVID-19 lockdown in northern parts of India. *Environment, Development and Sustainability*. DOI: http://dx.doi.org/10.1007/s10668-020-00994-6.

Gautam, S. 2020a. COVID-19: Air pollution remains low as people stay at home. *Air Quality, Atmosphere & Health* **13**(7): 853–857. DOI: http://dx.doi.org/10.1007/s11869-020-00842-6.

Gautam, S. 2020b. The influence of COVID-19 on air quality in India: A boon or inutile. *Bulletin of Environmental Contamination and Toxicology* **104**(6): 724–726. DOI: http://dx.doi.org/10.1007/s00128-020-02877-y.

Ghahremanloo, M, Lops, Y, Choi, Y, Mousavinezhad, S. 2020. Impact of the COVID-19 outbreak on air pollution levels in East Asia. *Science of the Total Environment* **754**. DOI: http://dx.doi.org/10.1016/j.scitotenv.2020.142226.

Giani, P, Castruccio, S, Anav, A, Howard, D, Hu, W, Crippa, P. 2020. Short-term and long-term health impacts of air pollution reductions from COVID-19 lockdowns in China and Europe: A modelling study. *The Lancet Planetary Health*. DOI: http://dx.doi.org/10.1016/S2542-5196(20)30224-2.

Goldberg, DL, Anenberg, SC, Griffin, D, McLinden, CA, Lu, Z, Streets, DG. 2020. Disentangling the impact of the COVID-19 lockdowns on urban NO_2 from natural variability. *Geophysical Research Letters*. DOI: http://dx.doi.org/10.1029/2020GL089269.

Google. 2020. Google Scholar. Available at https://scholar.google.com/. Assessed 1 October 2020.

Grell, GA, Peckham, SE, Schmitz, R, McKeen, SA, Frost, G, Skamarock, WC, Eder, B. 2005. Fully coupled "online" chemistry within the WRF model. *Atmospheric Environment* **39**(37): 6957–6975. DOI: http://dx.doi.org/10.1016/j.atmosenv.2005.04.027.

Griffith, SM, Huang, WS, Lin, CC, Chen, YC, Chang, KE, Lin, TH, Wang, SH, Lin, NH. 2020. Long-range air pollution transport in East Asia during the first week of the COVID-19 lockdown in China. *Science of the Total Environment* **741**. DOI: http://dx.doi.org/10.1016/j.scitotenv.2020.140214.

Gualtieri, G, Brilli, L, Carotenuto, F, Vagnoli, C, Zaldei, A, Gioli, B. 2020. Quantifying road traffic impact on air quality in urban areas: A Covid19-induced lockdown analysis in Italy. *Environmental Pollution* **267**. DOI: http://dx.doi.org/10.1016/j.envpol.2020.115682.

Guo, H, Sullivan, AP, Campuzano-Jost, P, Schroder, JC, Lopez-Hilfiker, FD, Dibb, JE, Jimenez, JL, Thornton, JA, Brown, SS, Nenes, A, Weber, RJ. 2016. Fine particle pH and the partitioning of nitric acid during winter in the northeastern United States. *Journal of Geophysical Research: Atmospheres* **121**(17): 10355–10376. DOI: http://dx.doi.org/10.1002/2016JD025311.

Hale, T, Webster, S, Petherick, A, Phillips, T, Kira, B. 2020. *Oxford COVID-19 government response tracker* [data set]. University of Oxford, UK: Government BSo. Available at https://www.bsg.ox.ac.uk/research/research-projects/coronavirus-government-response-tracker. Accessed 1 October 2020.

Han, BS, Park, K, Kwak, KH, Park, SB, Jin, HG, Moon, S, Kim, JW, Baik, JJ. 2020. Air quality change in Seoul, South Korea under COVID-19 social distancing: Focusing on $PM_{2.5}$. *International Journal of Environmental Research and Public Health* **17**(17). DOI: http://dx.doi.org/10.3390/ijerph17176208.

Harshita, S, Vivek, KP. 2020. Understanding the lockdown impact in Delhi due to COVID-19 by using micro level temporal analysis of six criteria pollutants. *Journal of Indian Geophysical Union* **24**(3): 72–79.

Hashim, BM, Al-Naseri, SK, Al-Maliki, A, Al-Ansari, N. 2020. Impact of COVID-19 lockdown on NO_2, O_3, $PM_{2.5}$ and PM_{10} concentrations and assessing air quality changes in Baghdad, Iraq. *Science of the Total Environment* **754**. DOI: http://dx.doi.org/10.1016/j.scitotenv.2020.141978.

He, G, Pan, Y, Tanaka, T. 2020. The short-term impacts of COVID-19 lockdown on urban air pollution in China. *Nature Sustainability* **3**: 1005–1011. DOI: http://dx.doi.org/10.1038/s41893-020-0581-y.

He, K. 2012. Multi-resolution Emission Inventory for China (MEIC): Model framework and 1990–2010 anthropogenic emissions. A32B-05. Available at https://ui.adsabs.harvard.edu/abs/2012AGUFM.A32B.05H. Accessed 15 November 2020.

Henze, DK, Hakami, A, Seinfeld, JH. 2007. Development of the adjoint of GEOS-Chem. *Atmospheric Chemistry and Physics* **7**(9): 2413–2433. DOI: http://dx.doi.org/10.5194/acp-7-2413-2007.

Higham, JE, Ramírez, CA, Green, MA, Morse, AP. 2020. UK COVID-19 lockdown: 100 days of air pollution reduction? *Air Quality, Atmosphere & Health*. DOI: http://dx.doi.org/10.1007/s11869-020-00937-0.

Homan, CD, Volk, CM, Kuhn, AC, Werner, A, Baehr, J, Viciani, S, Ulanovski, A, Ravegnani, F. 2010. Tracer measurements in the tropical tropopause layer during the AMMA/SCOUT-O3 aircraft campaign. *Atmospheric Chemistry and Physics* **10**(8): 3615–3627. DOI: http://dx.doi.org/10.5194/acp-10-3615-2010.

Huang, G, Sun, K. 2020. Non-negligible impacts of clean air regulations on the reduction of tropospheric NO_2 over East China during the COVID-19 pandemic observed by OMI and TROPOMI. *Science of the Total Environment* **745**. DOI: http://dx.doi.org/10.1016/j.scitotenv.2020.141023.

Huang, X, Ding, A, Gao, J, Zheng, B, Zhou, D, Qi, X, Tang, R, Wang, J, Ren, C, Nie, W, Chi, X, Xu, Z, Chen, L, Li, Y, Che, F, Pang, N, Wang, H, Tong, D, Qin, W, Cheng, W, Liu, W, Fu, Q, Liu, B, Chai, F, Davis, SJ, Zhang, Q, He, K. 2020. Enhanced secondary pollution offset reduction of primary emissions during COVID-19 lockdown in China. *National Science Review* **8**(2). DOI: http://dx.doi.org/10.1093/nsr/nwaa137.

Hudda, N, Simon, MC, Patton, AP, Durant, JL. 2020. Reductions in traffic-related black carbon and ultrafine particle number concentrations in an urban neighborhood during the COVID-19 pandemic. *Science of the Total Environment* **742**. DOI: http://dx.doi.org/10.1016/j.scitotenv.2020.140931.

Inness, A, Ades, M, Agustí-Panareda, A, Barré, J, Benedictow, A, Blechschmidt, AM, Dominguez, JJ, Engelen, R, Eskes, H, Flemming, J, Huijnen, V, Jones, L, Kipling, Z, Massart, S, Parrington, M, Peuch, VH, Razinger, M, Remy, S, Schulz, M, Suttie, M. 2019. The CAMS reanalysis of atmospheric composition. *Atmospheric Chemistry and Physics* **19**(6): 3515–3556. DOI: http://dx.doi.org/10.5194/acp-19-3515-2019.

Jain, S, Sharma, T. 2020. Social and travel lockdown impact considering coronavirus Disease (COVID-19) on air quality in megacities of India: Present benefits, future challenges and way forward. *Aerosol and Air Quality Research* **20**: 1222–1236. DOI: http://dx.doi.org/10.4209/aaqr.2020.04.0171.

Jakovljević, I, Štrukil, ZS, Godec, R, Davila, S, Pehnec, G. 2020. Influence of lockdown caused by the COVID-19 pandemic on air pollution and carcinogenic content of particulate matter observed in Croatia. *Air Quality, Atmosphere & Health*. DOI: http://dx.doi.org/10.1007/s11869-020-00950-3.

Jia, C, Fu, X, Bartelli, D, Smith, L. 2020a. Insignificant impact of the "Stay-At-Home" order on ambient air quality in the Memphis metropolitan area, U.S.A. *Atmosphere* **11**(6). DOI: http://dx.doi.org/10.3390/atmos11060630.

Jia, H, Huo, J, Fu, Q, Duan, Y, Lin, Y, Jin, X, Hu, X, Cheng, J. 2020b. Insights into chemical composition, abatement mechanisms and regional transport of atmospheric pollutants in the Yangtze River Delta region, China during the COVID-19 outbreak control period. *Environmental Pollution* **267**. DOI: http://dx.doi.org/10.1016/j.envpol.2020.115612.

Jiayu, L, Federico, T. 2020. Changes in air quality during the COVID-19 lockdown in Singapore and associations with human mobility trends. *Aerosol and Air Quality Research* **20**: 1748–1758. DOI: http://dx.doi.org/10.4209/aaqr.2020.06.0303.

Ju, MJ, Oh, J, Choi, Y-H. 2020. Changes in air pollution levels after COVID-19 outbreak in Korea. *Science of the Total Environment* **750**. DOI: http://dx.doi.org/10.1016/j.scitotenv.2020.141521.

Kanniah, KD, Kamarul Zaman, NAF, Kaskaoutis, DG, Latif, MT. 2020. COVID-19's impact on the atmospheric environment in the Southeast Asia region. *Science of the Total Environment* **736**. DOI: http://dx.doi.org/10.1016/j.scitotenv.2020.139658.

Kant, Y, Mitra, D, Chauhan, A. 2020. Space-based observations on the impact of COVID-19-induced lockdown on aerosols over India. *Current Science* **119**(3): 539–544. DOI: http://dx.doi.org/ 10.18520/cs/v119/i3/539-544.

Kerimray, A, Baimatova, N, Ibragimova, OP, Bukenov, B, Kenessov, B, Plotitsyn, P, Karaca, F. 2020. Assessing air quality changes in large cities during COVID-19 lockdowns: The impacts of traffic-free urban conditions in Almaty, Kazakhstan. *Science of the Total Environment* **730**. DOI: http://dx.doi.org/10.1016/j.scitotenv.2020.139179.

Khoder, MI. 2009. Diurnal, seasonal and weekdays–weekends variations of ground level ozone concentrations in an urban area in greater Cairo. *Environmental Monitoring and Assessment* **149**(1): 349–362. DOI: http://dx.doi.org/10.1007/s10661-008-0208-7.

Kiendler-Scharr, A, Mensah, AA, Friese, E, Topping, D, Nemitz, E, Prevot, ASH, Äijälä, M, Allan, J, Canonaco, F, Canagaratna, M, Carbone, S, Crippa, M, Dall Osto, M, Day, DA, De Carlo, P, Di Marco, CF, Elbern, H, Eriksson, A, Freney, E, Hao, L, Herrmann, H, Hildebrandt, L, Hillamo, R, Jimenez, JL, Laaksonen, A, McFiggans, G, Mohr, C, O'Dowd, C, Otjes, R, Ovadnevaite, J, Pandis, SN, Poulain, L, Schlag, P, Sellegri, K, Swietlicki, E, Tiitta, P, Vermeulen, A, Wahner, A, Worsnop, D,

Wu, HC. 2016. Ubiquity of organic nitrates from nighttime chemistry in the European submicron aerosol. *Geophysical Research Letters* **43**(14): 7735–7744. DOI: http://dx.doi.org/10.1002/2016GL069239.

Krecl, P, Targino, AC, Oukawa, GY, Cassino Junior, RP. 2020. Drop in urban air pollution from COVID-19 pandemic: Policy implications for the megacity of São Paulo. *Environmental Pollution* **265**. DOI: http://dx.doi.org/10.1016/j.envpol.2020.114883.

Kristiansen, NI, Arnold, D, Maurer, C, Vira, J, Rădulescu, R, Martin, D, Stohl, A, Stebel, K, Sofiev, M, O'Dowd, C, Wotawa, G. 2016. Improving model simulations of volcanic emission clouds and assessing model uncertainties, in Riley, K, Webley, P, Thompson, M, Webley, P eds., *Natural Hazard Uncertainty Assessment*. Available at https://doi.org/10.1002/9781119028116.ch8.

Kroll, JH, Heald, CL, Cappa, CD, Farmer, DK, Fry, JL, Murphy, JG, Steiner, AL. 2020. The complex chemical effects of COVID-19 shutdowns on air quality. *Nature Chemistry* **12**(9): 777–779. DOI: http://dx.doi.org/10.1038/s41557-020-0535-z.

Kumar, P, Hama, S, Omidvarborna, H, Sharma, A, Sahani, J, Abhijith, KV, Debele, SE, Zavala-Reyes, JC, Barwise, Y, Tiwari, A. 2020. Temporary reduction in fine particulate matter due to 'anthropogenic emissions switch-off' during COVID-19 lockdown in Indian cities. *Sustainable Cities and Society* **62**. DOI: http://dx.doi.org/10.1016/j.scs.2020.102382.

Kumari, P, Toshniwal, D. 2020. Impact of lockdown measures during COVID-19 on air quality—A case study of India. *International Journal of Environmental Health Research* 1–8. DOI: http://dx.doi.org/10.1080/09603123.2020.1778646.

Kumari, S, Lakhani, A, Kumari, KM. 2020. COVID-19 and air pollution in Indian cities: World's most polluted cities. *Aerosol and Air Quality Research* **20**. DOI: http://dx.doi.org/10.4209/aaqr.2020.05.0262.

Laughner, JL, Cohen, RC. 2019. Direct observation of changing NO_x lifetime in North American cities. *Science* **366**(6466): 723. DOI: http://dx.doi.org/10.1126/science.aax6832.

Le, T, Wang, Y, Liu, L, Yang, J, Yung, YL, Li, G, Seinfeld, JH. 2020a. Unexpected air pollution with marked emission reductions during the COVID-19 outbreak in China. *Science* **369**(6504): 702. DOI: http://dx.doi.org/10.1126/science.abb7431.

Le, VV, Huynh, TT, Ölçer, A, Hoang, AT, Le, AT, Nayak, SK, Pham, VV. 2020b. A remarkable review of the effect of lockdowns during COVID-19 pandemic on global PM emissions. *Energy Sources, Part A: Recovery, Utilization, and Environmental Effects* 1–16. DOI: http://dx.doi.org/10.1080/15567036.2020.1853854.

Lei, MT, Monjardino, J, Mendes, L, Gonçalves, D, Ferreira, F. 2020. Statistical forecast of pollution episodes in Macao during national holiday and COVID-19. *International Journal of Environmental Research and Public Health* **17**(14). DOI: http://dx.doi.org/10.3390/ijerph17145124.

Le Quéré, C, Jackson, RB, Jones, MW, Smith, AJP, Abernethy, S, Andrew, RM, De-Gol, AJ, Willis, DR, Shan, Y, Canadell, JG, Friedlingstein, P, Creutzig, F, Peters, GP. 2020. Temporary reduction in daily global CO_2 emissions during the COVID-19 forced confinement. *Nature Climate Change* **10**(7): 647–653. DOI: http://dx.doi.org/10.1038/s41558-020-0797-x.

Li, L, Li, Q, Huang, L, Wang, Q, Zhu, A, Xu, J, Liu, Z, Li, H, Shi, L, Li, R, Azari, M, Wang, Y, Zhang, X, Liu, Z, Zhu, Y, Zhang, K, Xue, S, Ooi, MCG, Zhang, D, Chan, A. 2020a. Air quality changes during the COVID-19 lockdown over the Yangtze River Delta Region: An insight into the impact of human activity pattern changes on air pollution variation. *Science of the Total Environment* **732**. DOI: http://dx.doi.org/10.1016/j.scitotenv.2020.139282.

Li, Z, Meng, J, Zhou, L, Zhou, R, Fu, M, Wang, Y, Yi, Y, Song, A, Guo, Q, Hou, Z, Yan, L. 2020b. Impact of the COVID-19 Event on the Characteristics of Atmospheric Single Particle in the Northern China. *Aerosol and Air Quality Research* **20**(8): 1716–1726. DOI: http://dx.doi.org/10.4209/aaqr.2020.06.0321.

Lian, X, Huang, J, Huang, R, Liu, C, Wang, L, Zhang, T. 2020. Impact of city lockdown on the air quality of COVID-19-hit of Wuhan city. *Science of the Total Environment* **742**. DOI: http://dx.doi.org/10.1016/j.scitotenv.2020.140556.

Liu, F, Page, A, Strode, SA, Yoshida, Y, Choi, S, Zheng, B, Lamsal, LN, Li, C, Krotkov, NA, Eskes, H, van der, AR, Veefkind, P, Levelt, PF, Hauser, OP, Joiner, J. 2020a. Abrupt decline in tropospheric nitrogen dioxide over China after the outbreak of COVID-19. *Science Advances* **6**(28). DOI: http://dx.doi.org/10.1126/sciadv.abc2992.

Liu, F, Wang, M, Zheng, M. 2021a. Effects of COVID-19 lockdown on global air quality and health. *Science of the Total Environment* **755**. DOI: http://dx.doi.org/10.1016/j.scitotenv.2020.142533.

Liu, Q, Harris, JT, Chiu, LS, Sun, D, Houser, PR, Yu, M, Duffy, DQ, Little, MM, Yang, C. 2021b. Spatiotemporal impacts of COVID-19 on air pollution in California, USA. *Science of the Total Environment* **750**. DOI: http://dx.doi.org/10.1016/j.scitotenv.2020.141592.

Liu, T, Wang, X, Hu, J, Wang, Q, An, J, Gong, K, Sun, J, Li, L, Qin, M, Li, J, Tian, J, Huang, Y, Liao, H, Zhou, M, Hu, Q, Yan, R, Wang, H, Huang, C. 2020b. Driving forces of changes in air quality during the COVID-19 lockdown period in the Yangtze River Delta region, China. *Environmental Science & Technology Letters* **7**(11): 779–786. DOI: http://dx.doi.org/10.1021/acs.estlett.0c00511.

Liu, Y, Ni, S, Jiang, T, Xing, S, Zhang, Y, Bao, X, Feng, Z, Fan, X, Zhang, L, Feng, H. 2020c. Influence of Chinese New Year overlapping COVID-19 lockdown on HONO sources in Shijiazhuang. *Science of the Total*

Environment **745**. DOI: http://dx.doi.org/10.1016/j.scitotenv.2020.141025.

Liu, Y, Stanturf, J, Goodrick, S. 2010. Trends in global wildfire potential in a changing climate. *Forest Ecology and Management* **259**(4): 685–697. DOI: http://dx.doi.org/10.1016/j.foreco.2009.09.002.

Liu, Z, Ciais, P, Deng, Z, Lei, R, Davis, SJ, Feng, S, Zheng, B, Cui, D, Dou, X, Zhu, B, Guo, R, Ke, P, Sun, T, Lu, C, He, P, Wang, Y, Yue, X, Wang, Y, Lei, Y, Zhou, H, Cai, Z, Wu, Y, Guo, R, Han, T, Xue, J, Boucher, O, Boucher, E, Chevallier, F, Tanaka, K, Wei, Y, Zhong, H, Kang, C, Zhang, N, Chen, B, Xi, F, Liu, M, Bréon, F-M, Lu, Y, Zhang, Q, Guan, D, Gong, P, Kammen, DM, He, K, Schellnhuber, HJ. 2020d. Near-real-time monitoring of global CO_2 emissions reveals the effects of the COVID-19 pandemic. *Nature Communications* **11**(1): 5172. DOI: http://dx.doi.org/10.1038/s41467-020-18922-7.

Ljubenkov, I, Haddout, S, Priya, KL, Hoguane, AM. 2020. SARS-CoV-2 epidemic: Changes in air quality during the lockdown in Zagreb (Republic of Croatia). *Toxicological & Environmental Chemistry* **102**(5–6): 302–303. DOI: http://dx.doi.org/10.1080/02772248.2020.1778703.

Ma, C-J, Kang, G-U. 2020. Air quality variation in Wuhan, Daegu, and Tokyo during the explosive outbreak of COVID-19 and its health effects. *International Journal of Environmental Research and Public Health* **17**(11). DOI: http://dx.doi.org/10.3390/ijerph17114119.

Mahato, S, Ghosh, KG. 2020. Short-term exposure to ambient air quality of the most polluted Indian cities due to lockdown amid SARS-CoV-2. *Environmental Research* **188**. DOI: http://dx.doi.org/10.1016/j.envres.2020.109835.

Mahato, S, Pal, S, Ghosh, KG. 2020. Effect of lockdown amid COVID-19 pandemic on air quality of the megacity Delhi, India. *Science of the Total Environment* **730**. DOI: http://dx.doi.org/10.1016/j.scitotenv.2020.139086.

Martorell-Marugán, J, Villatoro-García, JA, García-Moreno, A, López-Domínguez, R, Requena, F, Merelo, JJ, Lacasaña, M, de Dios Luna, J, Díaz-Mochón, JJ, Lorente, JA, Carmona-Sáez, P. 2021. DatAC: A visual analytics platform to explore climate and air quality indicators associated with the COVID-19 pandemic in Spain. *Science of the Total Environment* **750**. DOI: http://dx.doi.org/10.1016/j.scitotenv.2020.141424.

Masum, MH, Pal, SK. 2020. Statistical evaluation of selected air quality parameters influenced by COVID-19 lockdown. *Global Journal of Environmental Science and Management* **6**: 85–94. DOI: http://dx.doi.org/10.22034/GJESM.2019.06.SI.08.

McFiggans, G, Mentel, TF, Wildt, J, Pullinen, I, Kang, S, Kleist, E, Schmitt, S, Springer, M, Tillmann, R, Wu, C, Zhao, D, Hallquist, M, Faxon, C, Le Breton, M, Hallquist, ÅM, Simpson, D, Bergström, R, Jenkin, ME, Ehn, M, Thornton, JA, Alfarra, MR, Bannan, TJ, Percival, CJ, Priestley, M, Topping, D, Kiendler-Scharr, A. 2019. Secondary organic aerosol reduced by mixture of atmospheric vapours. *Nature* **565**(7741): 587–593. DOI: http://dx.doi.org/10.1038/s41586-018-0871-y.

Mendez-Espinosa, JF, Rojas, NY, Vargas, J, Pachón, JE, Belalcazar, LC, Ramírez, O. 2020. Air quality variations in Northern South America during the COVID-19 lockdown. *Science of the Total Environment* **749**. DOI: http://dx.doi.org/10.1016/j.scitotenv.2020.141621.

Menut, L, Bessagnet, B, Siour, G, Mailler, S, Pennel, R, Cholakian, A. 2020. Impact of lockdown measures to combat Covid-19 on air quality over Western Europe. *Science of the Total Environment* **741**. DOI: http://dx.doi.org/10.1016/j.scitotenv.2020.140426.

Metya, A, Dagupta, P, Halder, S, Chakraborty, S, Tiwari, YK. 2020. COVID-19 lockdowns improve air quality in the South-East Asian regions, as seen by the remote sensing satellites. *Aerosol and Air Quality Research* **20**(8): 1772–1782. DOI: http://dx.doi.org/10.4209/aaqr.2020.05.0240.

Miyazaki, K, Bowman, K, Sekiya, T, Jiang, Z, Chen, X, Eskes, H, Ru, M, Zhang, Y, Shindell, D. 2020. Air quality response in China linked to the 2019 novel coronavirus (COVID-19) lockdown. *Geophysical Research Letters* **47**(19). DOI: http://dx.doi.org/10.1029/2020GL089252.

Mohd Nadzir, MS, Ooi, MCG, Alhasa, KM, Bakar, MAA, Mohtar, AAA, Nor, MFFM, Latif, MT, Hamid, HHA, Ali, SHM, Ariff, NM, Anuar, J, Ahamad, F, Azhari, A, Hanif, NM, Subhi, MA, Othman, M, Nor, MZM. 2020. The impact of Movement Control Order (MCO) during pandemic COVID-19 on local air quality in an urban area of Klang Valley, Malaysia. *Aerosol and Air Quality Research* **20**(6): 1237–1248. DOI: http://dx.doi.org/10.4209/aaqr.2020.04.0163.

Naeger, AR, Murphy, K. 2020. Impact of COVID-19 containment measures on air pollution in California. *Aerosol and Air Quality Research* **20**. DOI: http://dx.doi.org/10.4209/aaqr.2020.05.0227.

Nakada, LYK, Urban, RC. 2020. COVID-19 pandemic: Impacts on the air quality during the partial lockdown in São Paulo state, Brazil. *Science of the Total Environment* **730**. DOI: http://dx.doi.org/10.1016/j.scitotenv.2020.139087.

Naqvi, HR, Datta, M, Mutreja, G, Siddiqui, MA, Naqvi, DF, Naqvi, AR. 2020. Improved air quality and associated mortalities in India under COVID-19 lockdown. *Environmental Pollution* **268**. DOI: http://dx.doi.org/10.1016/j.envpol.2020.115691.

Nault, BA, Campuzano-Jost, P, Day, DA, Schroder, JC, Anderson, B, Beyersdorf, AJ, Blake, DR, Brune, WH, Choi, Y, Corr, CA, de Gouw, JA, Dibb, J, DiGangi, JP, Diskin, GS, Fried, A, Huey, LG, Kim, MJ, Knote, CJ, Lamb, KD, Lee, T, Park, T, Pusede, SE, Scheuer, E, Thornhill, KL, Woo, JH, Jimenez, JL. 2018. Secondary organic aerosol production from local emissions dominates the organic aerosol budget over Seoul, South Korea, during KORUS-AQ. *Atmospheric Chemistry and Physics* **18**(24): 17769–

17800. DOI: http://dx.doi.org/10.5194/acp-18-17769-2018.

Navinya, C, Patidar, G, Phuleria, HC. 2020. Examining effects of the COVID-19 national lockdown on Ambient air quality across urban India. *Aerosol and Air Quality Research* **20**(8): 1759–1771. DOI: http://dx.doi.org/10.4209/aaqr.2020.05.0256.

Nichol, JE, Bilal, M, Ali, MA, Qiu, Z. 2020. Air pollution scenario over China during COVID-19. *Remote Sensing* **12**(13). DOI: http://dx.doi.org/10.3390/rs12132100.

Ordóñez, C, Garrido-Perez, JM, García-Herrera, R. 2020. Early spring near-surface ozone in Europe during the COVID-19 shutdown: Meteorological effects outweigh emission changes. *Science of the Total Environment* **747**. DOI: http://dx.doi.org/10.1016/j.scitotenv.2020.141322.

Otmani, A, Benchrif, A, Tahri, M, Bounakhla, M, Chakir, EM, El Bouch, M, Krombi, Mh. 2020. Impact of Covid-19 lockdown on PM_{10}, SO_2 and NO_2 concentrations in Salé City (Morocco). *Science of the Total Environment* **735**. DOI: http://dx.doi.org/10.1016/j.scitotenv.2020.139541.

Pacheco, H, Díaz-López, S, Jarre, E, Pacheco, H, Méndez, W, Zamora-Ledezma, E. 2020. NO_2 levels after the COVID-19 lockdown in Ecuador: A trade-off between environment and human health. *Urban Climate* **34**. DOI: http://dx.doi.org/10.1016/j.uclim.2020.100674.

Pan, S, Jung, J, Li, Z, Hou, X, Roy, A, Choi, Y, Gao, HO. 2020. Air quality implications of COVID-19 in California. *Sustainability* **12**(17). DOI: http://dx.doi.org/10.3390/su12177067.

Panda, S, Mallik, C, Nath, J, Das, T, Ramasamy, B. 2020. A study on variation of atmospheric pollutants over Bhubaneswar during imposition of nationwide lockdown in India for the COVID-19 pandemic. *Air Quality, Atmosphere & Health* **14**: 97–108. DOI: http://dx.doi.org/10.1007/s11869-020-00916-5.

Pant, G, Alka Garlapati, D, Gaur, A, Hossain, K, Singh, SV, Gupta, AK. 2020. Air quality assessment among populous sites of major metropolitan cities in India during COVID-19 pandemic confinement. *Environmental Science and Pollution Research* **27**(35): 44629–44636. DOI: http://dx.doi.org/10.1007/s11356-020-11061-y.

Park, H, Jeong, S, Koo, J-H, Sim, S, Bae, Y, Kim, Y, Park, C, Bang, J. 2020. Lessons from COVID-19 and Seoul: Effects of reduced human activity from social distancing on urban CO_2 concentration and air quality. *Aerosol and Air Quality Research* **20**. DOI: http://dx.doi.org/10.4209/aaqr.2020.07.0376.

Parra, R, Espinoza, C. 2020. Insights for air quality management from modeling and record studies in Cuenca, Ecuador. *Atmosphere* **11**(9). DOI: http://dx.doi.org/10.3390/atmos11090998.

Patel, H, Talbot, N, Salmond, J, Dirks, K, Xie, S, Davy, P. 2020. Implications for air quality management of changes in air quality during lockdown in Auckland (New Zealand) in response to the 2020 SARS-CoV-2 epidemic. *Science of the Total Environment* **746**. DOI: http://dx.doi.org/10.1016/j.scitotenv.2020.141129.

Pei, Z, Han, G, Ma, X, Su, H, Gong, W. 2020. Response of major air pollutants to COVID-19 lockdowns in China. *Science of the Total Environment* **743**. DOI: http://dx.doi.org/10.1016/j.scitotenv.2020.140879.

Petetin, H, Bowdalo, D, Soret, A, Guevara, M, Jorba, O, Serradell, K, Pérez García-Pando, C. 2020. Meteorology-normalized impact of the COVID-19 lockdown upon NO_2 pollution in Spain. *Atmospheric Chemistry and Physics* **20**(18): 11119–11141. DOI: http://dx.doi.org/10.5194/acp-20-11119-2020.

Petherick, A, Kira, B, Hale, T, Phillips, T, Webster, S, Cameron-Blake, E, Hallas, L, Majumdar, S, Tatlow, H. 2020. Variation in government responses to COVID-19. Available at https://www.bsg.ox.ac.uk/research/publications/variation-government-responses-covid-19. Accessed 1 October 2020.

Petzold, A, Thouret, V, Gerbig, C, Zahn, A, Brenninkmeijer, CAM, Cameron-Blake, E, Hallas, L, Majumdar, S, Tatlow, H. 2015. Global-scale atmosphere monitoring by in-service aircraft—Current achievements and future prospects of the European Research Infrastructure IAGOS. *Tellus B: Chemical and Physical Meteorology* **67**(1). DOI: http://dx.doi.org/10.3402/tellusb.v67.28452.

Phillips, CA, Caldas, A, Cleetus, R, Dahl, KA, Declet-Barreto, J, Licker, R, Merner, LD, Ortiz-Partida, JP, Phelan, AL, Spanger-Siegfried, E, Talati, S, Trisos, CH, Carlson, CJ. 2020. Compound climate risks in the COVID-19 pandemic. *Nature Climate Change* **10**(7): 586–588. DOI: http://dx.doi.org/10.1038/s41558-020-0804-2.

Qiu, Y, Ma, Z, Li, K, Lin, W, Tang, Y, Dong, F, Liao, H. 2020. Markedly enhanced levels of Peroxyacetyl Nitrate (PAN) during COVID-19 in Beijing. *Geophysical Research Letters* **47**(19). DOI: http://dx.doi.org/10.1029/2020GL089623.

Ranjan, AK, Patra, AK, Gorai, AK. 2020. Effect of lockdown due to SARS COVID-19 on aerosol optical depth (AOD) over urban and mining regions in India. *Science of the Total Environment* **745**. DOI: http://dx.doi.org/10.1016/j.scitotenv.2020.141024.

Raymond, C, Horton, RM, Zscheischler, J, Martius, O, AghaKouchak, A, Balch, J, Bowen, SG, Camargo, SJ, Hess, J, Kornhuber, K, Oppenheimer, M, Ruane, AC, Wahl, T, White, K. 2020. Understanding and managing connected extreme events. *Nature Climate Change* **10**(7): 611–621. DOI: http://dx.doi.org/10.1038/s41558-020-0790-4.

Resmi, CT, Nishanth, T, Satheesh Kumar, MK, Manoj, MG, Balachandramohan, M, Valsaraj, KT. 2020. Air quality improvement during triple-lockdown in the coastal city of Kannur, Kerala to combat Covid-19 transmission. *PeerJ* **8**: e9642–e9642. DOI: http://dx.doi.org/10.7717/peerj.9642.

Rodríguez-Urrego, D, Rodríguez-Urrego, L. 2020. Air quality during the COVID-19: $PM_{2.5}$ analysis in the 50 most polluted capital cities in the world.

Environmental Pollution **266**. DOI: http://dx.doi.org/10.1016/j.envpol.2020.115042.

Ropkins, K, Tate, J. 2020. Early observations on the impact of the COVID-19 lockdown on air quality trends across the UK. *Science of the Total Environment* **754**. DOI: http://dx.doi.org/10.1016/j.scitotenv.2020.142374.

Şahin, ÜA. 2020. The effects of COVID-19 measures on air pollutant concentrations at urban and traffic sites in Istanbul. *Aerosol and Air Quality Research* **20**(9): 1874–1885. DOI: http://dx.doi.org/10.4209/aaqr.2020.05.0239.

Seinfeld, JH, Pandis, SN. 2006. *Atmospheric chemistry and physics: From air pollution to climate change*. Second edition. Hoboken, NJ: Wiley-Interscience Publication.

Selvam, S, Muthukumar, P, Venkatramanan, S, Roy, PD, Manikanda Bharath, K, Jesuraja, K. 2020. SARS-CoV-2 pandemic lockdown: Effects on air quality in the industrialized Gujarat state of India. *Science of the Total Environment* **737**: 140391–140391. DOI: http://dx.doi.org/10.1016/j.scitotenv.2020.140391.

Shah, V, Jacob, DJ, Li, K, Silvern, RF, Zhai, S, Liu, M, Lin, J, Zhang, Q. 2020. Effect of changing NO_x lifetime on the seasonality and long-term trends of satellite-observed tropospheric NO_2 columns over China. *Atmospheric Chemistry and Physics* **20**(3): 1483–1495. DOI: http://dx.doi.org/10.5194/acp-20-1483-2020.

Shah, V, Jaeglé, L, Thornton, JA, Lopez-Hilfiker, FD, Lee, BH, Schroder, JC, Campuzano-Jost, P, Jimenez, JL, Guo, H, Sullivan, AP, Weber, RJ, Green, JR, Fiddler, MN, Bililign, S, Campos, TL, Stell, M, Weinheimer, AJ, Montzka, DD, Brown, SS. 2018. Chemical feedbacks weaken the wintertime response of particulate sulfate and nitrate to emissions reductions over the eastern United States. *Proceedings of the National Academy of Sciences* **115**(32): 8110. DOI: http://dx.doi.org/10.1073/pnas.1803295115.

Shakil, MH, Munim, ZH, Tasnia, M, Sarowar, S. 2020. COVID-19 and the environment: A critical review and research agenda. *Science of the Total Environment* **745**. DOI: http://dx.doi.org/10.1016/j.scitotenv.2020.141022.

Shakoor, A, Chen, X, Farooq, TH, Shahzad, U, Ashraf, F, Rehman, A, Sahar, Ne, Yan, W. 2020. Fluctuations in environmental pollutants and air quality during the lockdown in the USA and China: Two sides of COVID-19 pandemic. *Air Quality, Atmosphere & Health* **13**: 1335–1342. DOI: http://dx.doi.org/10.1007/s11869-020-00888-6.

Sharma, M, Jain, S, Lamba, BY. 2020a. Epigrammatic study on the effect of lockdown amid Covid-19 pandemic on air quality of most polluted cities of Rajasthan (India). *Air Quality, Atmosphere & Health* **13**(10): 1157–1165. DOI: http://dx.doi.org/10.1007/s11869-020-00879-7.

Sharma, S, Zhang, M, Anshika, Gao, J, Zhang, H, Kota, SH. 2020b. Effect of restricted emissions during COVID-19 on air quality in India. *Science of the Total Environment* **728**. DOI: http://dx.doi.org/10.1016/j.scitotenv.2020.138878.

Shen, L, Zhao, T, Wang, H, Liu, J, Bai, Y, Kong, S, Zheng, H, Zhu, Y, Shu, Z. 2021. Importance of meteorology in air pollution events during the city lockdown for COVID-19 in Hubei Province, Central China. *Science of the Total Environment* **754**. DOI: http://dx.doi.org/10.1016/j.scitotenv.2020.142227.

Shenfeld, L. 1970. Meteorological aspects of air pollution control. *Atmosphere* **8**(1): 3–13. DOI: http://dx.doi.org/10.1080/00046973.1970.9676578.

Shi, X, Brasseur, GP. 2020. The response in air quality to the reduction of Chinese Economic activities during the COVID-19 outbreak. *Geophysical Research Letters* **47**(11). DOI: http://dx.doi.org/10.1029/2020GL088070.

Sicard, P, De Marco, A, Agathokleous, E, Feng, Z, Xu, X, Paoletti, E, Rodriguez, JJD, Calatayud, V. 2020. Amplified ozone pollution in cities during the COVID-19 lockdown. *Science of the Total Environment* **735**. DOI: http://dx.doi.org/10.1016/j.scitotenv.2020.139542.

Siciliano, B, Carvalho, G, da Silva, CM, Arbilla, G. 2020a. The impact of COVID-19 partial lockdown on primary pollutant concentrations in the atmosphere of Rio de Janeiro and São Paulo Megacities (Brazil). *Bulletin of Environmental Contamination and Toxicology* **105**(1): 2–8. DOI: http://dx.doi.org/10.1007/s00128-020-02907-9.

Siciliano, B, Dantas, G, da Silva, CM, Arbilla, G. 2020b. Increased ozone levels during the COVID-19 lockdown: Analysis for the city of Rio de Janeiro, Brazil. *Science of the Total Environment* **737**. DOI: http://dx.doi.org/10.1016/j.scitotenv.2020.139765.

Siddiqui, A, Halder, S, Chauhan, P, Kumar, P. 2020. COVID-19 Pandemic and city-level Nitrogen Dioxide (NO_2) reduction for urban centres of India. *Journal of the Indian Society of Remote Sensing* **48**(7): 999–1006. DOI: http://dx.doi.org/10.1007/s12524-020-01130-7.

Sillman, S. 1999. The relation between ozone, NO_x and hydrocarbons in urban and polluted rural environments. *Atmospheric Environment* **33**(12): 1821–1845. DOI: http://dx.doi.org/10.1016/S1352-2310(98)00345-8.

Silver, B, He, X, Arnold, SR, Spracklen, DV. 2020. The impact of COVID-19 control measures on air quality in China. *Environmental Research Letters* **15**(8). DOI: http://dx.doi.org/10.1088/1748-9326/aba3a2.

Singh, RP, Chauhan, A. 2020. Impact of lockdown on air quality in India during COVID-19 pandemic. *Air Quality, Atmosphere & Health* **13**(8): 921–928. DOI: http://dx.doi.org/10.1007/s11869-020-00863-1.

Singh, V, Singh, S, Biswal, A, Kesarkar, AP, Mor, S, Ravindra, K. 2020. Diurnal and temporal changes in air pollution during COVID-19 strict lockdown over different regions of India. *Environmental*

Pollution **266**. DOI: http://dx.doi.org/10.1016/j.envpol.2020.115368.

Son, JY, Fong, KC, Heo, S, Kim, H, Lim, CC, Bell, ML. 2020. Reductions in mortality resulting from reduced air pollution levels due to COVID-19 mitigation measures. *Science of the Total Environment* **744**. DOI: http://dx.doi.org/10.1016/j.scitotenv.2020.141012.

Srivastava, S, Kumar, A, Bauddh, K, Gautam, AS, Kumar, S. 2020. 21-Day lockdown in India dramatically reduced air pollution indices in Lucknow and New Delhi, India. *Bulletin of Environmental Contamination and Toxicology* **105**(1): 9–17. DOI: http://dx.doi.org/10.1007/s00128-020-02895-w.

Stratoulias, D, Nuthammachot, N. 2020. Air quality development during the COVID-19 pandemic over a medium-sized urban area in Thailand. *Science of the Total Environment* **746**. DOI: http://dx.doi.org/10.1016/j.scitotenv.2020.141320.

Stringency Index. 2020. Our world in data. Available at https://ourworldindata.org/grapher/covid-stringency-index. Accessed 1 October 2020.

Su, T, Li, Z, Zheng, Y, Luan, Q, Guo, J. 2020. Abnormally shallow boundary layer associated with severe air pollution during the COVID-19 lockdown in China. *Geophysical Research Letters* **47**. DOI: http://dx.doi.org/10.1029/2020GL090041.

Suhaimi, NF, Jalaludin, J, Latif, MT. 2020. Demystifying a possible relationship between COVID-19, air quality and meteorological factors: Evidence from Kuala Lumpur, Malaysia. *Aerosol and Air Quality Research* **20**(7): 1520–1529. DOI: http://dx.doi.org/10.4209/aaqr.2020.05.0218.

Sun, W, Shao, M, Granier, C, Liu, Y, Ye, CS, Zheng, JY. 2018. Long-term trends of anthropogenic SO_2, NO_x, CO, and NMVOCs emissions in China. *Earth's Future* **6**(8): 1112–1133. DOI: http://dx.doi.org/10.1029/2018EF000822.

Sun, Y, Lei, L, Zhou, W, Chen, C, He, Y, Sun, J, Li, Z, Xu, W, Wang, Q, Ji, D, Fu, P, Wang, Z, Worsnop, DR. 2020. A chemical cocktail during the COVID-19 outbreak in Beijing, China: Insights from six-year aerosol particle composition measurements during the Chinese New Year holiday. *Science of the Total Environment* **742**. DOI: http://dx.doi.org/10.1016/j.scitotenv.2020.140739.

Tanzer-Gruener, R, Li, J, Eilenberg, SR, Robinson, AL, Presto, AA. 2020. Impacts of modifiable factors on Ambient air pollution: A case study of COVID-19 shutdowns. *Environmental Science & Technology Letters* **7**(8): 554–559. DOI: http://dx.doi.org/10.1021/acs.estlett.0c00365.

Tobías, A, Carnerero, C, Reche, C, Massagué, J, Via, M, Minguillón, MC, Alastuey, A, Querol, X. 2020. Changes in air quality during the lockdown in Barcelona (Spain) one month into the SARS-CoV-2 epidemic. *Science of the Total Environment* **726**. DOI: http://dx.doi.org/10.1016/j.scitotenv.2020.138540.

United Nations. 2020. United Nations framework convention on climate change. Available at https://unfccc.int/parties-observers#:~:text=Annex%20I%20Parties%20include%20the,Central%20and%20Eastern%20European%20States. Accessed 15 November 2020.

Vadrevu, KP, Eaturu, A, Biswas, S, Lasko, K, Sahu, S, Garg, JK, Justice, C. 2020. Spatial and temporal variations of air pollution over 41 cities of India during the COVID-19 lockdown period. *Scientific Reports* **10**(1): 16574. DOI: http://dx.doi.org/10.1038/s41598-020-72271-5.

Venter, ZS, Aunan, K, Chowdhury, S, Lelieveld, J. 2020. COVID-19 lockdowns cause global air pollution declines. *Proceedings of the National Academy of Sciences* **117**(32): 18984–18990. DOI: http://dx.doi.org/10.1073/pnas.2006853117.

Wan, S, Cui, K, Wang, Y-F, Wu, J-L, Huang, W-S, Xu, K, Zhang, J. 2020. Impact of the COVID-19 Event on Trip Intensity and Air Quality in Southern China. *Aerosol and Air Quality Research* **20**(8): 1727–1747. DOI: http://dx.doi.org/10.4209/aaqr.2020.07.0364.

Wang, G, Zhang, R, Gomez, ME, Yang, L, Levy Zamora, M, Hu, M, Lin, Y, Peng, J, Guo, S, Meng, J, Li, J, Cheng, C, Hu, T, Ren, Y, Wang, Y, Gao, J, Cao, J, An, Z, Zhou, W, Li, G, Wang, J, Tian, P, Marrero-Ortiz, W, Secrest, J, Du, Z, Zheng, J, Shang, D, Zeng, L, Shao, M, Wang, W, Huang, Y, Wang, Y, Zhu, Y, Li, Y, Hu, J, Pan, B, Cai, L, Cheng, Y, Ji, Y, Zhang, F, Rosenfeld, D, Liss, PS, Duce, RA, Kolb, CE, Molina, MJ. 2016. Persistent sulfate formation from London Fog to Chinese haze. *Proceedings of the National Academy of Sciences* **113**(48): 13630. DOI: http://dx.doi.org/10.1073/pnas.1616540113.

Wang, H, Miao, Q, Shen, L, Yang, Q, Wu, Y, Wei, H, Yin, Y, Zhao, T, Zhu, B, Lu, W. 2020a. Characterization of the aerosol chemical composition during the COVID-19 lockdown period in Suzhou in the Yangtze River Delta, China. *Journal of Environmental Sciences*. DOI: http://dx.doi.org/10.1016/j.jes.2020.09.019.

Wang, L, Li, M, Yu, S, Chen, X, Li, Z, Zhang, Y, Jiang, L, Xia, Y, Li, J, Liu, W, Li, P, Lichtfouse, E, Rosenfeld, D, Seinfeld, JH. 2020b. Unexpected rise of ozone in urban and rural areas, and sulfur dioxide in rural areas during the coronavirus city lockdown in Hangzhou, China: implications for air quality. *Environmental Chemistry Letters*. DOI: http://dx.doi.org/10.1007/s10311-020-01028-3.

Wang, P, Chen, K, Zhu, S, Wang, P, Zhang, H. 2020c. Severe air pollution events not avoided by reduced anthropogenic activities during COVID-19 outbreak. *Resources, Conservation and Recycling* **158**. DOI: http://dx.doi.org/10.1016/j.resconrec.2020.104814.

Wang, X, Zhang, R. 2020. How did air pollution change during the COVID-19 outbreak in China? *Bulletin of the American Meteorological Society* **101**(10): E1645–E1652. DOI: http://dx.doi.org/10.1175/BAMS-D-20-0102.1.

Wang, Y, Chen, Y, Wu, Z, Shang, D, Bian, Y, Du, Z, Schmitt, SH, Su, R, Gkatzelis, GI, Schlag, P, Hohaus, T, Voliotis, A, Lu, K, Zeng, L, Zhao, C, Alfarra, MR, McFiggans, G, Wiedensohler, A, Kiendler-Scharr, A, Zhang, Y, Hu, M. 2020d. Mutual promotion between aerosol particle liquid water and particulate nitrate enhancement leads to severe nitrate-dominated particulate matter pollution and low visibility. *Atmospheric Chemistry and Physics* **20**(4): 2161–2175. DOI: http://dx.doi.org/10.5194/acp-20-2161-2020.

Wang, Y, Wen, Y, Wang, Y, Zhang, S, Zhang, KM, Zheng, H, Xing, J, Wu, Y, Hao, J. 2020e. Four-month changes in air quality during and after the COVID-19 lockdown in six megacities in China. *Environmental Science & Technology Letters* **7**(11): 802–808. DOI: http://dx.doi.org/10.1021/acs.estlett.0c00605.

Wang, Y, Yuan, Y, Wang, Q, Liu, C, Zhi, Q, Cao, J. 2020f. Changes in air quality related to the control of coronavirus in China: Implications for traffic and industrial emissions. *Science of the Total Environment* **731**. DOI: http://dx.doi.org/10.1016/j.scitotenv.2020.139133.

Wang, Z, Uno, I, Yumimoto, K, Itahashi, S, Chen, X, Yang, W, Wang, Z. 2021. Impacts of COVID-19 lockdown, Spring Festival and meteorology on the NO_2 variations in early 2020 over China based on in-situ observations, satellite retrievals and model simulations. *Atmospheric Environment* **244**. DOI: http://dx.doi.org/10.1016/j.atmosenv.2020.117972.

Warneke, C, de Gouw, JA, Holloway, JS, Peischl, J, Ryerson, TB, Atlas, E, Blake, D, Trainer, M, Parrish, DD. 2012. Multiyear trends in volatile organic compounds in Los Angeles, California: Five decades of decreasing emissions. *Journal of Geophysical Research: Atmospheres* **117**(D21). DOI: http://dx.doi.org/10.1029/2012JD017899.

World Health Organization. 2019. *2018 WHO health and climate change survey report: Tracking global progress*. Geneva, Switzerland: World Health Organization.

Wilkins, KL, Benedetti, A, Kristiansen, NI, Lange, AC. 2016. Applications of satellite observations of volcanic ash in atmospheric dispersion modeling, in Mackie, S, Cashman, K, Ricketts, H, Rust, A, Watson, M eds., *Volcanic ash*. Amsterdam, the Netherlands: Elsevier: 233–246. Available at https://10.1016/b978-0-08-100405-0.00019-7.

Williams, J, Petrik, L, Wichmann, J. 2020. $PM_{2.5}$ chemical composition and geographical origin of air masses in Cape Town, South Africa. *Air Quality, Atmosphere & Health*. DOI: http://dx.doi.org/10.1007/s11869-020-00947-y.

Womack, CC, McDuffie, EE, Edwards, PM, Bares, R, de Gouw, JA, Docherty, KS, Dubé, WP, Fibiger, DL, Franchin, A, Gilman, JB, Goldberger, L, Lee, BH, Lin, JC, Long, R, Middlebrook, AM, Millet, DB, Moravek, A, Murphy, JG, Quinn, PK, Riedel, TP, Roberts, JM, Thornton, JA, Valin, LC, Veres, PR, Whitehill, AR, Wild, RJ, Warneke, C, Yuan, B, Baasandorj, M, Brown, SS. 2019. An odd oxygen framework for wintertime ammonium nitrate aerosol pollution in urban areas: NO_x and VOC control as mitigation strategies. *Geophysical Research Letters* **46**(9): 4971–4979. DOI: http://dx.doi.org/10.1029/2019GL082028.

Wong, DC, Pleim, J, Mathur, R, Binkowski, F, Otte, T, Gilliam, R, Pouliot, G, Xiu, A, Young, JO, Kang, D. 2012. WRF-CMAQ two-way coupled system with aerosol feedback: Software development and preliminary results. *Geoscientific Model Development* **5**(2): 299–312. DOI: http://dx.doi.org/10.5194/gmd-5-299-2012.

Wyche, KP, Nichols, M, Parfitt, H, Beckett, P, Gregg, DJ, Smallbone, KL, Monks, PS. 2020. Changes in ambient air quality and atmospheric composition and reactivity in the south east of the UK as a result of the COVID-19 lockdown. *Science of the Total Environment* **755**. DOI: http://dx.doi.org/10.1016/j.scitotenv.2020.142526.

Xiang, J, Austin, E, Gould, T, Larson, T, Shirai, J, Liu, Y, Marshall, J, Seto, E. 2020. Impacts of the COVID-19 responses on traffic-related air pollution in a Northwestern US city. *Science of the Total Environment* **747**. DOI: http://dx.doi.org/10.1016/j.scitotenv.2020.141325.

Xu, J, Ge, X, Zhang, X, Zhao, W, Zhang, R, Zhang, Y. 2020a. COVID-19 impact on the concentration and composition of submicron particulate matter in a typical city of Northwest China. *Geophysical Research Letters* **47**. DOI: http://dx.doi.org/10.1029/2020GL089035.

Xu, K, Cui, K, Young, L-H, Hsieh, Y-K, Wang, Y-F, Zhang, J, Wan, S. 2020b. Impact of the COVID-19 Event on Air Quality in Central China. *Aerosol and Air Quality Research* **20**(5): 915–929. DOI: http://dx.doi.org/10.4209/aaqr.2020.04.0150.

Xu, K, Cui, K, Young, L-H, Wang, Y-F, Hsieh, Y-K, Wan, S, Zhang, J. 2020c. Air quality index, indicatory air pollutants and impact of COVID-19 event on the air quality near central China. *Aerosol and Air Quality Research* **20**(6): 1204–1221. DOI: http://dx.doi.org/10.4209/aaqr.2020.04.0139.

Yan, X, Ohara, T, Akimoto, H. 2005. Statistical modeling of global soil NO_x emissions. *Global Biogeochemical Cycles* **19**(3). DOI: http://dx.doi.org/10.1029/2004GB002276.

Yang, Y, Ren, L, Li, H, Wang, H, Wang, P, Chen, L, Yue, X, Liao, H. 2020. Fast climate responses to aerosol emission reductions during the COVID-19 pandemic. *Geophysical Research Letters* **47**(19). DOI: http://dx.doi.org/10.1029/2020GL089788.

Yuan, Q, Qi, B, Hu, D, Wang, J, Zhang, J, Yang, H, Zhang, S, Liu, L, Xu, L, Li, W. 2021. Spatiotemporal variations and reduction of air pollutants during the COVID-19 pandemic in a megacity of Yangtze River Delta in China. *Science of the Total Environment* **751**. DOI: http://dx.doi.org/10.1016/j.scitotenv.2020.141820.

Zalakeviciute, R, Vasquez, R, Bayas, D, Buenano, A, Mejia, D, Zegarra, R, Diaz, V, Lamb, B. 2020. Drastic improvements in air quality in Ecuador during the COVID-19 outbreak. *Aerosol and Air Quality Research* **20**(8): 1783–1792. DOI: http://dx.doi.org/10.4209/aaqr.2020.05.0254.

Zambrano-Monserrate, MA, Ruano, MA. 2020. Has air quality improved in Ecuador during the COVID-19 pandemic? A parametric analysis. *Air Quality, Atmosphere & Health* **13**(8): 929–938. DOI: http://dx.doi.org/10.1007/s11869-020-00866-y.

Zangari, S, Hill, DT, Charette, AT, Mirowsky, JE. 2020. Air quality changes in New York City during the COVID-19 pandemic. *Science of the Total Environment* **742**. DOI: http://dx.doi.org/10.1016/j.scitotenv.2020.140496.

Zhang, J, Cui, K, Wang, Y-F, Wu, J-L, Huang, W-S, Wan, S, Xu, K. 2020a. Temporal variations in the air quality index and the impact of the COVID-19 event on air quality in Western China. *Aerosol and Air Quality Research* **20**(7): 1552–1568. DOI: http://dx.doi.org/10.4209/aaqr.2020.06.0297.

Zhang, L, Yang, L, Zhou, Q, Zhang, X, Xing, W, Zhang, H, Toriba, A, Hayakawa, K, Tang, N. 2020b. Impact of the COVID-19 outbreak on the long-range transport of particulate PAHs in East Asia. *Aerosol and Air Quality Research* **20**: 2035–2046. DOI: http://dx.doi.org/10.4209/aaqr.2020.07.0388.

Zhang, Q, Pan, Y, He, Y, Walters, WW, Ni, Q, Liu, X, Xu, G, Shao, J, Jiang, C. 2021. Substantial nitrogen oxides emission reduction from China due to COVID-19 and its impact on surface ozone and aerosol pollution. *Science of the Total Environment* **753**. DOI: http://dx.doi.org/10.1016/j.scitotenv.2020.142238.

Zhang, R, Zhang, Y, Lin, H, Feng, X, Fu, T-M, Wang, Y. 2020c. NO_x emission reduction and recovery during COVID-19 in East China. *Atmosphere* **11**(4). DOI: http://dx.doi.org/10.3390/atmos11040433.

Zhang, Z, Arshad, A, Zhang, C, Hussain, S, Li, W. 2020d. Unprecedented temporary reduction in global air pollution associated with COVID-19 forced confinement: A continental and city scale analysis. *Remote Sensing* **12**(15). DOI: http://dx.doi.org/10.3390/rs12152420.

Zhao, K, Bao, Y, Huang, J, Wu, Y, Moshary, F, Arend, M, Wang, Y, Lee, X. 2019. A high-resolution modeling study of a heat wave-driven ozone exceedance event in New York City and surrounding regions. *Atmospheric Environment* **199**: 368–379. DOI: http://dx.doi.org/10.1016/j.atmosenv.2018.10.059.

Zhao, N, Wang, G, Li, G, Lang, J, Zhang, H. 2020a. Air pollution episodes during the COVID-19 outbreak in the Beijing–Tianjin–Hebei region of China: An insight into the transport pathways and source distribution. *Environmental Pollution* **267**. DOI: http://dx.doi.org/10.1016/j.envpol.2020.115617.

Zhao, Y, Zhang, K, Xu, X, Shen, H, Zhu, X, Zhang, Y, Hu, Y, Shen, G. 2020b. Substantial changes in Nitrogen Dioxide and Ozone after excluding meteorological impacts during the COVID-19 outbreak in Mainland China. *Environmental Science & Technology Letters* **7**(6): 402–408. DOI: http://dx.doi.org/10.1021/acs.estlett.0c00304.

Zheng, B, Tong, D, Li, M, Liu, F, Hong, C, Geng, G, Li, H, Li, X, Peng, L, Qi, J, Yan, L, Zhang, Y, Zhao, H, Zheng, Y, He, K, Zhang, Q. 2018. Trends in China's anthropogenic emissions since 2010 as the consequence of clean air actions. *Atmospheric Chemistry and Physics* **18**(19): 14095–14111. DOI: http://dx.doi.org/10.5194/acp-18-14095-2018.

Zheng, H, Kong, S, Chen, N, Yan, Y, Liu, D, Zhu, B, Xu, K, Cao, W, Ding, Q, Lan, B, Zhang, Z, Zheng, M, Fan, Z, Cheng, Y, Zheng, S, Yao, L, Bai, Y, Zhao, T, Qi, S. 2020. Significant changes in the chemical compositions and sources of $PM_{2.5}$ in Wuhan since the city lockdown as COVID-19. *Science of the Total Environment* **739**. DOI: http://dx.doi.org/10.1016/j.scitotenv.2020.140000.

Zoran, MA, Savastru, RS, Savastru, DM, Tautan, MN. 2020. Assessing the relationship between surface levels of $PM_{2.5}$ and PM_{10} particulate matter impact on COVID-19 in Milan, Italy. *Science of the Total Environment* **738**. DOI: http://dx.doi.org/10.1016/j.scitotenv.2020.139825.

How to cite this article: Gkatzelis, GI, Gilman, JB, Brown, SS, Eskes, H, Gomes, AR, Lange, AC, McDonald, BC, Peischl, J, Petzold, A, Thompson, CR, Kiendler-Scharr, A. 2021. The global impacts of COVID-19 lockdowns on urban air quality: A critical review and recommendations. *Elementa: Science of the Anthropocene* 9(1). DOI: https://doi.org/10.1525/elementa.2021.00176

Domain Editor-in-Chief: Detlev Helmig, Boulder AIR LLC, Boulder, CO, USA

Associate Editor: Frank Flocke, National Center for Atmospheric Research, Boulder, CO, USA

Knowledge Domain: Atmospheric Science

Published: April 2, 2021 **Accepted:** January 31, 2021 **Submitted:** December 4, 2020

ELEMENTA Science of the Anthropocene

Elem Sci Anth is a peer-reviewed open access journal published by University of California Press.

OPEN ACCESS